The Thesis Committee for Ghazal Dashti
Certifies that this is the approved version of the following thesis:

A Study of Microemulsion Viscosity with Consideration of Polymer and Co-solvent Additives

APPROVED BY
SUPERVISING COMMITTEE:

Supervisor:

Mojdeh Delshad

Kishore Mohanty

A Study of Microemulsion Viscosity with Consideration of Polymer and Co-solvent Additives

by

Ghazal Dashti, B.S.P.E.

Thesis

Presented to the Faculty of the Graduate School of

The University of Texas at Austin

in Partial Fulfillment

of the Requirements

for the Degree of

Master of Science in Engineering

The University of Texas at Austin

May 2014

Dedication

To my beloved husband, Farhad Tarahhom, for his love, support, and patience

To my lovely daughter Tannaz

To my mother Parvin

And to the memory of my father Houshang

Acknowledgements

I would like to express my deepest appreciation and sincerest gratitude to my supervisor, Dr. Mojdeh Delshad, who gave me the opportunity to work in this area. Words cannot express my sincere appreciation for her guidance. She provided me with the knowledge, support and invaluable insights I needed to make graduate school a fulfilling experience.

My gratitude further continues to my second reader, Dr. Kishore Mohanty, for supporting this research and providing us his laboratories for developing the needed experiments for this project.

I owe a great debt of thanks to all the individuals who made this experience possible. I also would like to give special thanks to Dr. Krishna Panthi for his great effort in providing me with laboratory experiments needed for this project.

I would also like to express my gratitude to Dr. Abdoljalil Varavei and Mohammad Lotfollahi for their help during my research.

I would like to express my deepest gratitude to my husband, Farhad Tarahhom, for his endless love and support throughout my study. My achievement would not have been possible without his help.

Abstract

A Study of Microemulsion Viscosity with Consideration of Polymer and Co-solvent Additives

Ghazal Dashti, M.S.E.

The University of Texas at Austin, 2014

Supervisor: Mojdeh Delshad

With the dramatic increase in the worldwide demand for the crude oil and with the fact that the oil and gas resources are depleting, the enhanced oil recovery process plays an important role to increase the production from the existing hydrocarbon reservoirs. Chemical enhanced oil recovery is one of the most important techniques to unlock significant amount of trapped oil from oil reservoirs. Surface agent materials (Surfactants) are used to lower the interfacial tension (IFT) between water and oil phases to ultralow values and mobilize the trapped oil. When surfactant, water, and oil are mixed together they form a thermodynamically stable phase called microemulsion which can be characterized by ultralow interfacial tension and the ability to solubilize both aqueous and oil compounds.

Another characteristic of microemulsion solution is its viscosity which plays an important role in the creation and movement of the oil bank. The microemulsion micro-structure is complex and its viscosity is difficult to predict. Various viscosity models and correlations are presented in the literature to describe microemulsion viscosity behavior,

but they fail to represent the rheological behavior of many microemulsion mixtures. Most of these models are valid in the lower and higher ranges of solute where one of the domains is discontinuous. The majority of the models fail to calculate the rheology of microemulsion phase in bicontinuous domains.

In this work, we present a systematic study of the rheological behavior of microemulsion systems and the effect of additives such as polymer and co-solvent on rheological properties of microemulsions. Several laboratory experiments were conducted to determine the rheological behavior of surfactant solutions.

A new empirical model for the viscosity of microemulsion phase as a function of salinity is introduced. The model consists of three different correlations one for each phase type of Windsor phase behaviors. The proposed model is validated using a number of experimental results presented in this document.

The proposed viscosity model is implemented in the UTCHEM simulator and the simulator results are compared with the coreflood experiments. Excellent matches were obtained for the pressure. We further improved the proposed viscosity model to incorporate the effect of polymer and co-solvent on the microemulsion viscosity.

Table of Contents

List of Tables xi

List of Figures xiv

Chapter 1: Introduction 1

Chapter 2: Literature Review 4

2.1 Introduction 4

2.2 Phase Behavior Screening 5

2.3 Microemulsion Types 5

2.4 Interfacial Tension 7

2.5 Microemulsion Viscosity 8

2.6 Polymeric Microemulsions 10

2.7 Co-Solvent 11

2.7.1 Effect of co-solvent on phase behavior and optimal salinity 13

2.7.2 Effect of co-solvent on microemulsion viscosity 16

2.8 Alcohol partitioning 20

Chapter 3: Methodology and Data Analysis 21

3.1 Experimental Equipment 21

Borosilicate Pipettes 21

Pipette Repeater 21

Oxygenated Propane Torch 22

Water Deionizer 22

Convection Ovens 22

3.1.1 Phase Behavior Screening Description 22

3.1.2 Samples solution preparation 23

Electrolytes and Brines 23

Surfactant Stock 23

Polymer Stock 23

3.2 Set Up Procedure 24

3.3 Interpretation and Measurement 26
3.3.1 Solubilization Ratio 26
Oil Solubilization Ratio 26
Water Solubilization Ratio....27
Optimum Solubilization Ratio 27
3.3.2 Interfacial Tension 27
3.4 Microemulsion Viscosity Measurements....28
3.4.1 Microemulsion Rheology Testing Description....28
Sample Preparation 28
Equilibration 29
Phase Extraction....29
3.4.2 Microemulsion Viscosity Measurements....30
ARG2 VISCOMETER....30
Chapter 4: Experimental Results 32
4.1 Microemulsion Rheology....32
4.1.1 AO 41-50 Data Set....32
Oleic Phase Viscosity 34
Microemulsion Phase Viscosity....35
4.1.2 AO 352 Data Set 48
Microemulsion Phase Viscosity....49
4.1.3 AO 03 Data Set 54
Microemulsion Phase Viscosity....55
Chapter 5: Development of New Viscosity Model for Microemulsion 58
5.1 Verification of New Viscosity Model....59
5.1.1 AO 41-50 Data Set....60
5.1.2 AO 352 Data Set 62
5.1.3 AO 03 Data Set 65
5.1.4 PCN 78-79 68
5.1.5 PCN-128 Data Set....72
5.1.6 Field A Data Set....75

5.2 Effect of Polymer on Microemulsion Rheology 77
5.2.1 Effect of Polymer on Microemulsion Phase Behavior 79
5.2.2 AO 352 Data Set with Polymer 81
Oil Phase Viscosity 81
Aqueous Phase Viscosity in Type III Systems 84
Microemulsion Phase Viscosity 87
5.2.3 AO 03 Data Set 92
Type I phase behavior 93
Type II Phase Behavior 94
Type III Phase Behavior 94
5.2.4 PCN 128 Data Set 97

Chapter 6: Simulation Case Study 100
6.1 UTCHEM Simulator 100
6.1.1 UTCHEM Viscosity Model 101
6.2 PCN-01 ACP Coreflood History Match 103
6.3 PCN-04 ACP Coreflood History Match 113

Chapter 7: Effect of Co-Solvent on Microemulsion Viscosity 122
7.1 Data Set 1 123
7.2 Viscosity Model to Incorporate Co-solvent Effects 127
7.2.1 Type I Phase Behavior 132
7.2.2 Type III Phase Behavior 134
7.2.3 Type II Phase Behavior 137
7.2.4 Model Verification 139
7.3 Summary 142

Chapter 8: Summary, Conclusions, and Recommendations 144
8.1 Summary and Conclusions 144
8.2 Recommendations 146

BIBLIOGRAPHY **148**

List of Tables

Table 2.1: The Effect of IBA on Flattening Time, IFT, IFV, Partition Coefficient, and Oil Displacement Efficiency (Chiang & Shah., 1980) 20

Table 4.1: Formation brine (FB).....36

Table 4.2: Synthetic formation brine (SFB) 37

Table 4.3: Summary of AO samples and the type of phase behavior for each sample. 38

Table 4.4: Phase behavior types for AO 352 formulation 50

Table 4.5: Top phase viscosity measurements vs. shear rates for AO 352 data set.50

Table 4.6: Middle phase microemulsion viscosity measurements vs. shear rates for AO 352 data set.....51

Table 4.7: Lower phase viscosity measurements vs. shear rates for AO 352 data set. 51

Table 5.1: Microemulsion viscosity at shear rate of 10 sec^{-1} for AO 41-50.....61

Table 5.2: Constant parameters used in Eq. (5.2) for AO 41-50 61

Table 5.3: Model results vs. lab measurements for AO 41-50 61

Table 5.4: Viscosity results for shear rate 10 sec^{-1} for surfactant formulation AO 352 63

Table 5.5: Constant parameters used in Eq. (5.2) for AO 352.....63

Table 5.6: Model results vs. lab measurements for AO 352.....64

Table 5.7: Phase behavior for AO 03 samples.....66

Table 5.8: Viscosity results for shear rate of 10 sec^{-1} for surfactant formulation AO 03 66

Table 5.9: Constant parameters used in Eq. (5.2) for AO 03 data set 66

Table 5.10: Model results vs. lab measurements for AO 03 data set.....67
Table 5.11: PCN-78 and PCN-79 microemulsion viscosity measurements 69
Table 5.12: Model results vs. lab measurements for PCN-78 69
Table 5.13: Model results vs. lab measurements for PCN-79 70
Table 5.14: PCN-128 microemulsion viscosity measurements 73
Table 5.15: Model results vs. lab measurements for PCN-128 74
Table 5.16: Viscosity measurements at shear rates of 1 and 10 sec^{-1} for KL-48ME at 85 °C 76
Table 5.17: Viscosity measurements at shear rates of 1 and 10 sec^{-1} for KL-46ME at 85 °C 76
Table 5.18: Viscosity measurements at shear rates of 1 and 10 sec^{-1} for KL-46ME at 65 °C 77
Table 5.19: Phase behavior for AO 352.....80
Table 5.20: Phase behavior for AO 03 data set 80
Table 5.21: Bottom phase aqueous viscosities for samples with Type I phase behavior (AO 03 data set).....94
Table 5.22: Microemulsion viscosities for the cases with and without polymer in Type III (AO 03 data set).....96
Table 5.23: Microemulsion viscosities with and without polymer at shear rate of 1 sec^{-1} 98
Table 6.1: PCN-01 core properties 105
Table 6.2: Compositions of synthetic brine (PCNSSB) for PCN-01 coreflood. .105
Table 6.3: ASP slug and polymer drive used in PCN-01 coreflood 106
Table 6.4: Co-solvent and soap phase behavior UTCHEM input parameters (Xu, 2012). 109

Table 6.5: Polymer input parameters (Xu, 2012) 110
Table 6.6: Input parameters for co-solvent/microemulsion properties (Xu, 2012)110
Table 6.7: Viscosity parameters for the original and the new viscosity models..110
Table 6.8: PCN-04 core properties 116
Table 6.9: Compositions of synthetic brine (PCNSSB) for PCN-04 coreflood. .116
Table 6.10: ASP slug and polymer drive used in PCN-04 coreflood 116
Table 6.11: Co-solvent and soap phase behavior input parameters (Xu, 2012). .117
Table 6.12: Polymer input parameters (Xu, 2012) 118
Table 6.13: Input parameters for co-solvent/microemulsion properties (Xu, 2012)118
Table 6.14: Viscosity parameters for the original and the new viscosity models118
Table 7.1: Microemulsion viscosity at different surfactant and co-solvent concentrations 125
Table 7.2: RF at different co-solvent concentrations.....139
Table 7.3: Microemulsion viscosities for sample with 37.5 wt% alcohol concentration 140
Table 7.4: Model parameters at 37.5 wt% alcohol concentration.....140
Table 7.5: Microemulsion viscosities for sample with 50 wt% alcohol concentration 141

List of Figures

Figure 2.1: Winsor classification of microemulsion phase environments 7

Figure 2.2: Interfacial tension and solubilization parameters (Healy & Reed, 1974) 8

Figure 2.3: Viscosity of the system A in the single-phase region (Jones & Dreher, 1976) 15

Figure 2.4: Microemulsion viscosity and volume (Healy & Reed, 1976) 17

Figure 2.5: Microemulsion viscosity vs. salinity at different alcohol concentrations (Salter, 1977).....18

Figure 3.1: Pipette Racks Maintained at Reservoir Temperature in the Oven 25

Figure 3.2: ARG2 rheometer (Costello, 2005) 31

Figure 4.1: Phase behavior with 0.375% TDA-13PO-SO4, as a surfactant, 0.125% C20-24 IOS as a co-surfactant, 0.75% IBA as a co-solvent, 0.5 % $Na2CO_3$ and scanning with 0-2.5% NaCl. 38

Figure 4.2: AO 41-50 microemulsion viscosity vs. salinity at different shear rates (in s^{-1}) 39

Figure 4.3: Match of solubilization ratios for AO 41-50 samples 40

Figure 4.4: Viscosity match (Model vs. lab data) at shear rate of 1.0 $s^{-1}$for AO 41-50 41

Figure 4.5: Viscosity match for the Newtonian viscosity of AO 41-50 samples ..41

Figure 4.6: Viscosity of pure oil and three equilibrium phases at optimum salinity of 0.3025 meq/ml vs. shear rate 42

Figure 4.7: Top phase viscosity (oleic phase) vs. shear rate for samples with salinity in Type I phase behavior (AO 41-46) 43

Figure 4.8: Top phase viscosity (excess oil phase) vs. shear rate for samples with salinity in Type III phase behavior (AO 48-50).....44
Figure 4.9: Microemulsion phase (bottom phase) viscosity vs. shear rate for samples with salinity in Type I phase behavior (AO 41-46) 45
Figure 4.10: Microemulsion phase (bottom phase) viscosity vs. salinity for samples with Type I phase behavior shown at different shear rates in s^{-1}.....46
Figure 4.11: Microemulsion phase (middle phase) viscosity vs. shear rate for samples with salinity in Type III phase behavior. 47
Figure 4.12: Microemulsion phase (middle phase) viscosity vs. salinity for samples with Type III phase behavior measured at different shear rates in s^{-1}.48
Figure 4.13: Microemulsion viscosity vs. salinity for samples with Type I phase behavior (AO 352 data set) at different shear rates in Sec^{-1}. 52
Figure 4.14: Microemulsion viscosity vs. salinity for samples with Type III phase behavior (AO 352 data set) at different shear rates in Sec^{-1}. 53
Figure 4.15: Upper phase microemulsion phase viscosity vs. salinity for samples with Type II phase behavior (AO 352 data set) at different shear rates in Sec^{-1} 54
Figure 4.16: Microemulsion viscosity vs. salinity for samples with Type I phase behavior (AO 03 data set) for different shear rates in s^{-1}.....56
Figure 4.17: Microemulsion viscosity vs. salinity for samples with Type III phase behavior (AO 03 data set) for different shear rates in s^{-1}.....57
Figure 5.1: Validation of new viscosity model with experimental measurements for AO 41-50 62
Figure 5.2: Validation of proposed viscosity model with experimental measurements for AO 352 65

Figure 5.3: Validation of new viscosity model with experimental measurements for AO 03 data set.....68
Figure 5.4: Validation of new viscosity model with experimental measurements for PCN-78 71
Figure 5.5: Validation of new viscosity model with experimental measurements for PCN-79 72
Figure 5.6: Validation of new viscosity model with experimental measurements for PCN-128 75
Figure 5.7: Lab measurements vs. model results for Field A data. 77
Figure 5.8: Effect of polymer on solubilization ratio (AO 352). 81
Figure 5.9: Oil phase viscosities vs. shear rates at different salinity for samples with Type I phase behavior (AO 352 samples with and without polymer).83
Figure 5.10: Oil phase viscosities vs. shear rates at different salinity for samples with Type III phase behavior (AO 352 samples with and without polymer). 84
Figure 5.11: Polymer viscosity measurements vs. salinity at different shear rates in sec^{-1}. 86
Figure 5.12: Aqueous phase viscosity for samples with Type III phase behavior at different shear rate of Sec^{-1} 87
Figure 5.13: Viscosity vs. salinity for samples with Type I phase behavior (AO 352 with polymer) for different shear rates in Sec^{-1}. 89
Figure 5.14: Viscosity vs. salinity for samples with Type III phase behavior (AO 352 with polymer) for different shear rates in Sec^{-1}. 90

Figure 5.15: Comparison between microemulsion viscosities (with and without polymer) for system with Type I phase behavior at shear rate of 10 sec^{-1}. 91

Figure 5.16: Comparison between microemulsion viscosities (with and without polymer) for system with Type III phase behavior at shear rate of 10 sec^{-1}. 92

Figure 5.17: Comparison of polymer viscosity and bottom phase viscosities for samples with and without polymer in a Type III phase behavior (AO 03 data set) 96

Figure 5.18: Microemulsion phase viscosity with and without polymer for a Type III phase behavior (AO 03 data set). 97

Figure 5.19: Comparison of microemulsion phase viscosity with and without polymer (PCN 128 data set). 99

Figure 6.1: Microemulsion viscosity with 1.5% Butyl-5EO in PCNSSB at 16000 ppm TDS in 30% oil. 107

Figure 6.2: PCN-01 apparent viscosity and total relative mobility. 108

Figure 6.3: Oil recovery, oil saturation, and oil cut for PNC-01 coreflood. 109

Figure 6.4: Pressure drop across entire core for PCN-01 coreflood. 111

Figure 6.5: Oil saturation for PCN-01 coreflood. 112

Figure 6.6: Cumulative oil recovery for PCN-01 coreflood. 113

Figure 6.7: Oil recovery, oil saturation, and oil cut for PNC-04 coreflood. 117

Figure 6.8: Pressure drop across entire core for PCN-04 coreflood. 119

Figure 6.9: Cumulative oil recovery for PCN-04 coreflood. 120

Figure 6.10: Oil saturation for PCN-04 coreflood. 121

Figure 7.1: Middle phase viscosities vs. shear rates at different surfactant and co-solvent concentrations.....125
Figure 7.2: Microemulsion viscosity vs. co-solvent concentration at constant surfactant concentration and a given salinity.....127
Figure 7.3: Microemulsion viscosity vs. salinity for Surfactant AA TAA (12.5). CSEL and CSEU nearly coincide (Salter, 1977) 129
Figure 7.4: Microemulsion viscosity vs. salinity for Surfactant AA TAA (25) (Salter, 1977) 130
Figure 7.5: Microemulsion viscosity vs. salinity for Surfactant AA TAA (37.5) (Salter, 1977).....131
Figure 7.6: Microemulsion viscosity vs. salinity for Surfactant AA TAA (50) (Salter, 1977) 132
Figure 7.7: Viscosity vs. normalized salinity for Type I samples with different co-solvent concentrations (indicated in the parenthesis) of Salter (Salter, 1977) 134
Figure 7.8: Viscosity vs. normalized salinity for Type III samples at different concentrations of co-solvent vs normalized salinity using data of Salter (Salter, 1977).....136
Figure 7.9: Microemulsion viscosity vs. normalized salinity for Type II samples at different concentrations of co-solvent vs normalized salinity using Salter's data (Salter, 1977).....138
Figure 7.10: Model validation for microemulsion viscosities at 37.5 and 50 wt% alcohol concentrations (Date from Salter (Salter, 1977). 142

Chapter 1: Introduction

With the dramatic increase in the worldwide demand for the crude oil and with the fact that the oil and gas resources are depleting, the enhanced oil recovery process plays an important role to increase the production from the existing hydrocarbon reservoirs. Chemical enhanced oil recovery is one of the most important techniques to unlock significant amount of trapped oil from the oil reservoirs. Surface agent materials (Surfactants) are used to lower the interfacial tension (IFT) between water and oil phases to ultralow values and mobilize the trapped oil. When surfactant, water, and oil are mixed together they form a thermodynamically stable phase called microemulsion which can be characterized by ultralow interfacial tension and the ability to solubilize both aqueous and oil compounds.

Many characteristics of microemulsion solutions are of interest to many researchers. Viscosity of microemulsion phase finds a special status in literatures. The viscosity of a solution is an indication of fluid consistency and is a measure of its internal resistance to flow. The importance of viscosity in chemical flooding makes it one of the most important and measured transport properties.

Viscosity of microemulsion phase is a measurable property that can describe the flow behavior and is of considerable interest in oil industry due to its importance in EOR applications. It is one of the most important parameters in the ability of the microemulsion to recover oil in enhanced oil recovery processes. The knowledge of microemulsion phase viscosity and the capability to control it is an important factor in oil recovery. The microemulsion micro-structure is complex and its viscosity is difficult to predict.

Various viscosity models and correlations are presented in the literature to describe microemulsion viscosity behavior and are capable of modeling the microemulsion rheology of number of systems but they fail to represent the rheological behavior of complex microemulsion mixtures. Most of these models are valid in the lower and higher ranges of solute where we have continuous phases. The majority of the models fail to calculate the rheology of microemulsion phase in bicontinuous systems.

Adding polymer or co-solvent to surfactant solutions often results in interesting rheological properties. The complex microscopic and macroscopic structures of such systems lead to viscosity behaviors that are very different than the conventional Newtonian and non-Newtonian fluids. Despite very interesting rheological behavior of bicontinuous microemulsion complexes, there are only very few literature studies for the rheological properties of these systems.

The purpose of this research was to study the rheology of microemulsions and the effect of co-solvent and polymer on the microemulsion viscosity. The rheological behaviors of microemulsion systems are largely depend on their phase behaviors i.e. oil in water or water in oil emulsions. Different phase behavior can have significantly different rheological properties. We introduce a new empirical viscosity model for the viscosity of microemulsion phase as a function of salinity. The model is not a continuous correlation that covers all three different types of phase behaviors; rather, we introduce empirical correlations for the microemulsion phase for each phase behavior type. We implemented the new viscosity model into UTCHEM simulator and verified it by matching results of coreflood laboratory experiments. We have also introduced several factors and new concepts to incorporate the effect of polymer and co-solvent on the microemulsion viscosity.

A literature review of microemulsion rheology and the effect of polymer and co-solvent on the microemulsion viscosity are presented in Chapter 2. A brief description of the equipment and materials are covered in Chapter 3. Analysis used to develop a new viscosity model based on the rheology properties of microemulsion phase is described in Chapter 4 and Chapter 5. Implementation and verification of the newly developed viscosity model into UTCHEM numerical simulator are presented in Chapter 6. Chapter 7 describes the modifications to the new viscosity model to account for the effect of co-solvent on microemulsion viscosity. Finally, the conclusions and recommendations are given in Chapter 8.

Chapter 2: Literature Review

2.1 INTRODUCTION

Enhanced oil recovery (EOR) is becoming more important to the oil and gas industry as the economy of the industry pushes the limits and requires the examination of the chemical flooding methods. The use of chemical materials such as surfactant/co-solvent solutions to enhance the recovery of hydrocarbons from reservoir is widely recognized in oil industries since the mid-1920s (Beckstrom & Van Tuyl, 1927). The chemical solution is usually mixed on site and delivered for injection into vertical or horizontal wells. Solubilization of oil into aqueous phase is the primary recovery mechanism in surfactant/co-solvent flooding. Upon contact with oil, the surfactant/co-solvent mixture increases the total solubility of oil in aqueous phase and improves the recovery of the remaining or trapped oil in the reservoir. Solubilization mechanism requires that the surfactant concentration be greater than critical micelles concentration (CMC) and be maintained as the mixture flows through porous media. In addition to solubilization mechanism, surfactant/co-solvent mixture can improve the oil recovery through mobilization. The surfactant/co-surfactant mixture reduces the interfacial tension between the oil phase and the aqueous phase which in turn reduces the capillary force that traps the oil into the pores of the rock.

Many characteristics of microemulsion solutions are of interest to many researchers. Viscosity of microemulsion phase finds a special status in the literature. The viscosity of a solution is an indication of fluid consistency and is a measure of fluid internal resistance to flow. The importance of viscosity in chemical flooding makes it one of the most important and measured transport properties.

The purpose of this research was to study the rheology of microemulsions and the effect of co-solvent and polymer on the microemulsion viscosity.

2.2 PHASE BEHAVIOR SCREENING

Thermodynamically stable phase can be formed with oil, water and surfactant mixtures [(Winsor, 1954); (Bourrel & Schechter, 1988)]. Surfactants form micellar structures at concentrations above the critical micelle concentration (CMC) (Bourrel & Schechter, 1988). A microemulsion is a distinct phase consisting of surfactant, oil and water and sometimes co-solvents and other components. This phase is thermodynamically stable in the sense that it will return to the same phase volume at a given temperature (Bourrel & Schechter, 1988).

Crude oil is a complex mixture consisting of more than 200 different organic compounds. There is no unique formulation for chemical EOR design. There are various chemical interactions between the injected formulation and the reservoir rock.

Chemicals for EOR application are usually characterized by phase behavior screening. A chemical formulation for an EOR application should first be designed to work well in phase behavior before being tested in a core flood experiment.

The phase transition is examined by keeping all variables fixed except for the scanning variable. The scanning variable may include salinity, surfactant, cosurfactant, alcohol, or oil.

2.3 MICROEMULSION TYPES

The formation of a distinct, thermodynamically stable phase when surfactant, brine, and oil are mixed is called microemulsion (Winsor, 1954). Microemulsion phase is different from emulsions, which are thermodynamically unstable.

Microemulsion phase behavior tests involve mixing the surfactant solution with oil and allowing it to reach equilibrium at the desired temperature. The number of phases and the volume changes are the characteristics of the phase behavior test. Microemulsion phase behavior was originally described by Winsor as Type I, Type II, and Type III. At lower salinity, Type I or oil-in-water microemulsions occur, which are characterized by coexistence with an excess brine phase. At very high salinity, Type II or water-in-oil microemulsions are formed, which are characterized by coexistence with an excess oil phase. Type III occurs between the Type I and Type II in which microemulsions are formed as a middle phase. Type III microemulsion has both excess oil and excess water phases. The salinities at which the transition happens between Type I and Type III phase behaviors is referred to as the lower critical salinity, and the salinity of the transition between Type III and Type II is referred to as the upper critical salinity. Figure 2.1 illustrates Winsor phase transitions brought by increasing either salinity (in case of ionic surfactants) or temperature (for non-ionics).

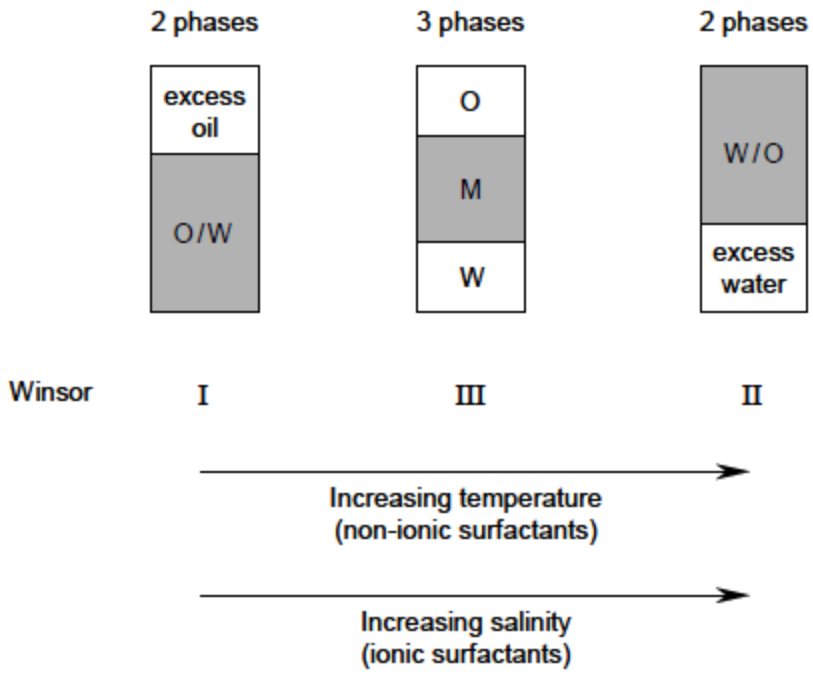

Figure 2.1: Winsor classification of microemulsion phase environments

2.4 INTERFACIAL TENSION

The optimum microemulsion mixture may consist of one or more of the following components: surfactant, co-solvent, alcohol, salt, and polymer. Alcohol or salt is used to optimize a microemulsion mixture. Salter, 1977 and others demonestrated the salt screening method to optimize a microemulsion mixtures by measuring the interfacial tension. The optimum salinity is defined as the salinity at which the interfacial tension for both oil/microemulsion and brine/microemulsion are at the minimum (Figure 2.2).

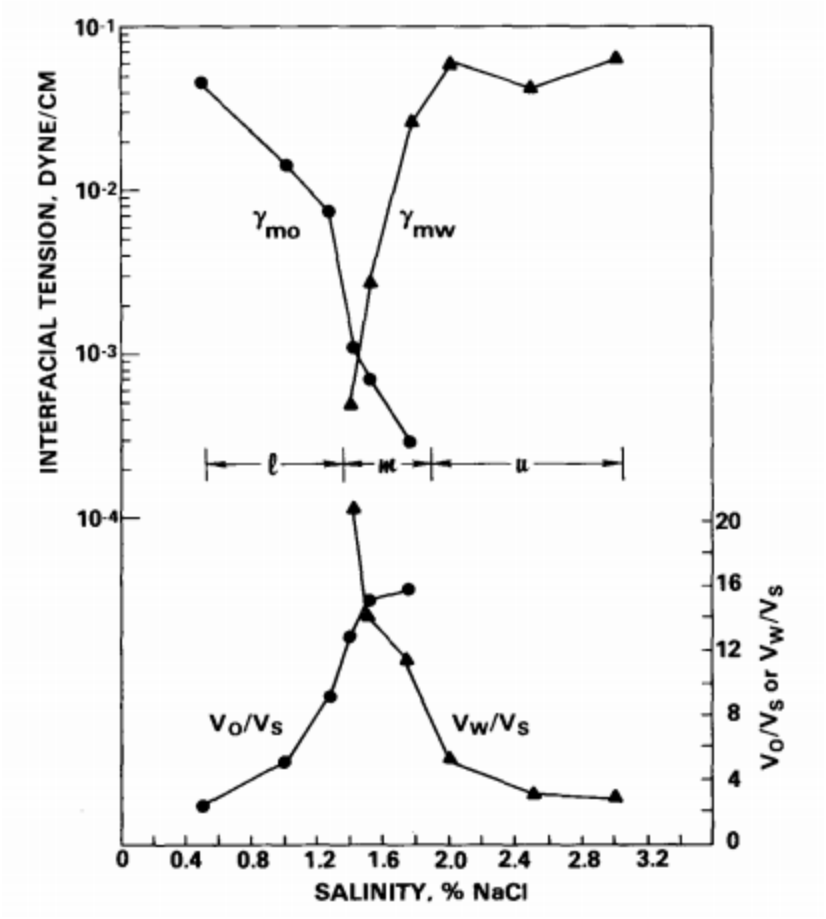

Figure 2.2: Interfacial tension and solubilization parameters (Healy & Reed, 1974)

2.5 MICROEMULSION VISCOSITY

Viscosity as a characteristic of a system mainly depends on the microscopic and macroscopic structures of the system and their internal interactions. Many factors affect the viscosity of the microemulsion phase. Anionic and cationic surfactants show different microemulsion viscosity behavior when additives are added to the solution. Garcia-Rio et al. (1994) reported that the viscosity and the water solubilization capacity of cationic microemulsion phase decreases with the increase in salts, HCl, NaOH concentration.

Ajith et al. (1994) presented the increase in anionic microemulsion viscosity by increasing salinity.

The viscosity of a microemulsion phase is highly affected by system compositions. A system that is oil continuous can change into a bicontinuous system and finally to a water continuous system. These phases (oil continuous, bicontinuous, or water continuous phases) have very different structures and result in distinct changes in viscosity. In Winsor Type I and Type II systems we have isolated aggressions and the viscosity of microemulsion phase is very close to the viscosity of continuous oil and aqueous phases, while in Winsor Type III, where we have a bicontinuous phase, larger viscosity values is observed.

Microemulsions have complex rheological behavior. Droplet clustering and fusion which is known as microemulsion percolation changes the internal structure of microemulsion and affects the viscosity (Eicke, et al., 1984). Percolation is known as a process of transitioning from isolated droplets to an interconnected bicontinuous system.

Various viscosity models and correlations are presented in the literature to describe microemulsion viscosity and are capable of modeling the microemulsion rheology of number of systems but they fail to represent the rheology of complex microemulsion mixtures. Most of these models are valid in the lower and higher ranges of solute where we have continuous phases. The majority fails to model the rheology of microemulsion phase in bicontinuous systems.

The viscosity of a microemulsion system is a measurable quantity that characterizes a given system. The viscosity of dilute microemulsion can be modeled by Einstein’s well-known viscosity relation as follow:

$$\eta_r = 1 + 2.5\phi \tag{2.1}$$

where η_r is the relative viscosity of the solution, and ϕ is the volume fraction of the solute or dispersed phase. However, this relation is not valid at higher concentration and for the system with complex structures, most likely due to many body interactions. There is a lack of accurate theory on viscosity of microemulsions. Other forms of equations have been used to represent the rheology of microemulsion systems. One of these equations is Moody equation examined by (Baker, et al., 1984):

$$\eta_r = \exp\frac{a\varphi}{1 - k\varphi} \tag{2.2}$$

where η_r is the relative viscosity $\left(\eta_{so\ln}/\eta_{solv}\right)$, φ is the volume fraction of water, and *a* and *k* are constants. The constant *a* is related to intrinsic viscosity and *k* accounts for particle interaction. (Vand, 1948) presented an equation very similar to Moody equation as follow:

$$\ln\eta_r = \frac{v\varphi}{1 - Q\varphi} \tag{2.3}$$

where constant v is the particle shape factor and Q accounts for inter-particle interaction. (Bidyut & Satya, 2000) listed few of these correlations.

2.6 POLYMERIC MICROEMULSIONS

Mobility control is a key in improving the sweep efficiency of surfactant flooding. Without mobility control, aqueous phase which has lower viscosity and higher mobility will move faster than the displaced fluid such as viscous oil and creates fingering problem. Once fingering happens, a high mobility channels are formed between injectors and producers and lowers the efficiency of the process.

By adding polymer to the surfactant slug the viscosity of the chemical slug increases which is needed to offset the aqueous relative permeability when IFT is

reduced. Higher water viscosity or low mobility ratio also increases the sweep efficiency by preventing the viscous fingering due to fluid properties and channeling due to reservoir heterogeneities. The mobility ratio is a dimensionless number that is used to characterize the displacement efficiency between two fluids and is defined by the ratio of the displacing fluid to the displaced phase mobility as follow (Lake, 1989):

$$M = \frac{\lambda_{displacing\_fluid}}{\lambda_{displaced\_fluid}} \tag{2.4}$$

where M is the mobility ratio, $\lambda_{displacing\_fluid}$ is the mobility of the displacing fluid (i.e. effective permeability divided by viscosity of water phase)and $\lambda_{displaced\_fluid}$ is the mobility of displaced fluid (i.e. oil phase).

Adding polymer to surfactant solutions often results in interesting rheological properties. The complex microscopic and macroscopic structures of such systems lead to viscosity behaviors that are very different than the conventional Newtonian and non-Newtonian fluids. Despite very interesting rheological behavior of bicontinuous microemulsion complexes, there are only very few literature studies for the rheological properties of these systems [(Chen & Warr, 1992), (Anklam, et al., 1995)]. Laboratory experiments are required to measure the mobility of a polymer solution in porous media. Polymer solutions including microemulsion complex with polymer are non-Newtonian fluids and their shear flow behaviors are always changing. In another word, their viscosities are shear rate dependent (Sorbie, 1991).

2.7 CO-SOLVENT

Co-solvents such as alcohols Disrupt interfacial structures to prevent the formation of gels and liquid crystals and promote rapid equilibration to low-viscosity microemulsion [(Snaz & Pope, 1995); (Lelanne-Casso, et al., 1983)]. Also, they decrease

the separation time and enhance the coalescence of microemulsion. Additionally, the use of co-solvents improves the adjustment of the optimal salinity of a formulation (Lelanne-Casso, et al., 1983).

Alcohol is used in many surfactant flooding formulations. There are many different types of alcohols with different properties. Some of the alcohols such as Methanol are relatively polar and very soluble in water while some types like hexanol are almost insoluble in water. The water-soluble alcohols make micellar to become more hydrophilic while the water-insoluble alcohols make system more lipophilic (Jones & Dreher, 1976). The differences in alcohol properties and the opinion regarding the effect of alcohol on surfactant flooding differ greatly among different authors (Salter, 1977).

Proper choice of co-surfactant has a big impact on micellar solution. Systems that are using methanol as the co-surfactant are usually sensitive to temperature. Glycerin usually makes thick micellar solutions and requires large quantities (Gogarty & Tosch, 1968).

Since at least there are three components in microemulsion – oil, water and surfactant – the phase behavior of the system must be specified at least with three members. Therefore it is convenient to use ternary diagram for compositional state of the system. If components presented in the system behave collectively, they can be considered as a single pseudo component to simplify the methodology and phase behavior calculation. Many of the phase behavior calculation consider surfactant and co-surfactant/alcohol as a single component. However, studies show that in some cases surfactant entirely is partitioned in microemulsion phase while alcohol is partitioned in significant fraction among phases or vice versa. Because of these observations, it is

recommended that for some cases the system should be treated with four components (Prouvost, et al., 1985).

Despite the role and effect of co-surfactants on oil recovery, very few systematic quantitative studies regarding their effects on chemical phase behavior and microemulsion phase properties have been done in the petroleum literatures.

2.7.1 Effect of co-solvent on phase behavior and optimal salinity

Both optimal salinity and the solubility of surfactant are affected by type and the amount of the alcohol (Salter, 1977). The relative solubility of alcohol plays the key role to its characterization. Some of researchers stated that alcohol increases the water solubility of the surfactant and decreases surfactant adsorption (Trushenski, et al., 1974) while some stated the alcohol reduces the viscosity of the microemulsion phase (Healy & Reed, 1974). Tosch et al. (1969) stated that effect of surfactant on alcohol partitioning is negligible. This observation was applied in the study by (Salter, 1977). For those types of alcohols that affected the optimal salinity, if the alcohol partitioned least in the oil it results in a great increase in the optimal salinity while if the alcohol partitioned most into the oil it decreases the optimal salinity the most. Also the height of multiphase region increases as the amount of alcohol increases which in turn results in a smaller amount of microemulsion phase at a given amount of surfactant. In addition to the above mentioned effects, the amount and type of alcohol changes the ranges of salinities that phase changes happen.

The phase behavior of a chemical flooding system is not simple since there are always more than three pure components and three or more phases in equilibrium in some part of multiphase regions. Adding co-surfactant to the system substantially alters the phase behavior, viscosity, and the micellar structure (Healy & Reed, 1974). In general,

co-surfactant reduces the micellar viscosity and order of magnitude in viscosity reduction is usual when 1 or 2 percent isopropyl or normal butyl alcohol is added (Gogarty & Tosch, 1968).

In a study by Jones and Dreher (1976) adding a small amount of 2-propanol (IPA) to a system consisting of an aqueous phase and a microemulsion phase caused the microemulsion phase to shrunk. The IPA expelled more water from the microemulsion phase while adding additional IPA resulted in a single phase system. The system remains a single-phase until IPA started to expel more hydrocarbons from the microemulsion phase. Figure 2.3 shows the phase boundary and the viscosity of the microemulsion phase for their study.

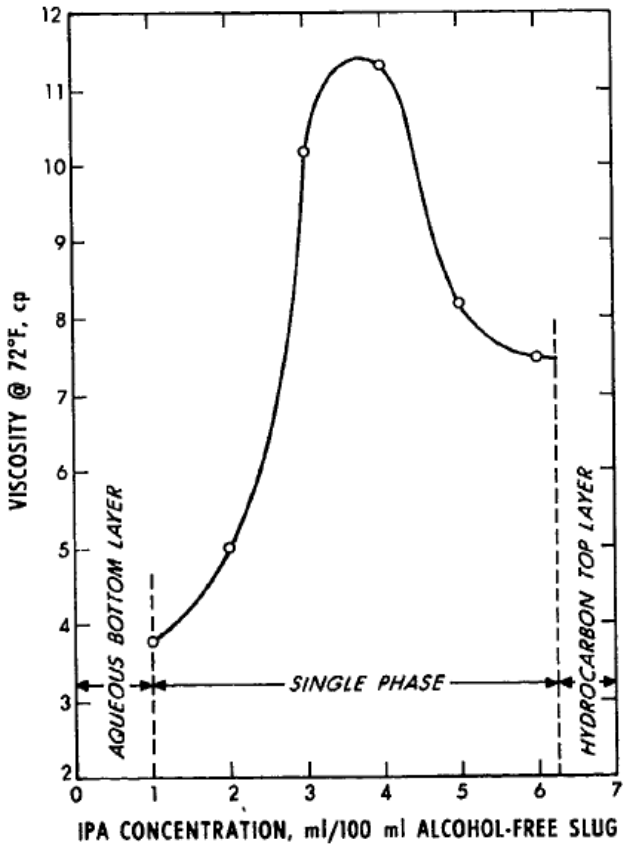

Figure 2.3: Viscosity of the system A in the single-phase region (Jones & Dreher, 1976)

The location of plait point is greatly affected by optimal salinity. The optimal salinity is the salinity at which the minimum concentration of surfactant is required to make a mixture of a single phase 50:50 water and oil. The minimum area of the multiphase region occurs at the optimal salinity.

The maximum oil recovery efficiency can be found at optimal salinity at which middle phase microemulsion has equal and very low interfacial tension with both oil and brine. The optimized surfactant formulation for a given crude oil can be achieved by the proper selection of surfactant and alcohol and the proper alcohol to surfactant ratio (Hsieh & Shah, 1977 Copyright 1976).

The study by Hsieh and Shah, (1977 Copyright 1976) shows that the optimal salinity increases with the increase in the chain length of n-alcohols. They also stated that the optimal salinity is higher in an oil/brine/surfactant/alcohol system if the alcohol solubility is higher. Their results also show that there is an optimal alcohol concentration that results in an ultra-low interfacial tension and solubilize the maximum amount of oil and brine. This optimal alcohol concentration is a function of optimal salinity.

2.7.2 Effect of co-solvent on microemulsion viscosity

The viscosity and phase behavior of microemulsion phase depends on salinity. As salinity increases, microemulsion phase undergoes the transition from Winsor's Type I to Type III or from Type III to Type II. The viscosity changes sharply at these phase transitions related to the phase volume (Figure 2.4). These phenomena suggest that the phase changes are sharp transitions (Healy & Reed, 1976).

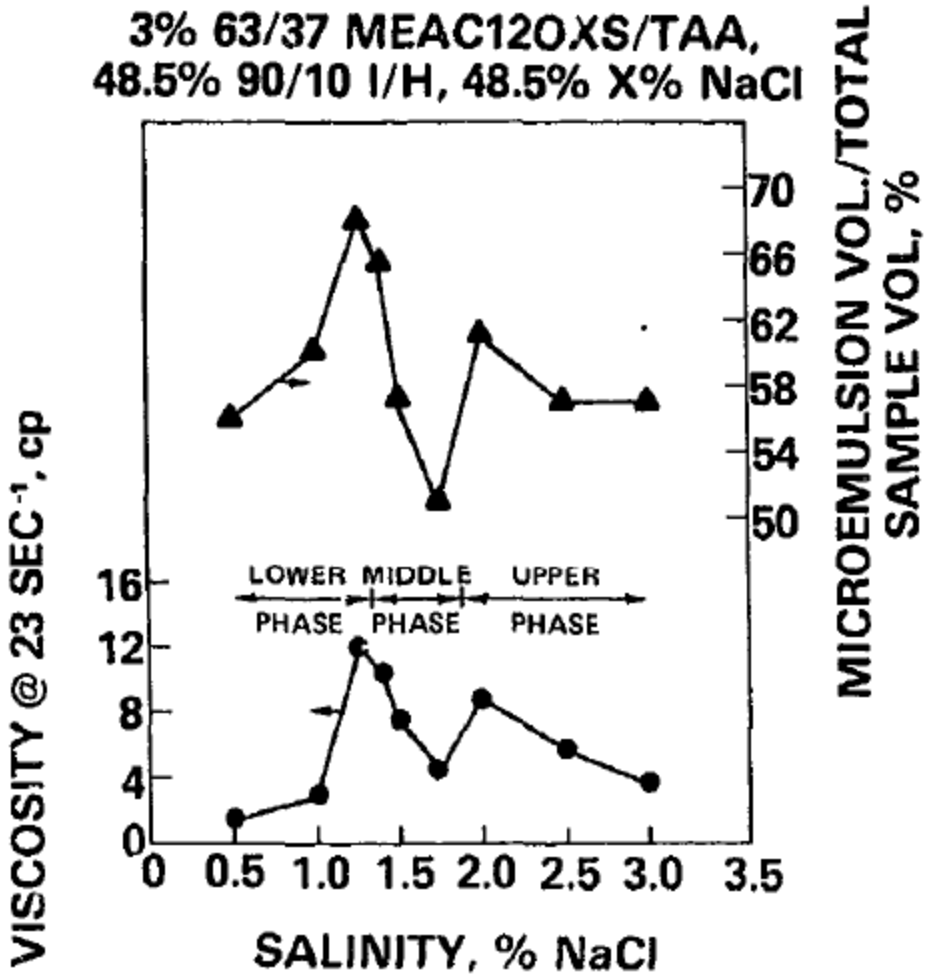

Figure 2.4: Microemulsion viscosity and volume (Healy & Reed, 1976)

Salter (1977) measured the viscosity of aqueous, oleic, and microemulsion phases at different shear rates and the reported values extrapolated/interpolated to shear rate of 10 s^{-1}. Based on his results, the viscosities of excess oil and water are independent of salinity. As salinity increases the microemulsion viscosity increases from a value less than the excess oil viscosity to a maximum value. The maximum viscosity occurs at salinity slightly greater than the salinity where the excess oil phase disappears. After this point, the microemulsion viscosity decreases as salinity increases (Salter, 1977).

The effect of alcohol on the microemulsion viscosity (Figure 2.5) can be summarized as follows (Salter, 1977):

- The maximum viscosity of the microemulsion phase decreases with the amount of alcohol
- The amount of alcohol does not affect the optimal salinity for TAA samples
- The increase in the amount of alcohol decreases the mass fraction of the microemulsion phase at any salinity
- The interfacial tension increases as the amount of alcohol increases at any salinity

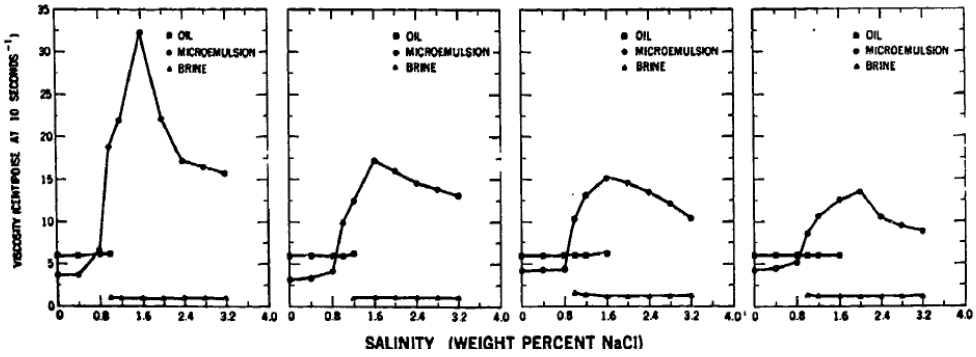

Figure 2.5: Microemulsion viscosity vs. salinity at different alcohol concentrations (Salter, 1977)

Salter (1977) stated that since the optimal salinity was independent of the amount of the alcohol, all of the above observations are resulted from the effect of alcohol on the system.

Laboratory results by Healy and Reed (1974) show that high viscosity appears everywhere in the system except toward the excess oil corner and there is a completely gel region toward the excess water corner. These very high viscosity regions in the ternary diagram limit the application of these compositions to tertiary oil recovery.

Adding amphiphilic components such as alcohol to the surfactant is one of the methods to reduce the viscosity (Healy & Reed, 1974). Adding 37 vol% tertiary amyl alcohol (TAA) to the surfactant for the case of 1% NaCl substantially reduced the single phase region viscosity. For their system, adding TAA increased the size of the water-external region in the ternary diagram. Alcohols that are more water-soluble produce lower-viscosity micellar slugs than the less water-soluble alcohols (Jones & Dreher, 1976).

The study by Chiang and Shah (1980) revealed that the interfacial tension and surfactant partitioning were not changed when isobutene was added to the system while the interfacial viscosity, oil drop flattening time, and displacement efficiency significantly affected by alcohol. The results show that the displacement efficiency increased as a result of adding iso-butanol to the formulation. Table 2.1 shows the effect of adding iso-butanol on various properties. They conclude that the rate of achieving the final value of interfacial tension was increased due to presence of alcohol which indicated that the surfactant is coming to the interface much faster in presence of alcohol.

Table 2.1: The Effect of IBA on Flattening Time, IFT, IFV, Partition Coefficient, and Oil Displacement Efficiency (Chiang & Shah., 1980)

SYSTEM	0.1% TRS 10-410 in 1.5% NaCl vs. n-Dodecane	0.1% TRS 10-410 + 0.06% IBA in 1.5% NaCl vs. n-Dodecane	0.05% TRS 10-80 in 1% NaCl vs. n-Octane	0.05% TRS 10-80 + 0.04% IBA in 1% NaCl vs. n-Octane
Run	S100-48	S100-43	S100-02	S100-44
Flattening Time	90 sec	< 1 sec	420 sec	< 1 sec
IFT (dynes/cm)	0.086	0.088	0.025	0.024
Interfacial Viscosity (s.p.)	0.096	0.086	0.023	0.018
Partition Coefficient	0.010	0.009	0.3	1.36
Secondary Recovery				
By Brine Flooding	-	-	61.2%	60.08%
By Surfactant Soln Flooding	84.37%	98.32%	60%	91%
Tertiary Recovery	-	-	0	76.84%
Final Oil Saturation	11.73%	1.28%	30%	5.36%

2.8 ALCOHOL PARTITIONING

For alcohols that are soluble in water, the fraction of alcohol partitioned in oil phase increases with increase in brine salinity. This effect is expected because the increase in brine salinity decreases the fraction of alcohol in brine phase which in turn increase the fraction of alcohol in oil phase (Salter, 1977).

According to (Hsieh & Shah, 1977 Copyright 1976) the assumption that alcohol only present in surfactant rich phase is not a valid assumption but it is a convenient assumption and does not have a significant effect on solubilization behavior.

Chapter 3: Methodology and Data Analysis

The viscosity of a solution is considered as a characteristic of its internal consistency. The experimental methodology is presented in this chapter. Microemulsion viscosity measurements are reported for solution prepared with commercial surfactants and a new viscosity model is introduced to better simulate the viscosity behavior. In most of the cases viscosities were measured with ARG2 Rheometer as a function of salinity. Accurate viscosities were then measured at different shear rates with an environmental chamber designed to control both temperature and evaporation.

3.1 EXPERIMENTAL EQUIPMENT

This section describes experimental equipment used in phase behavior screening and the microemulsion rheological measurements.

Borosilicate Pipettes

Fisherbrand standard 5 ml borosilicate pipettes with 5 mm inner diameter and 0.1 ml markings were used to hold fluid volumes for phase behavior experiments. The end of the pipettes were sealed using a Benzomatic Torch.

Pipette Repeater

The Eppendorf Repeater Plus dispenser was used to dispense the required amount of the solution or crude oil volumes into the borosilicate pipettes. Plastic tips were used in the dispenser and were disposed after use with one fluid.

Oxygenated Propane Torch

After the fluid is dispensed into the Pipettes, an oxygenated propane torch was used to flame-seal the pipette ends. The pipette ends would melt and mold together to seal after the exposure to the flame.

Water Deionizer

A Nanopure filtering system was used to remove all particulates to 0.45 microns from water in the water deionizer. The filtration of water continues until the resistivity of water shows that all ions are removed. All solutions including surfactant stock, polymer stock, and co-solvent stock were prepared using the deionized (DI) water.

Convection Ovens

To heat up the samples and preserve the consistency of the temperature for the phase behavior samples, convention ovens were used.

3.1.1 Phase Behavior Screening Description

Microemulsion phase behavior tests were used to evaluate the surfactant, co-surfactant, and co-solvent formulation. The formulation of the solution was varied by changing the concentration and the ratio of the components for each desired crude oil. Aqueous stability tests were also performed to find the salinity at which the solubility limit was reached. This is important since the surfactant solution needs to be stable up to at least the optimum salinity.

3.1.2 Samples solution preparation

Several experiments were conducted to study microemulsion viscosity behavior. These experiments generally included following steps: electrolyte mixtures with crude oil, the stock solution, observing the emulsions, recording properties and calculating the parameters.

Electrolytes and Brines

The electrolytes and brine stocks were mixed by weight in deionized water. Synthetic brines were created as surrogates for the field formulation for making the scan. To make the scan, brine solutions were diluted to necessary weight percent concentration. In order to observe the phase behavior over a range of salinities, different concentrated mixtures were used for a particular field application.

Surfactant Stock

A concentrated surfactant stock usually consisted of a primary surfactant, co-surfactant, and/or co-solvent mixed in deionized water. The mass of chemicals was calculated based on their activity and measured by the weight percent. The activity of the surfactant is provided by manufacturers as % (w/v) assuming density was equal to one g/mL. The order of addition was recorded on a mixing sheet.

Polymer Stock

Polymer stock was prepared at the desired concentration in NaCl solution. The NaCl solution was mixed with a stir bar and the dried polymer powder were sprinkled slowly to the shoulder of the vortex. The air on top of the solution was displaced by Argon and the container was covered. The polymer solution was continually stirred for more than 24 hours.

3.2 SET UP PROCEDURE

The phase behavior components were added volumetrically into the graduated 5 mL pipettes that were flame-sealed at their bottom. The components were dispensed in the following order: varied electrolyte, constant electrolyte, deionized water, surfactant and co-solvent stocks, and polymer stock. The air bubbles trapped at the bottom of the pipettes were tapped out before reading the initial interface of the samples. The aqueous fluid level in each pipette was recorded after that. Depending on the desired water-oil-ratio (WOR) crude oil was dispensed into the pipettes. Before sealing the pipettes, they were covered with argon gas to displace volatile gas. Using a propane-oxygen torch the pipettes were sealed and arranged in a rack to be transported to the convention ovens as displayed in Figure 3.1.

Figure 3.1: Pipette Racks Maintained at Reservoir Temperature in the Oven

The oven was set to the reservoir temperature for the crude oil being tested. After about 20 minutes the pipettes were inverted several times to mix the solution. Then, solutions were left in the oven so that they equilibrate. The fluid interface levels were recorded at increasing time intervals, such as 1 day, 3 days, one week, two weeks, and one month. In some cases, the equilibration time varies and it might be required to record the readings after 2-3 months as well.

3.3 INTERPRETATION AND MEASUREMENT

Phase behavior formulations were evaluated to pass the following criteria to be considered for testing in a core flood experiment: ultra-low IFT, high solubilization ratio, low microemulsion viscosity, aqueous phase stability, short equilibration time, good interface fluidity, and absence of gels or macroemulsions. Longer equilibration time is usually accompanied with the formation of gels and creation of macroemulsion which undesirable since their fluidity gets slow in the reservoir condition especially with low pressure gradient.

The measurements of the top and bottom interfaces were recorded for the solubilization ratio calculation.

3.3.1 Solubilization Ratio

The oil and water volumes are recognized from the readings of the initial aqueous and oil interface. After mixing the samples of the phase behavior and reading the interfaces, the volumes of the oil and water in the microemulsion can be recognized.

Oil Solubilization Ratio

The oil solubilization ratio σ_o is the volume of oil present in the microemulsion phase per volume of total active surfactant. The equation is:

$$\sigma_o = \frac{V_o}{V_s} \tag{3.1}$$

where V_o is the oil volume present in the microemulsion and V_s is the total surfactant volume present in the microemulsion phase. All the surfactant is assumed to be present in the microemulsion for the V_s calculation (i.e. corner plait point). The oil solubilized by the microemulsion, V_o, should be estimated based on the initial and top interface levels.

Water Solubilization Ratio

Water solubilization ratio, σ_W, is the volume of water present in a microemulsion per volume of total surfactant present in the sample. The equation is:

$$\sigma_W = \frac{V_W}{V_S} \tag{3.2}$$

where V_w is the water volume present in the microemulsion and V_s is the total surfactant volume present in the microemulsion phase.

Optimum Solubilization Ratio

The solubilization value where the oil and water solubilization ratios are equal is called the "Optimum Solubilization Ratio". The corresponding salinity at the optimum solubilization ratio is referred to as the "Optimal Salinity". Microemulsion at the optimum salinity is in the middle of the Winsor Type III microemulsion.

Higher solubilization ratios at optimum salinity are desirable in order to achieve lower interfacial tension (IFT) and to mobilize the trapped oil.

3.3.2 Interfacial Tension

(Healy & Reed, 1976) developed a correlation between oil and water solubilization ratio and interfacial tension between the microemulsion and each phase. Later, Huh (1979) developed a theoretical equation between the optimum salinity and the interfacial tension. According to Huh, the IFT, γ, is calculated as follows:

$$\gamma = \frac{C}{\sigma^2} \tag{3.3}$$

where C is approximately 0.3 dynes/cm and σ is the optimum solubilization ratio. According to Huh, a solubilization ratio of 10 or greater corresponds to an IFT of 0.003 dynes/cm or lower. Usually, the IFT necessary to recover the residual oil is aimed to be around this number.

When surfactant solution replaces the water phase, the residual oil becomes mobilized. This happens when the IFT between the residual oil and the aqueous phase is reduced. Surfactants that work well usually lower the IFT to 10^{-3} dynes/cm and reduce the capillary pressure greatly.

3.4 MICROEMULSION VISCOSITY MEASUREMENTS

The microemulsion samples were prepared in 20 ml tubes so that they could be used for viscosity measurements in the rheometer. The samples were with the same weight percent of the components represented in the phase behavior tests but in a larger volume. After checking the phase behavior tests and choosing the ones that are working well, the larger samples were prepared to be used for the viscosity measurement.

3.4.1 Microemulsion Rheology Testing Description

The following section describes the procedure performed to complete the rheological analysis of the microemulsion. The process begins with the preparation of a microemulsion sample. After preparing the samples, they were allowed to equilibrate in the oven. When equilibrated which usually took about 2-3 weeks, the sample were extracted for rheological measurements. Then, the rheological data were analyzed to investigate the trends of the microemulsion viscosity.

Sample Preparation

For the purpose of this research, the samples were made in 20 ml tubes and the extractions were done on all of the phases formed. Samples were extracted for the entire salinity scan that was prepared for each formulation. The components were injected in the same order that the components of the phase behavior samples were dispensed. After

dispensing the fluid, the tubes were covered by their caps and were located into the oven for equilibration.

Equilibration

The microemulsion samples were located in the oven to heat up and to equilibrate. Usually, the equilibration of the 20 ml samples would take more time than the phase behavior pipettes. After equilibration, the interfaces between the water, oil, and micellar solution were becoming distinct.

Phase Extraction

Once fully equilibrated microemulsion sample were ready for extraction. The sample was removed from the oven and the tube was kept still and vertical so not to mix the interfaces between the micellar solution, oil, or water. After removing the cap of the tube, the samples were extracted from oil, microemulsion, and water phases. Removing the excess oil phase from the top phase helps minimize contamination to the middle phase and the bottom phase during this stage. To prevent conning effect during the extraction of the middle phase, it is important to control the rate at which the middle phase is removed by the pipette. Finally, the bottom phase was extracted and transformed into the tub.

If there were Type I or Type II, the extractions were performed on the oil and the aqueous phases. If the tube was a Type III microemulsion, three small samples were extracted from all three phases. The extraction was performed using small pipettes which were made of glass and the small samples were transformed into small tubs to be ready for using in the rheometer.

3.4.2 Microemulsion Viscosity Measurements

After extracting the microemulsion samples, the samples were injected onto the ARG2 rheometer plate. The rheometer was set so that the viscosity of the small samples could also be measured. The samples had to be about 1 ml so that when the spinning bob was moved down, the bottom of the bob was entirely covered by the sample. The temperature of the rheometer was set to be 60 degree Celsius. The rheometer was attached to a computer and the machine was controlled by using the ARG2 viscometer software. After each measurement, the viscometer had to be cleaned to be used for the next sample. All the measurements were copied in the computer to be collected for analysis.

ARG2 VISCOMETER

Most of the bulk viscosity measurements were taken using ARG2 rheometer (Figure 3.2). The ARG2 rheometer is a combined motor and transducer instrument (CMT) type viscometer that analyzes shear stress between a spinning bob and a plate. The lower component of the measuring system is fixed, while the upper component is attached to a shaft that can be rotated by a torque produced by an induction motor. The instrument was designed to measure viscosities over a shear range of 0.001 to 100 sec^{-1} and required about 1 mL to operate properly. The stress is exerted on a thin wire that connects to the bob and the measurement is then converted into a viscosity.

Figure 3.2: ARG2 rheometer (Costello, 2005)

Chapter 4: Experimental Results

This chapter describes the design and performance of several different surfactant formulations that were used to develop and verify a new viscosity model for the microemulsion phase.

4.1 MICROEMULSION RHEOLOGY

Experiments were performed to measure the microemulsion viscosity of the surfactant formulations. The samples were prepared following the procedure described in Section 3.4.2. The results and analyses of these samples yielded important insight into microemulsion rheology in all types of phase behaviors.

4.1.1 AO 41-50 Data Set

In this section, we investigate the microemulsion viscosity for a surfactant formulation with the softened formation brine (formation brine without Ca and Mg). The solution mixture was formed with 0.75% TDA-13PO-SO4 as a surfactant, 0.25% C20-24 IOS as a co-surfactant, 0.75% IBA as a co-solvent, 0.5% Na_2CO_3 and scanned with 0.0-2.5 wt% NaCl. The oil used in this study is referred to as AO. Table 4.1 and Table 4.2 give the compositions of formation brine (FB) and synthetic formation brine (SFB) used in this experiment. Figure 4.1 shows the phase behavior of the surfactant formulation in soft brine.

There are a total of 10 samples at different salinities. Table 4.3 gives a summary of these samples. The viscosity is measured for all phases within a tube at different shear rates. The oil and microemulsion viscosities reported in Table 4.3 are the Newtonian viscosities for each phase. Among the 10 samples, the first 7 samples (salinity range from 0.0% - 1.5%) are Type I phase behavior and the last 3 samples (salinity range from

1.75% - 2.25%) are Type III phase behavior. As it is shown in Table 4.3, the microemulsion phase viscosities for samples with Type III phase behavior are much higher than the microemulsion phase viscosities of samples with Type I phase behavior.

A clear change in rheological behavior of the microemulsion is evident in Table 4.3 and from the microemulsion viscosity vs. salinity at different shear rates (Figure 4.2). To characterize the rheological properties of each phase we tried to match the measured viscosity in the lab with the viscosity model in UTCHEM. Liquid phase viscosities are modeled in terms of pure component viscosities and the phase concentrations of the oil, water, and surfactant as:

$$\mu_l = C_1 \mu_w e^{\alpha_1 (C_{2l} + C_{3l})} + C_{2l} \mu_o e^{\alpha_2 (C_{1l} + C_{3l})} + C_{3l} \alpha_3 e^{(\alpha_4 C_{1l} + \alpha_5 C_{2l})} \quad (4.1)$$

where the α parameters are determined by matching measured microemulsion viscosities at several compositions. In the absence of surfactant and polymer, water and oil viscosities reduce to pure water and oil viscosities (μ_w, μ_o). When polymer is present, μ_w is replaced by μ_p.

Matching experimental viscosity measurements using the above correlation is a big challenge and may not be possible in some cases. As the first step to match the viscosity, we tried to match the lab phase behavior using the phase behavior excel spreadsheet. Figure 4.3 shows a reasonable match between lab results and the model (Hand's Rule).

We used two sets of data to match the viscosity model presented in Eq. (4.1); one set is the lab measurements at the low shear rate (shear rate 1 sec^{-1}) and for the second set, we collected the viscosities at which there is no shear rate dependency (Newtonian

portion of the data). The water and oil viscosities of 1.3 cp and 14.4 cp are used in the calculation.

Figure 4.4 shows the match for the first set (viscosities at low shear rate) and Figure 4.5 shows the match for the second set (viscosities at which there is no shear rate dependency). Both results show that the viscosity model in Eq. (4.1) cannot match the lab results.

The lab results show that the microemulsion viscosities for the Type III phase behavior are significantly higher than the ones with Type I phase behavior. The low viscosity portion is where we have a two-phase system (Type I in this case). Once the third phase is formed, the viscosity of the microemulsion phase is extremely high. This enormous viscosity of microemulsion phase in Type III is an indication that the rheological properties of microemulsion phase in Type III system is very different than that in Type I. When there is a change from a two-phase to a three-phase behavior, we may need to develop either a different viscosity model or use different parameters in the current model corresponding to the phase behavior transition. A new viscosity model that addresses the rheological characteristic of microemulsion phase consistent with the phase behavior is the subject of this thesis.

In the following sections, we analyze the viscosity measurements of all phases in order to better understand the rheology of microemulsion phases in different types of phase behavior.

Oleic Phase Viscosity

Figure 4.6 shows the viscosity of oil and the three equilibrium phases at optimum salinity. The oil viscosity is independent of the shear rate (i.e. Newtonian). Another observation from Figure 4.6 is that the top excess oil viscosity is almost equal to the pure

oil viscosity. The middle phase and bottom aqueous phase viscosities are shear rate dependent. The middle phase viscosity is about 2 to 3 times more viscous at the ranges of 1-10 sec^{-1} shear rates.

An interesting observation is that the oleic phase viscosity in samples with Type I phase behavior is independent of shear rate and salinity, and is the same as pure oil viscosity (Figure 4.7). However, in samples with Type III phase behavior, the top phase (oleic phase) viscosity is shear rate dependent (Figure 4.8). This could be due to small presence of surfactant in the oleic phase or sample contamination.

Microemulsion Phase Viscosity

Similar to oil viscosity, the microemulsion viscosity shows different behavior for different ranges of salinity. One interesting observation that needs more attention is that the last three samples (AO 48-50) that are three phase samples (Type III), show extremely high microemulsion viscosity compared to other samples. The microemulsion viscosities in these samples are in the range of 100 cp to 300 cp compared to about 1 cp in other samples.

Lab results show that for sample with Type I phase behavior, microemulsion viscosity becomes almost independent of shear rate (Figure 4.9). The low shear rate data show inconsistency which could be due to measurement error at low shear rate.

To further investigate the rheology of the microemulsion phase for samples with Type I phase behavior, we plotted the viscosity of microemulsion phase vs. salinity at different shear rates (Figure 4.10). The results show that the viscosity increases as salinity increases and there is a linear trend in microemulsion viscosity vs. salinity for sample with Type I phase behavior. We use this observation to develop a new viscosity model for the microemulsion phase (bottom phase) for samples with Type I phase behavior.

At higher salinities (where three phases coexist), the microemulsion phase viscosity shows a shear thinning behavior. It seems that when the salinity is close to the lower salinity limit, the microemulsion viscosity is extremely high and shows more shear thinning behavior. Increasing salinity toward upper salinity reduces both the viscosity and its shear thinning behavior (Figure 4.11).

Microemulsion phase viscosities for samples with Type III phase behavior show a parabolic type of behavior. The viscosity increases with salinity and reaches a maximum and then decrease to another low value (Figure 4.12). We will develop a new viscosity model for microemulsion phase for samples with Type III phase behavior based on the above observations.

Table 4.1: Formation brine (FB)

Ion	**Concentration (ppm)**
Ca^{++}	180
Mg^{++}	70.5
Na^{+}	8027.8
K^{+}	101
HCO_3^{-}	893
Cl^{-}	12438
Total	21,272.50

Table 4.2: Synthetic formation brine (SFB)

Ion	**Concentration (ppm)**
Ca^{++}	0
Mg^{++}	0
Na^{+}	8027.8
K^{+}	101
HCO_3^{-}	893
Cl^{-}	12000
Total	21,022

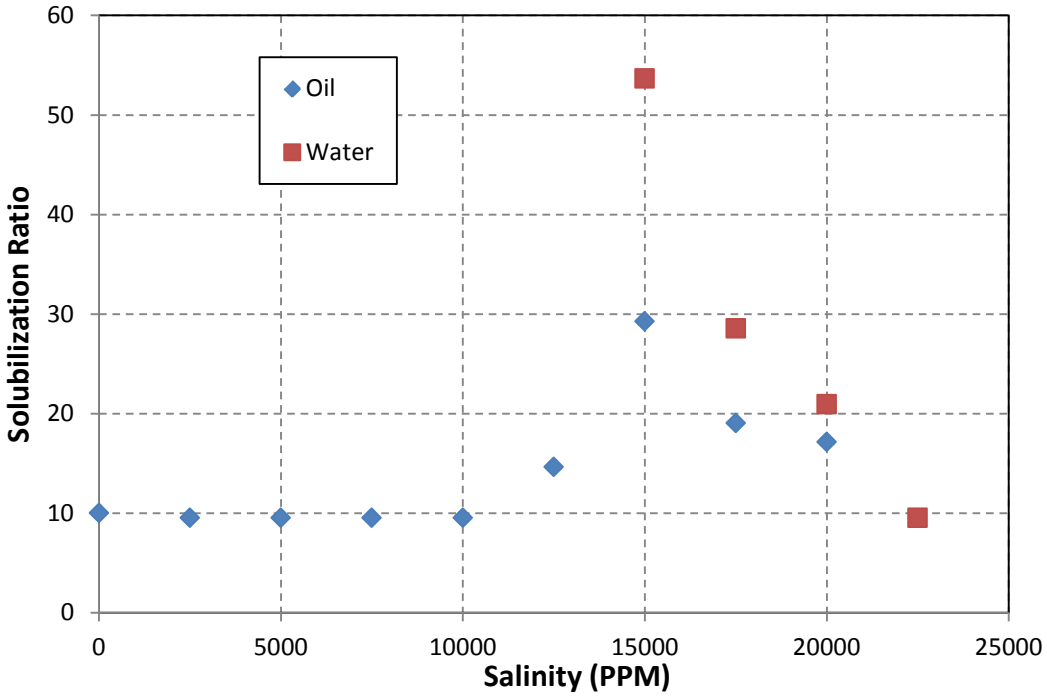

Figure 4.1: Phase behavior with 0.375% TDA-13PO-SO4, as a surfactant, 0.125% C20-24 IOS as a co-surfactant, 0.75% IBA as a co-solvent, 0.5 % $Na2CO_3$ and scanning with 0-2.5% NaCl.

Table 4.3: Summary of AO samples and the type of phase behavior for each sample.

Name	Salinity	Phase Type	Water Viscosity	Oil Viscosity	ME viscosity
AO-41	0.00%	I		11.5	1.20
AO-42	0.25%	I		11.5	1.20
AO-43	0.50%	I		11.4	1.66
AO-44	0.75%	I		11.6	2.00
AO-45	1.00%	I		11.8	2.30
AO-46	1.25%	I		11.1	2.40
AO-47	1.50%	I	5	13.8	
AO-48	1.75%	III	1.3	13.1	60
AO-49	2.00%	III	1.1	12.5	173
AO-50	2.25%	III	1.1	9.8	72

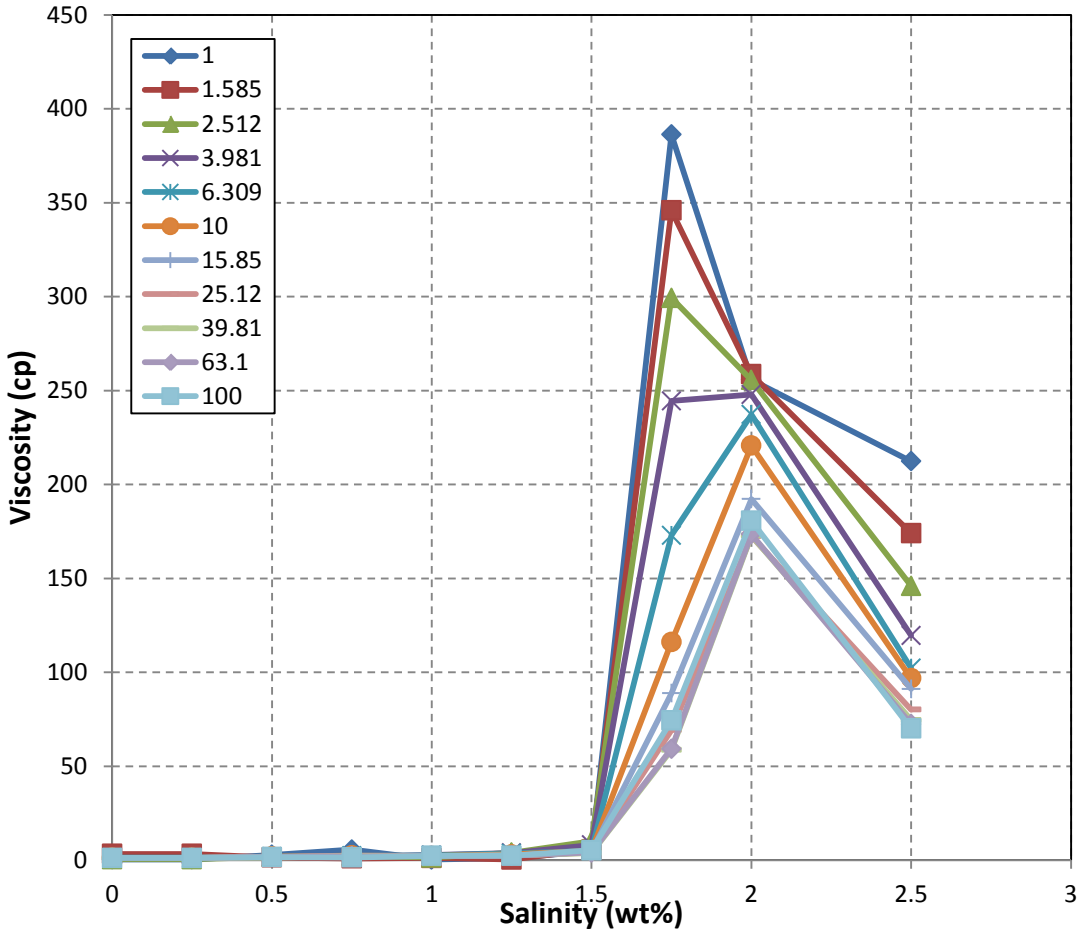

Figure 4.2: AO 41-50 microemulsion viscosity vs. salinity at different shear rates (in s^{-1})

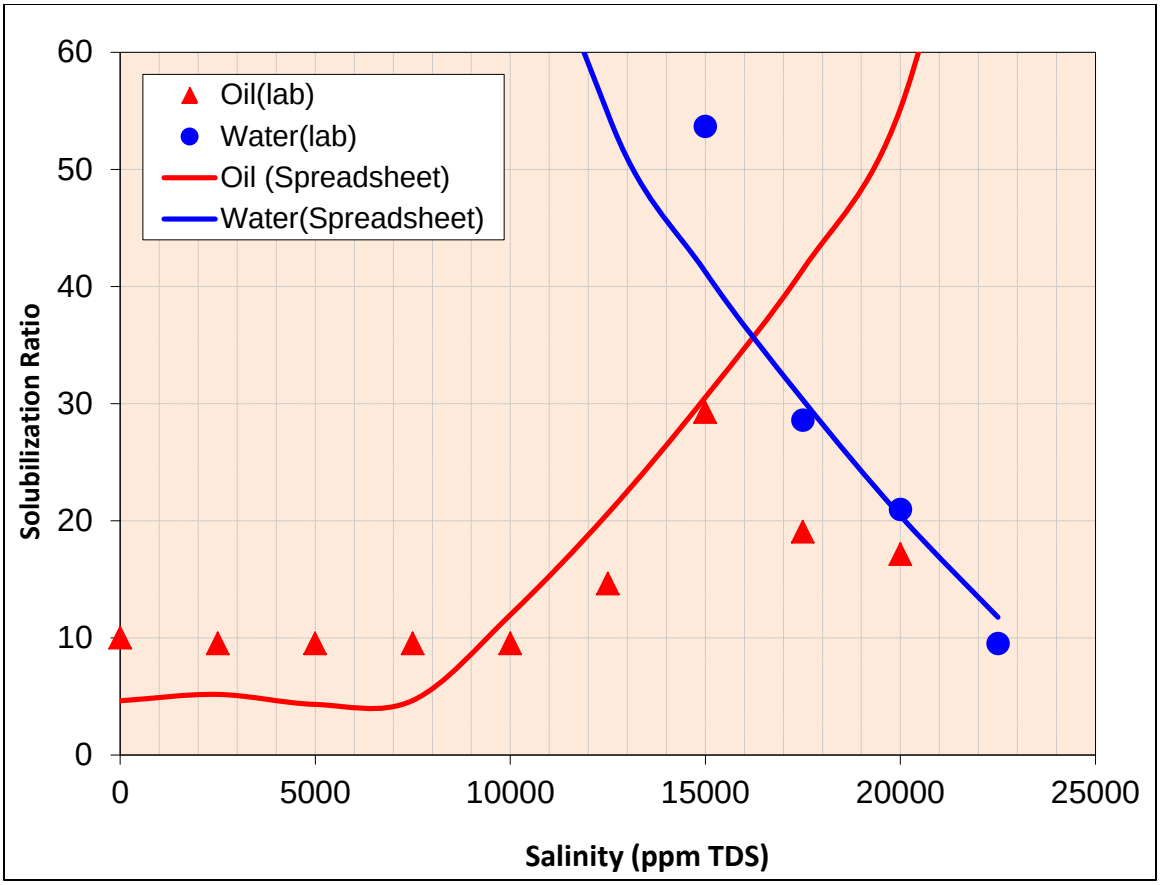

Figure 4.3: Match of solubilization ratios for AO 41-50 samples

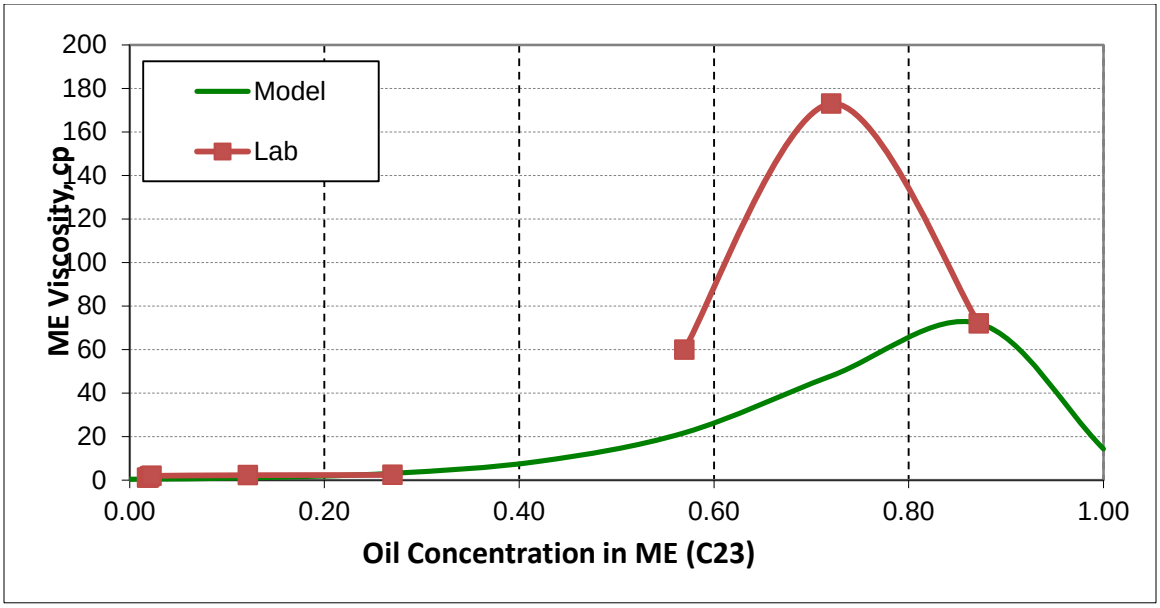

Figure 4.4: Viscosity match (Model vs. lab data) at shear rate of 1.0 $s^{-1}$for AO 41-50

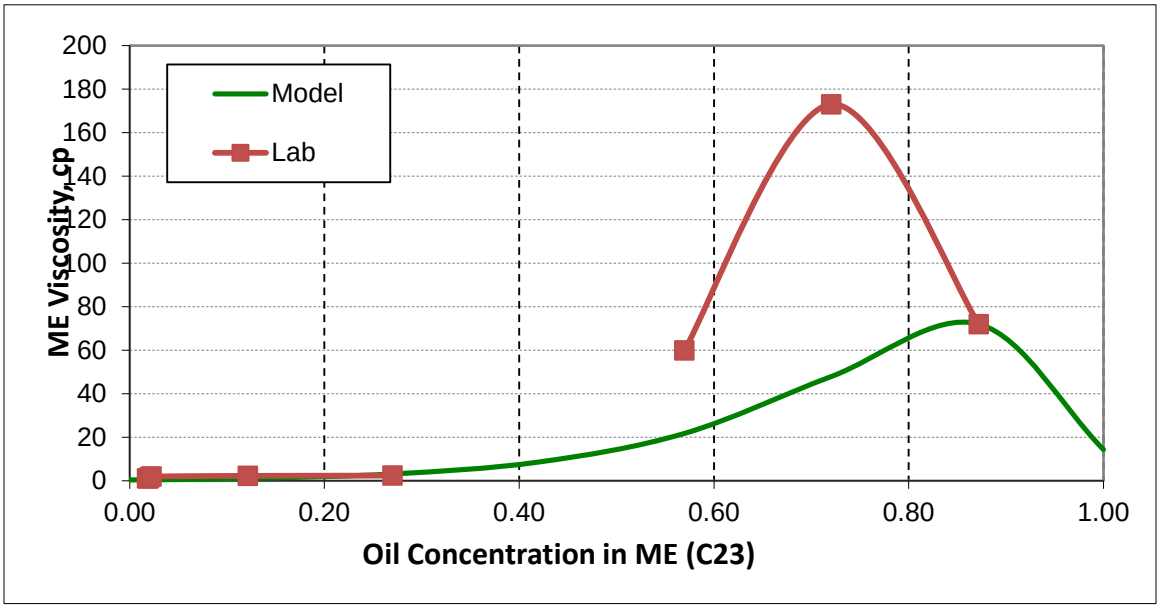

Figure 4.5: Viscosity match for the Newtonian viscosity of AO 41-50 samples

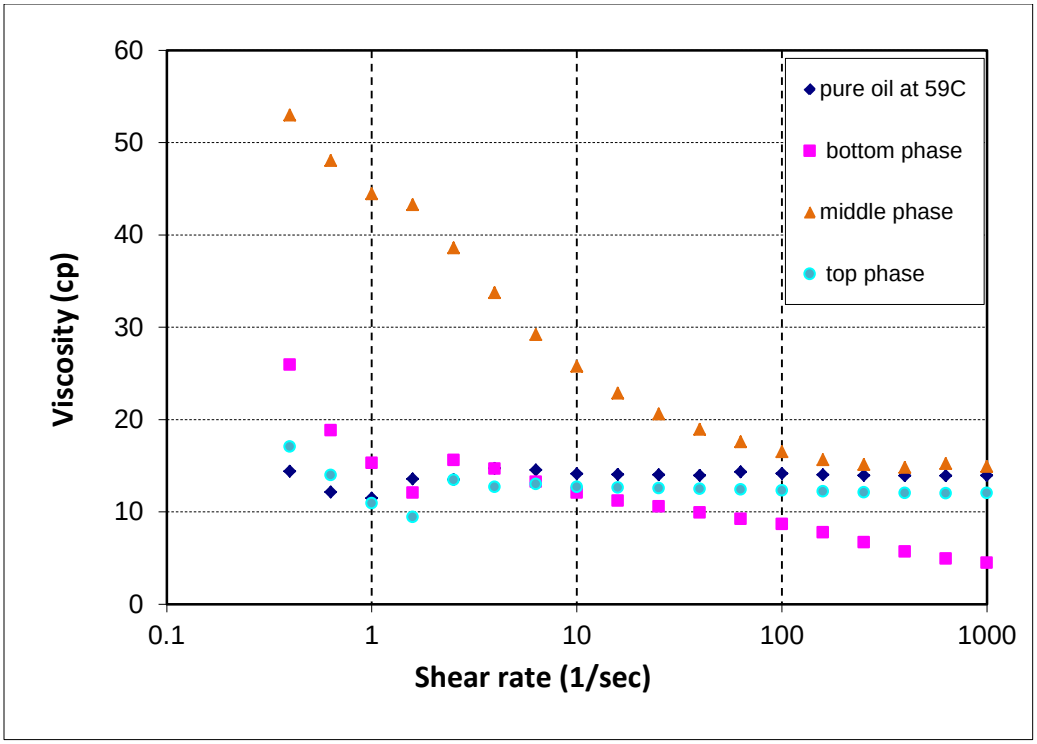

Figure 4.6: Viscosity of pure oil and three equilibrium phases at optimum salinity of 0.3025 meq/ml vs. shear rate

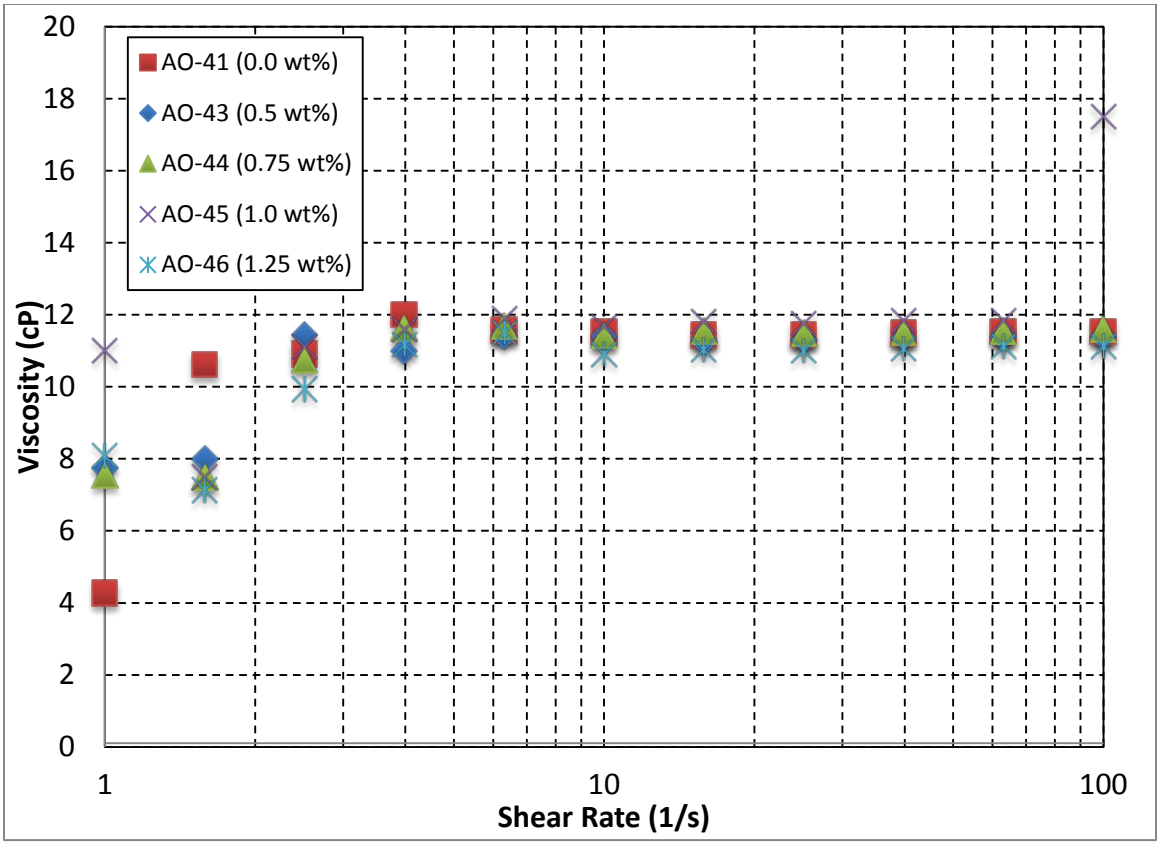

Figure 4.7: Top phase viscosity (oleic phase) vs. shear rate for samples with salinity in Type I phase behavior (AO 41-46)

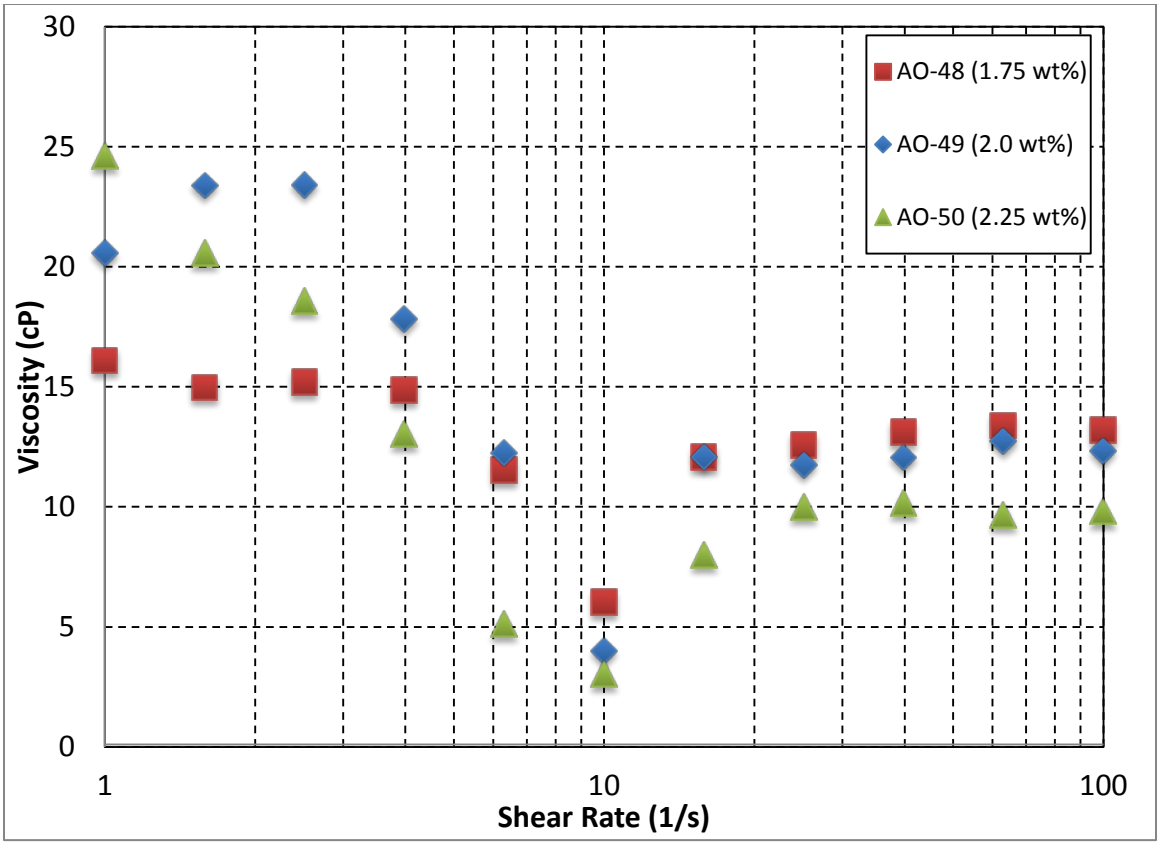

Figure 4.8: Top phase viscosity (excess oil phase) vs. shear rate for samples with salinity in Type III phase behavior (AO 48-50)

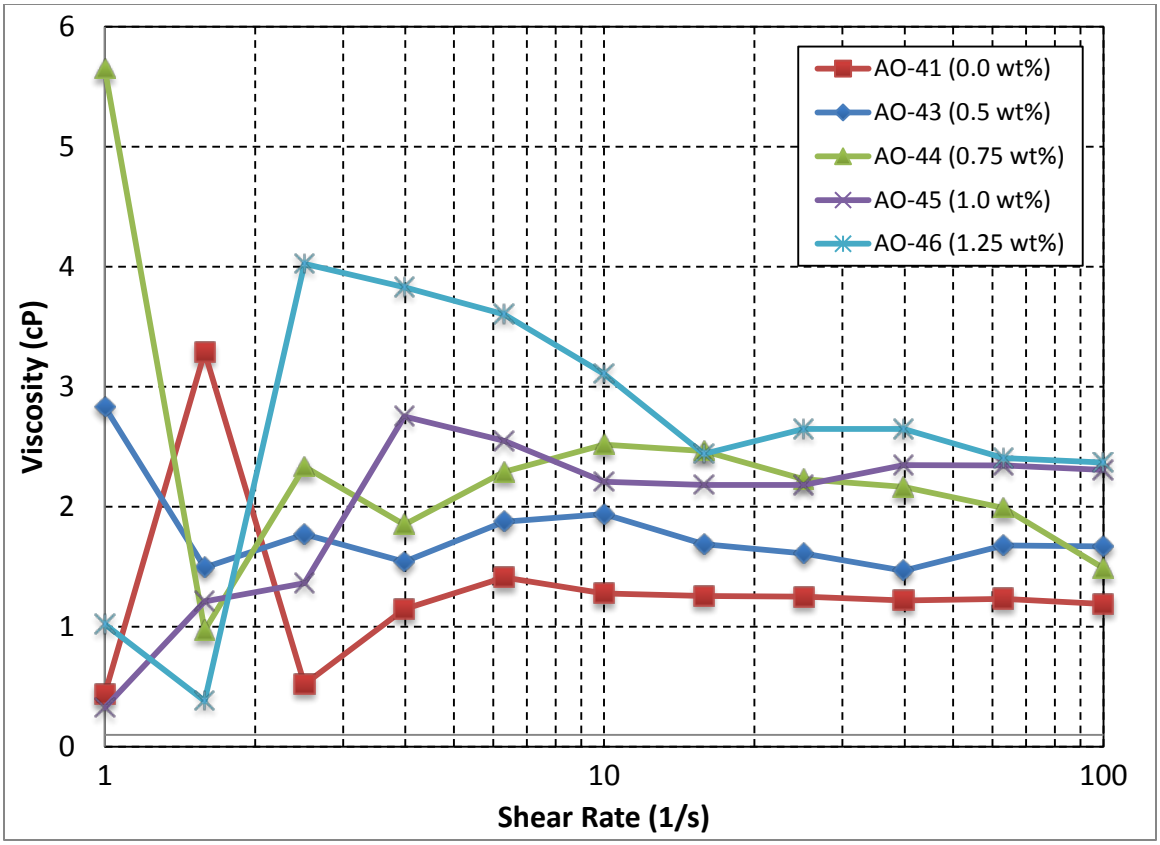

Figure 4.9: Microemulsion phase (bottom phase) viscosity vs. shear rate for samples with salinity in Type I phase behavior (AO 41-46)

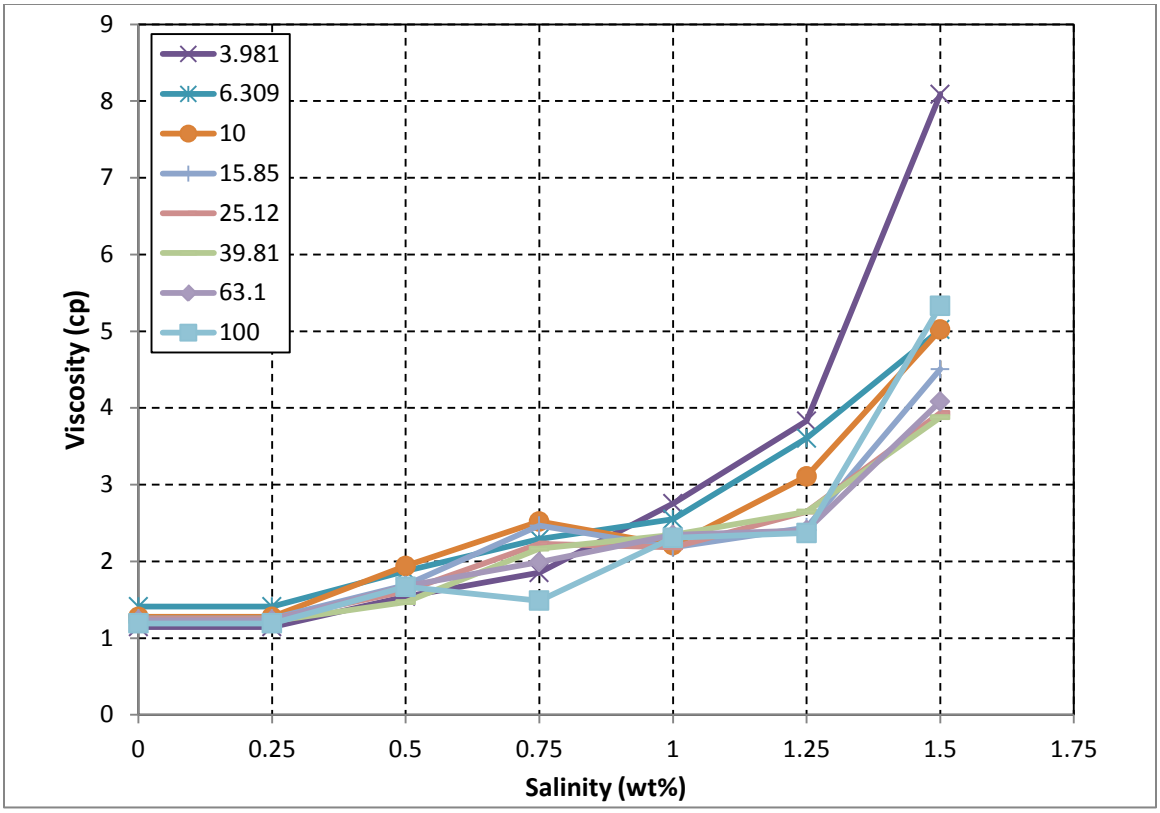

Figure 4.10: Microemulsion phase (bottom phase) viscosity vs. salinity for samples with Type I phase behavior shown at different shear rates in s^{-1}.

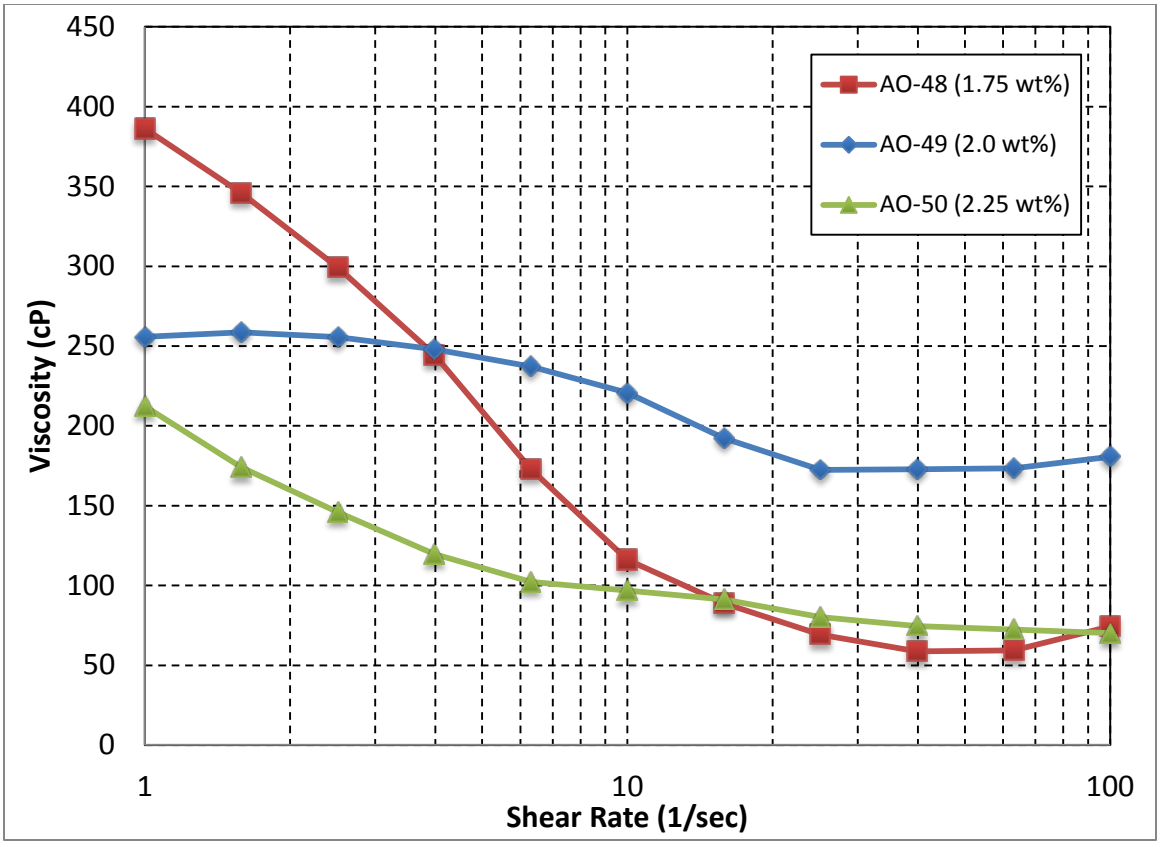

Figure 4.11: Microemulsion phase (middle phase) viscosity vs. shear rate for samples with salinity in Type III phase behavior.

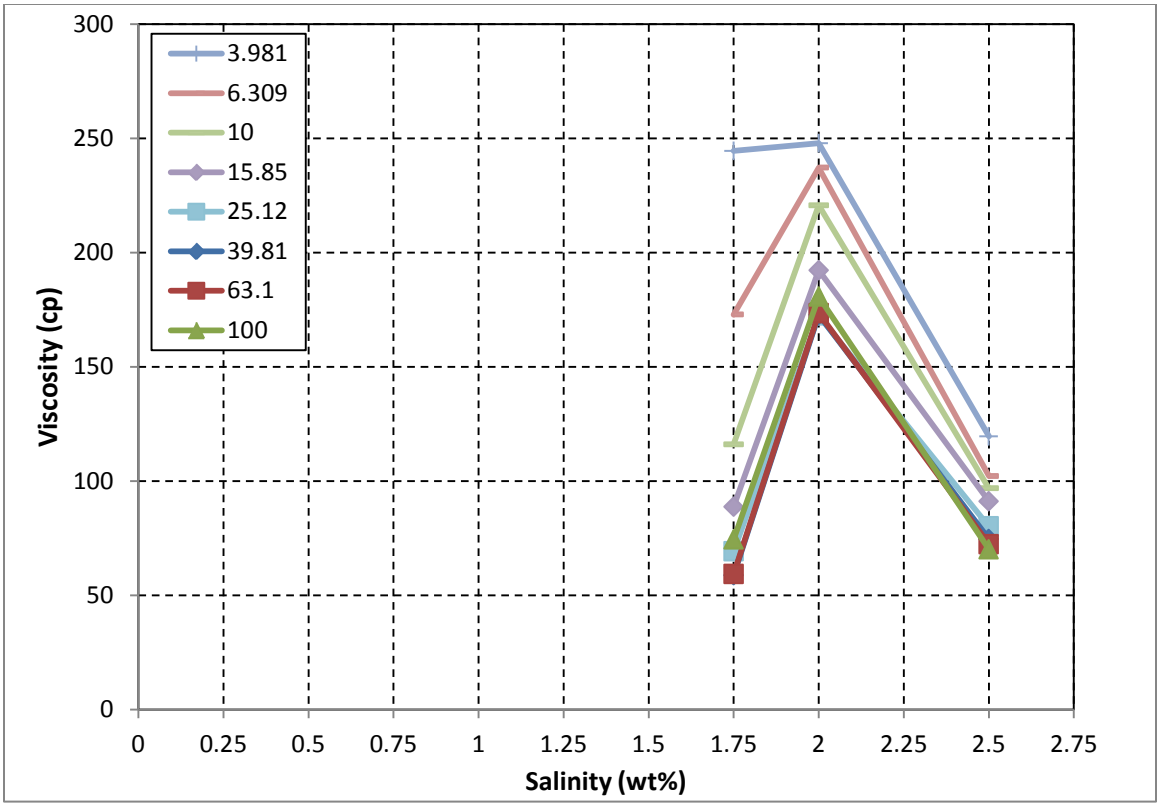

Figure 4.12: Microemulsion phase (middle phase) viscosity vs. salinity for samples with Type III phase behavior measured at different shear rates in s^{-1}.

4.1.2 AO 352 Data Set

In this section, we investigate the microemulsion viscosity for another surfactant formulation with the softened formation brine (formation brine without Ca and Mg). The solution mixture was formed with 0.375 wt% TDA-13PO-SO4 as a surfactant, 0.125 wt% C20-24 IOS as a co-surfactant, 0.75 wt% IBA as a co-solvent, 0.5 wt% Na_2CO_3 where the salinity scan was conducted with 0.0-2.5 wt% NaCl. The oil used in this study is referred as AO oil.

We have a total of 10 samples at different salinities. Table 4.4 shows a summary of these samples. In this data set, we have all three types of phase behavior (Type I, Type

II, and Type III). For each sample, we have measured the viscosity of each phase in the pipette at different shear rates. Table 4.5 through Table 4.7 give the phase viscosity in each test tube. We will use a similar approach used in previous section to analyze the viscosity data.

Water viscosity in all samples of Type II and Type III is about 0.5 cp. There is only one sample (sample with 1% salinity) that shows water viscosity twice as other sample. This could be due to some contamination during extracting the phase from the tube.

The excess oil phase viscosity in samples with Type I is about 13-14 cp. The first two test tubes in Type III also show the same oil viscosity but test tubes with salinity 1.5% and 1.75% have excess phase oil viscosity similar to that of microemulsion phase. One assumption is that these samples are contaminated during phase extraction (microemulsion phase may be extracted with the oil phase). This observation again confirms that the excess oil phase viscosity (top phase) in test tubes with Type I and Type III phase behavior is the same as pure oil viscosity.

Microemulsion Phase Viscosity

Type I test tubes show an increasing linear trend in viscosity with salinity (provided we remove samples with low shear rates where some measurements are in error). Type III test tubes show a parabolic type behavior. For Type III test tubes, the viscosity increases with salinity and reaches a maximum and then decreases to another low value. We have seen similar behavior for AO 41-50. Figure 4.13 and Figure 4.14 show viscosity of microemulsion phase for test tubes exhibiting Type I and Type III phase behaviors vs. salinity. Figure 4.14 also shows that the microemulsion viscosity for Type III phase behavior is highly affected by shear rate with power law behavior.

We only have two tubes with Type II phase behavior which limits us on drawing a solid conclusion but it is seen that the viscosity stays almost constant or have a linear trend with salinity for these type of phase behavior (Figure 4.15).

Table 4.4: Phase behavior types for AO 352 formulation

Salinity (wt% NaCl)	Type
0.00%	I
0.25%	I
0.50%	I
0.75%	I
1.00%	III
1.25%	III
1.50%	III
1.75%	III
2.00%	II
2.25%	II

Table 4.5: Top phase viscosity measurements vs. shear rates for AO 352 data set.

	AO 352 Type I Top	AO 352 Type I Top	AO 352 Type I Top	AO 352 Type I Top	AO 352 Type III Top	AO 352 Type III Top	AO 352 Type III Top	AO 352 Type III Top	AO 352 Type II Top	AO 352 Type II Top
Salinity	0.00	0.25	0.50	0.75	1.00	1.25	1.50	1.75	2.00	2.25
shear rate	viscosity (cP)	viscosity (cP)	viscosity (cP)	viscosity (cP)	viscosity (cP)	viscosity (cP)	viscosity (cP)	viscosity (cP)	viscosity (cP)	viscosity (cP)
1.00	14.20	11.41	10.65	9.99	12.41	15.81	45.06	21.62	18.15	15.91
1.59	11.21	9.82	10.36	12.78	14.17	14.04	42.37	25.13	19.12	17.41
2.51	8.34	9.61	13.29	12.68	14.38	13.67	41.13	21.45	17.21	18.08
3.98	13.16	13.46	13.38	12.27	14.10	13.24	38.62	22.45	17.48	17.62
6.31	13.88	14.30	13.61	11.90	14.01	13.32	35.68	21.92	17.15	17.58
10.00	14.09	14.50	13.58	11.90	14.03	13.33	32.57	21.99	17.11	17.59
15.85	14.07	14.42	13.58	11.88	14.01	13.41	29.64	21.80	16.99	17.55
25.12	14.09	14.38	13.61	11.88	14.05	13.49	27.03	21.32	16.85	17.48
39.81	14.09	14.45	13.66	11.90	14.08	13.60	24.64	20.92	16.72	17.46
63.10	14.11	14.38	13.77	11.93	14.14	13.78	22.89	20.59	16.65	17.41
100.00	14.16	14.07	13.71	11.98	14.12	13.75	21.24	20.37	16.54	17.21

Table 4.6: Middle phase microemulsion viscosity measurements vs. shear rates for AO 352 data set.

	AO 352 Type I Middle	AO 352 Type I Middle	AO 352 Type I Middle	AO 352 Type I Middle	AO 352 Type III Middle	AO 352 Type III Middle	AO 352 Type III Middle	AO 352 Type III Middle	AO 352 Type II Middle	AO 352 Type II Middle
Salinity	0.00	0.25	0.50	0.75	1.00	1.25	1.50	1.75	2.00	2.25
shear rate	viscosity (cP)	viscosity (cP)	viscosity (cP)	viscosity (cP)	viscosity (cP)	viscosity (cP)		viscosity (cP)	viscosity (cP)	viscosity (cP)
1.00					15.00	28.60	37.37	18.81		
1.59					14.32	26.57	35.18	19.07		
2.51					14.83	25.41	33.95	19.78		
3.98					14.54	24.31	32.58	19.22		
6.31					14.61	23.73	30.51	19.28		
10.00					14.59	22.61	27.81	19.19		
15.85					14.55	22.07	25.09	18.99		
25.12					14.60	20.28	22.60	18.84		
39.81					14.67	19.04	20.48	18.71		
63.10					14.65	17.57	18.86	18.61		
100.00					14.52	16.22	17.60	18.42		

Table 4.7: Lower phase viscosity measurements vs. shear rates for AO 352 data set.

	AO 352 Type I Bottom	AO 352 Type I Bottom	AO 352 Type I Bottom	AO 352 Type I Bottom	AO 352 Type III Bottom	AO 352 Type III Bottom	AO 352 Type III Bottom	AO 352 Type III Bottom	AO 352 Type II Bottom	AO 352 Type II Bottom
Salinity	0.00	0.25	0.50	0.75	1.00	1.25	1.50	1.75	2.00	2.25
shear rate							viscosity (cP)	viscosity (cP)	viscosity (cP)	viscosity (cP)
1.00	-2.62	-2.90	-2.47	2.69	1.92	1.20	3.24	-0.22	-0.97	1.67
1.59	-3.27	-4.03	1.19	1.77	1.51	-0.41	0.58	-1.24	-0.91	-0.96
2.51	-4.16	-4.33	1.84	2.08	1.66	0.95	0.28	1.44	1.38	1.45
3.98	0.49	-0.05	2.00	1.82	1.46	0.43	0.57	0.22	0.34	0.27
6.31	1.33	1.10	1.84	1.78	1.41	0.61	0.54	0.58	0.70	0.62
10.00	1.47	1.40	1.84	1.67	1.35	0.54	0.51	0.47	0.60	0.51
15.85	1.44	1.44	1.79	1.65	1.26	0.55	0.50	0.48	0.57	0.53
25.12	1.44	1.40	1.77	1.69	1.39	0.54	0.50	0.49	0.51	0.53
39.81	1.35	1.42	1.84	1.90	1.95	0.53	0.48	0.49	0.47	0.52
63.10	1.12	1.42	1.89	2.05	2.81	0.52	0.47	0.47	0.44	0.51
100.00	1.00	1.23	1.99	2.03	2.77	0.50	0.46	0.45	0.43	0.51

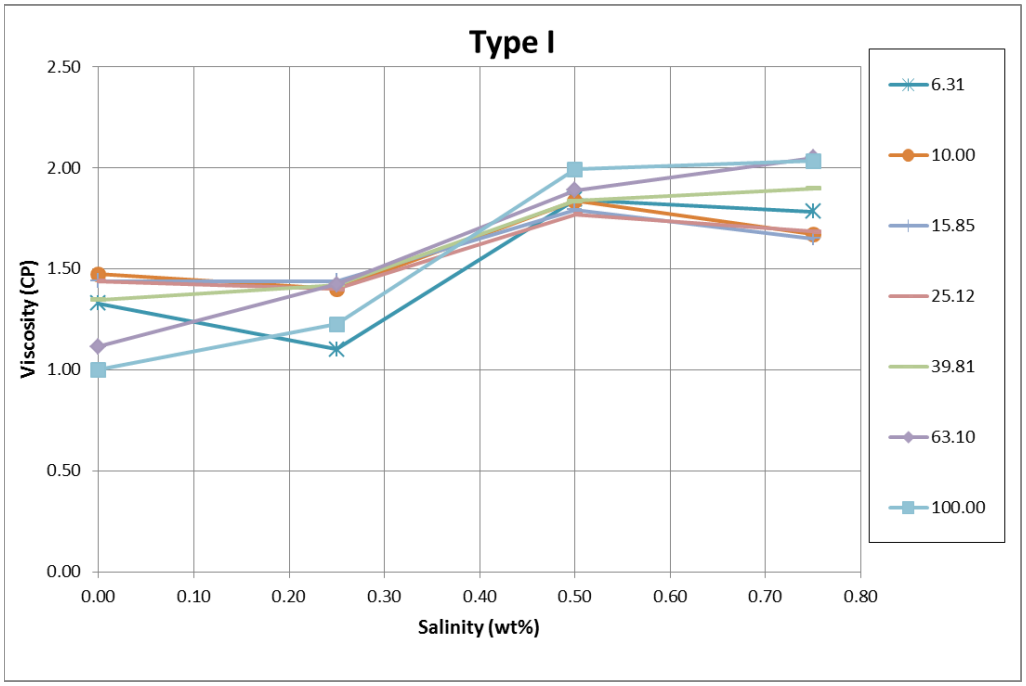

Figure 4.13: Microemulsion viscosity vs. salinity for samples with Type I phase behavior (AO 352 data set) at different shear rates in Sec^{-1}.

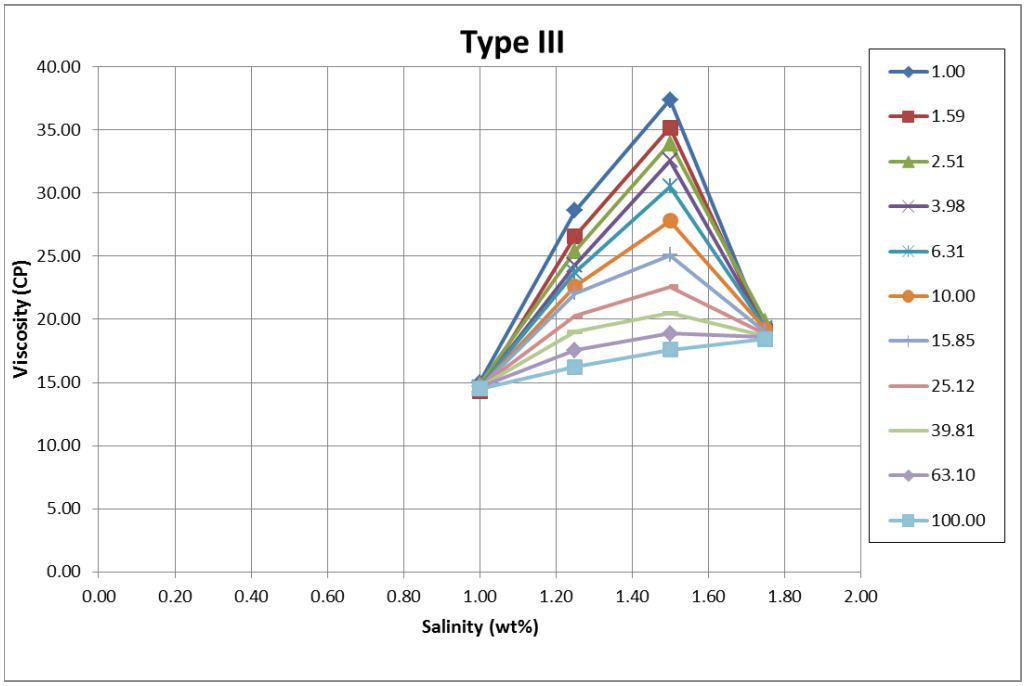

Figure 4.14: Microemulsion viscosity vs. salinity for samples with Type III phase behavior (AO 352 data set) at different shear rates in Sec^{-1}.

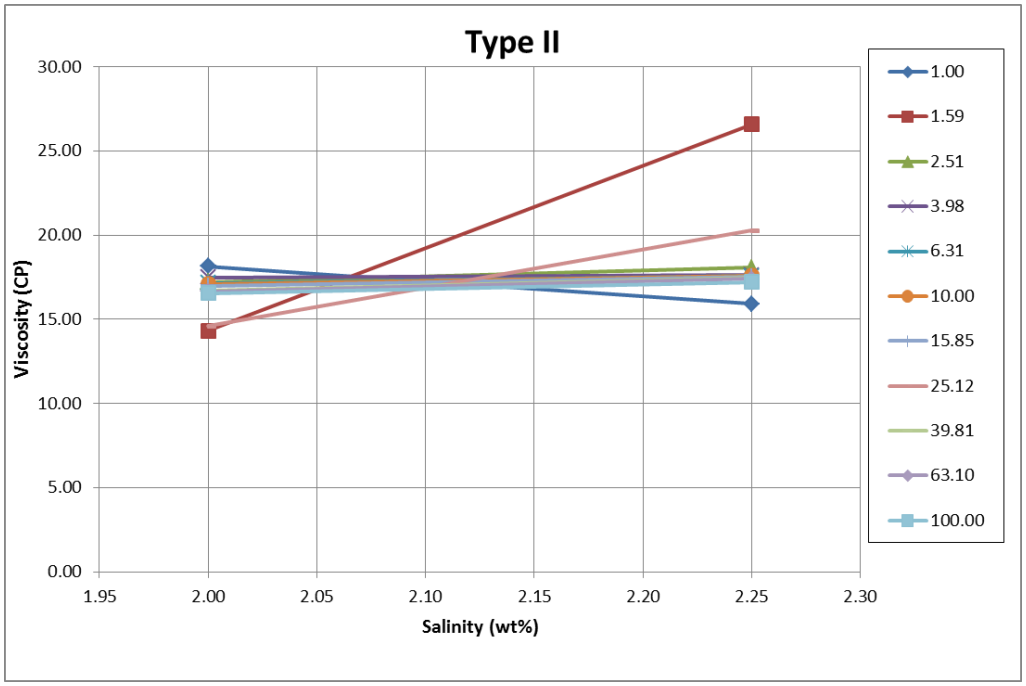

Figure 4.15: Upper phase microemulsion phase viscosity vs. salinity for samples with Type II phase behavior (AO 352 data set) at different shear rates in Sec^{-1}

4.1.3 AO 03 Data Set

The procedure to complete the rheological analysis of microemulsion phase began with sample preparation explained in Section 3.4. Once fully equilibrated, the phases can be extracted for rheological measurements. Following the viscosity measurements, the rheological measurements are analyzed to identify the trend in microemulsion phase viscosity vs. salinity. We prepared 20 samples for this data set; 10 samples with polymer and 10 samples without polymer scanning with 1.25% - 3.5% NaCl. The salinity increment was chosen such that we have enough data points for each type of phase behavior. Rheological measurements were made for each phase in each sample.

Microemulsion Phase Viscosity

Similar to the other two data sets, microemulsion viscosity for Type I test tubes shows a linear correlation with salinity (Figure 4.16). Also, Type III test tubes show a parabolic type of behavior. The viscosity increases with salinity and reaches a maximum and then decrease to another low value (Figure 4.17). We do not have tubes with Type II phase behavior in this data set.

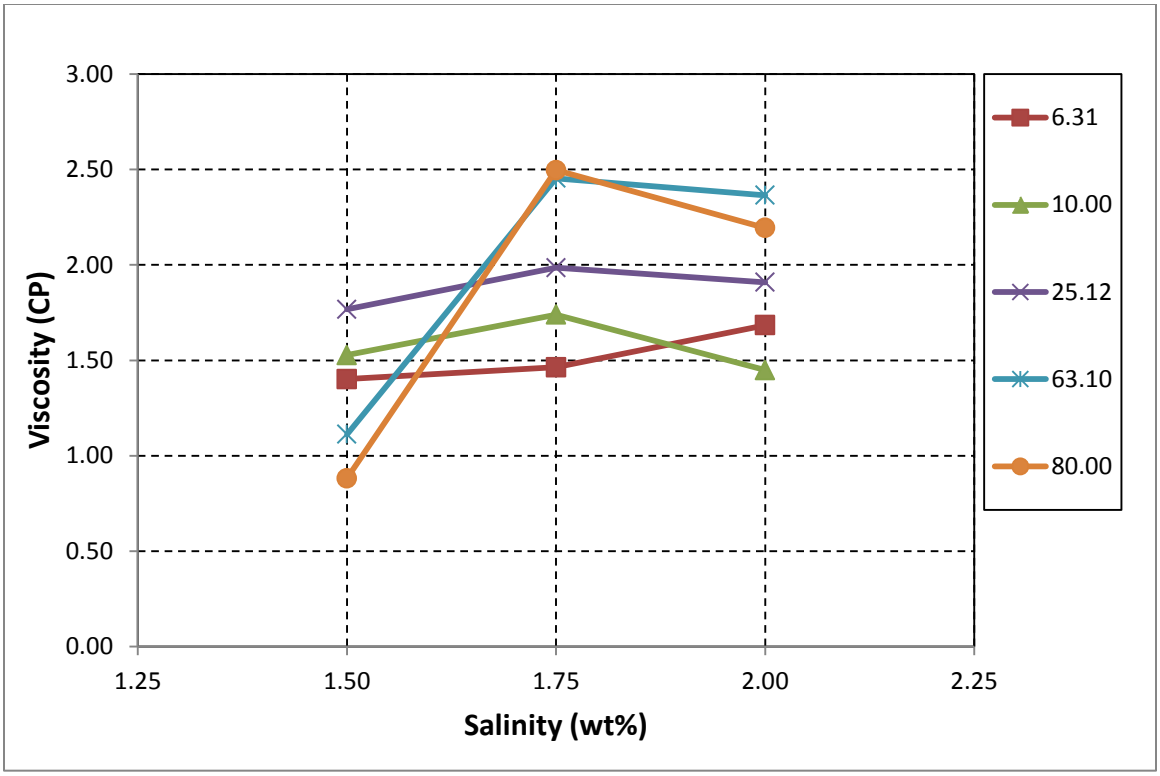

Figure 4.16: Microemulsion viscosity vs. salinity for samples with Type I phase behavior (AO 03 data set) for different shear rates in s^{-1}

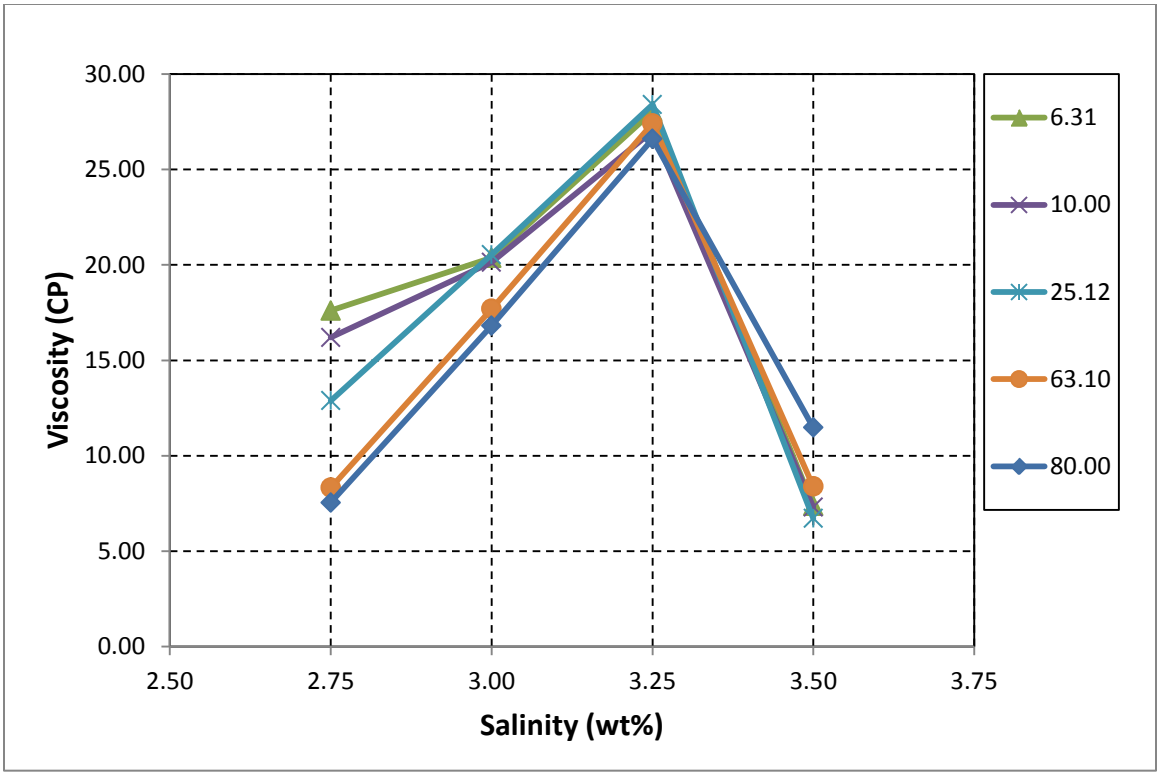

Figure 4.17: Microemulsion viscosity vs. salinity for samples with Type III phase behavior (AO 03 data set) for different shear rates in s^{-1}

Chapter 5: Development of New Viscosity Model for Microemulsion

Viscosity of microemulsion phase is of considerable interest in oil industry due to its importance in EOR application. The knowledge of microemulsion phase viscosity and the capability to control is an important factor in oil recovery. The magnitude and extent that microemulsion structure affects viscosity is complex and difficult to predict. Since no analytical model exists to predict microemulsion viscosity, the viscosity of microemulsion is measured experimentally for mixtures of water, oil, and surfactant.

The viscosity of a microemulsion system is a macroscopically measurable quantity that characterizes a given system. The viscosity of dilute microemulsion can be modeled by Einstein's well-known viscosity relation as follow:

$$\eta_r = 1 + 2.5\phi \tag{5.1}$$

where η_r is the relative viscosity of the solution, and ϕ is the volume fraction of the solute or dispersed phase. However, this relation is not valid at higher concentration and for the system with complex structures, most likely due to many body interactions. There is a lack of accurate theory on viscosity of microemulsions.

Salt such as NaCl can increase the viscosity of nonionic amphiphilic microemulsion solutions. The viscosity of a microemulsion phase is highly affected by system compositions. A system that is oil continuous can change into a bicontinuous system and finally to a water continuous system. These phases (oil continuous phase, bicontinuous phase, or water continuous phase) have very different structure organizations and result in distinct changes in viscosity. We have witnessed the same behavior in the microemulsion viscosity from our experimental lab measurements.

Based on the above statement and analysis performed and discussed in previous chapter, we propose a new empirical viscosity model for the viscosity of microemulsion

phase as a function of salinity. The proposed model is not a continuous across the phase behavior boundaries; rather, we introduce empirical correlations for the microemulsion phase for each type of phase behavior (consistent with the phase behavior using Hand's rule). The proposed viscosity model consists of the following correlations:

$$\mu_m = \begin{cases} \mu_w(\alpha_1 + \alpha_2 C_{SE}) & for\, C_{SE} < C_{SEL} \\ \mu_o(\alpha_3 + \alpha_4 C_{SE}) & for\, C_{SE} > C_{SEU} \\ \alpha_5 + \dfrac{\alpha_6}{C_{SE}^{0.5}} + \alpha_7 e^{C_{SE}} & for\, C_{SEL} \le C_{SE} \le C_{SEU} \end{cases} \tag{5.2}$$

where α parameters are matching parameters, μ_w is water viscosity, μ_o is oil viscosity, C_{SE} is the effective salinity, C_{SEL} is the lower limit salinity where Type III system forms, and C_{SEU} is the upper limit salinity where Type II systems forms.

The first and second correlations in the Eq. (5.2) are for the microemulsion viscosities in Type I and Type II phase behavior systems, respectively. These correlations have a linear trend with respect to salinity. The third correlation which has a parabolic form is for the microemulsion viscosity in Type III phase behavior.

5.1 VERIFICATION OF NEW VISCOSITY MODEL

Model validation is possibly the most important step in the model building steps. Validation of the new viscosity model is presented in this section. We use experimental lab measurements to verify the new viscosity model. In addition to lab results reported in previous sections, we have few other experimental measurements which we will use them for this step. We will validate and verify the new viscosity model with the following experimental lab measurements:

- AO 41-50 Data Set
- AO 352 Data Set
- AO 03 Data Set
- PCN 78-79
- PCN 128
- Field A Data Set

5.1.1 AO 41-50 Data Set

The detail analysis of AO 41-50 is presented in Section 4.1.2. To verify the model we use viscosities at shear rate of 10 sec^{-1} which is close to the shear rate of fluid at reservoir condition. Table 5.1 shows the microemulsion viscosity measurements at shear rate 10 sec^{-1}. We used a linear and non-linear curve fitting software package to match the new viscosity model [Eq. (5.2)] and determine the parameters. It is critical to ensure that the parameters are determined such that the model does not give negative viscosity. Generally, we do not have enough resolution on the experimental data around the salinities that the phase change happens and we have to find a workaround to eliminate getting negative viscosity around these phase changes. As a solution, we add the last point of the experimental data that we have in Type I to the Type III data set when we want to determine the model parameters. This workaround ensure that when we jump from Type I to Type III (especially in the simulation models), the model does not generate negative viscosity.

Table 5.2 contains parameters for this data set. Table 5.3 shows calculated results from our viscosity model and compare them with the lab results and Figure 5.1 shows the match graphically. The results show excellent match between experimental lab measurements and the results from the viscosity model.

Table 5.1: Microemulsion viscosity at shear rate of 10 sec^{-1} for AO 41-50

Salinity (wt %)	Type	Viscosity (cp)
0.00	Type I	1.28
0.25	Type I	1.28
0.50	Type I	1.94
0.75	Type I	2.52
1.00	Type I	2.21
1.25	Type I	3.11
1.50	Type I	5.02
1.75	Type III	116.10
2.00	Type III	220.70
2.25	Type III	96.82

Table 5.2: Constant parameters used in Eq. (5.2) for AO 41-50

α1	9.746
α2	0.657
α5	26176
α6	-6026
α7	-11133

Table 5.3: Model results vs. lab measurements for AO 41-50

Salinity	Viscosity (cp)		Relative Error (%)
	Measured	Model	
0.00	1.28	0.85	49.5
0.25	1.28	1.40	8.5
0.50	1.94	1.94	0.1
0.75	2.52	2.48	1.6
1.00	2.21	3.02	26.8
1.25	3.11	3.56	12.7
1.50	5.02	4.10	22.4
1.75	116.10	142.77	18.7
2.00	220.70	198.83	11.0
2.25	96.82	104.09	7.0

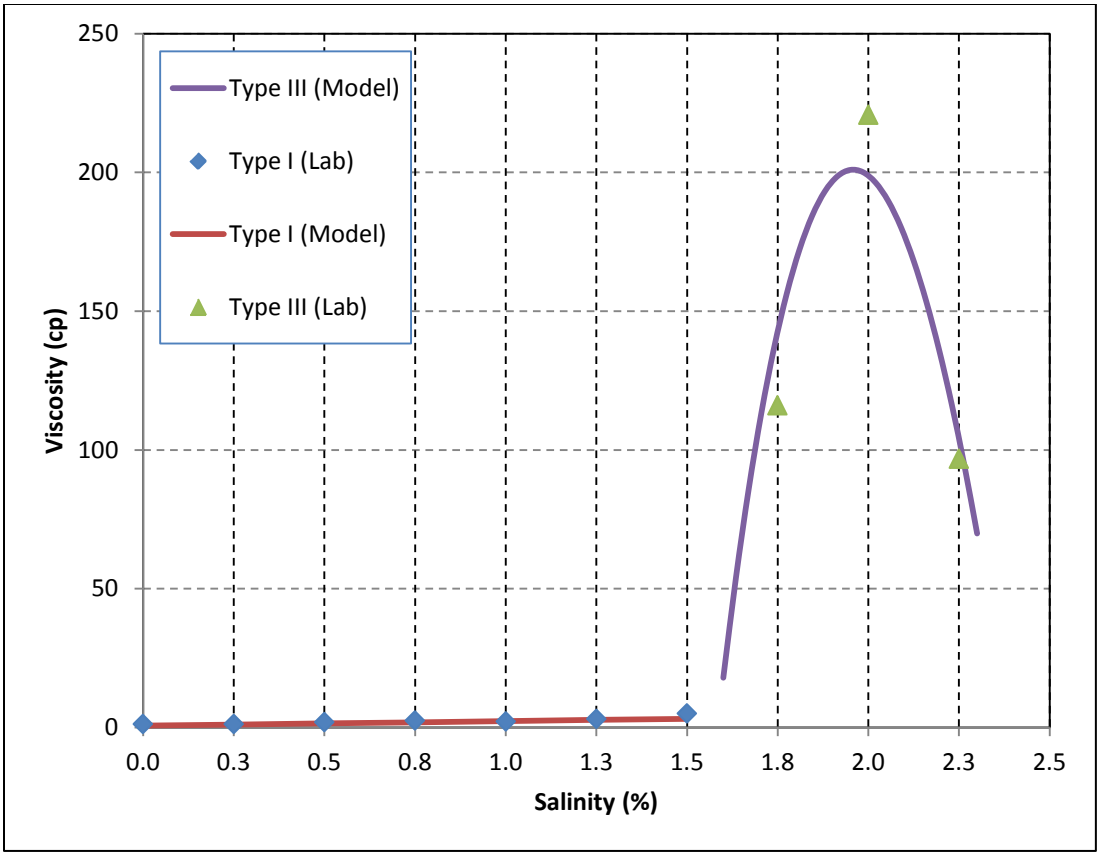

Figure 5.1: Validation of new viscosity model with experimental measurements for AO 41-50

5.1.2 AO 352 Data Set

The detail analysis of AO 352 is presented in Section 4.1.2. This is the only data set that has the viscosity measurements for all three types of microemulsion phase behaviors (Type I, Type II and Type III). To verify the model we use viscosities at shear rate 10 sec^{-1} which is close to the shear rate of fluid at reservoir condition. Table 5.4 shows the microemulsion viscosity measurements at shear rate 10 sec^{-1}. The water and oil viscosities of 0.5 cp and 14 cp are used in the calculation. We used a linear and non-linear curve fitting software package to match the new viscosity model [Eq. (5.2)] and determine the α parameters. Table 5.5 contains parameters α_1 to α_7 for this data set.

Table 5.6 shows calculated results from our viscosity model and compare them with the lab results and Figure 5.2 shows the match graphically. The results show excellent match between experimental lab measurements and the results from the viscosity model.

Table 5.4: Viscosity results for shear rate 10 sec^{-1} for surfactant formulation AO 352

Salinity (wt %)	Type	Viscosity (cp)
0.00	Type I	1.47
0.25	Type I	1.40
0.50	Type I	1.84
0.75	Type I	1.67
1.00	Type III	14.59
1.25	Type III	22.61
1.50	Type III	27.81
1.75	Type III	19.19
2.00	Type II	17.11
2.25	Type II	17.59

Table 5.5: Constant parameters used in Eq. (5.2) for AO 352

α1	2.8816
α2	0.8224
α3	0.9479
α4	0.1371
α5	487.6000
α6	-75.5000
α7	-242.3400

Table 5.6: Model results vs. lab measurements for AO 352

Salinity	Viscosity (cp)		Relative Error (%)
	Measured	Model	
0.00	1.47	1.44	2.2
0.25	1.40	1.54	9.3
0.50	1.84	1.65	11.6
0.75	1.67	1.75	4.5
1.00	14.59	16.56	11.9
1.25	22.61	23.64	4.4
1.50	27.81	26.21	6.1
1.75	19.19	22.50	14.7
2.00	17.11	17.11	0.0
2.25	17.59	17.59	0.0

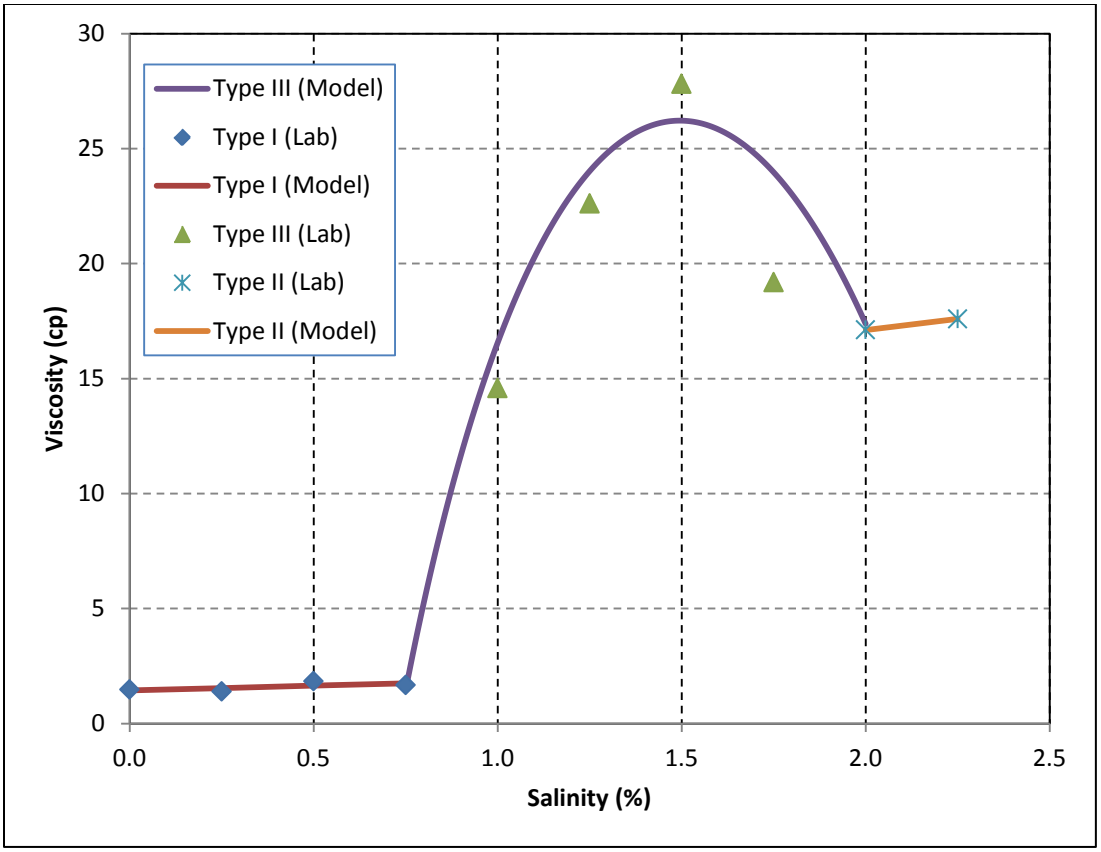

Figure 5.2: Validation of proposed viscosity model with experimental measurements for AO 352

5.1.3 AO 03 Data Set

The detail analysis of AO 03 data set is presented in Section 4.1.3. We have experimental measurements for Type I and Type III phase behavior. We did not see Type II phase behavior within the range of salinity used in this experiment. To verify the model we use viscosities at shear rate of 10 sec^{-1} which is close the shear rate of fluid at reservoir condition. Table 5.8 shows the microemulsion viscosity measurements at shear rate 10 sec^{-1} for Type I and Type III samples.

Table 5.9 contains parameters α_1 to α_7 for this data set. Table 5.10 shows calculated results from our viscosity model and compares them with the lab results and

Figure 5.3 shows the match graphically. The results show a good match between experimental lab measurements and the results from the viscosity model.

Table 5.7: Phase behavior for AO 03 samples

Sample #	Salinity (wt %)	Type
1	1.25	Type I
2	1.50	Type I
3	1.75	Type I
4	2.00	Type I
5	2.25	Type I
6	2.50	Type I
7	2.75	Type III
8	3.00	Type III
9	3.25	Type III
10	3.50	Type III

Table 5.8: Viscosity results for shear rate of 10 sec^{-1} for surfactant formulation AO 03

Sample #	Salinity (wt %)	Type	Viscosity (cp)
1	1.25	Type I	
2	1.50	Type I	1.53
3	1.75	Type I	1.74
4	2.00	Type I	1.45
5	2.25	Type I	
6	2.50	Type I	1.34
7	2.75	Type III	16.20
8	3.00	Type III	20.10
9	3.25	Type III	27.00
10	3.50	Type III	7.30

Table 5.9: Constant parameters used in Eq. (5.2) for AO 03 data set

α1	4.10
α2	-3.24
α5	3476
α6	-1281
α7	-996

Table 5.10: Model results vs. lab measurements for AO 03 data set

Salinity	Viscosity (cp)		Relative Error (%)
	Measured	Model	
1.25			
1.50	1.53	1.63	6.4
1.75	1.74	1.57	11.1
2.00	1.45	1.50	3.1
2.25			
2.50	1.34	1.36	1.3
2.75	16.20	14.75	9.8
3.00	20.10	24.70	18.6
3.25	27.00	22.25	21.4
3.50	7.30	8.97	18.6

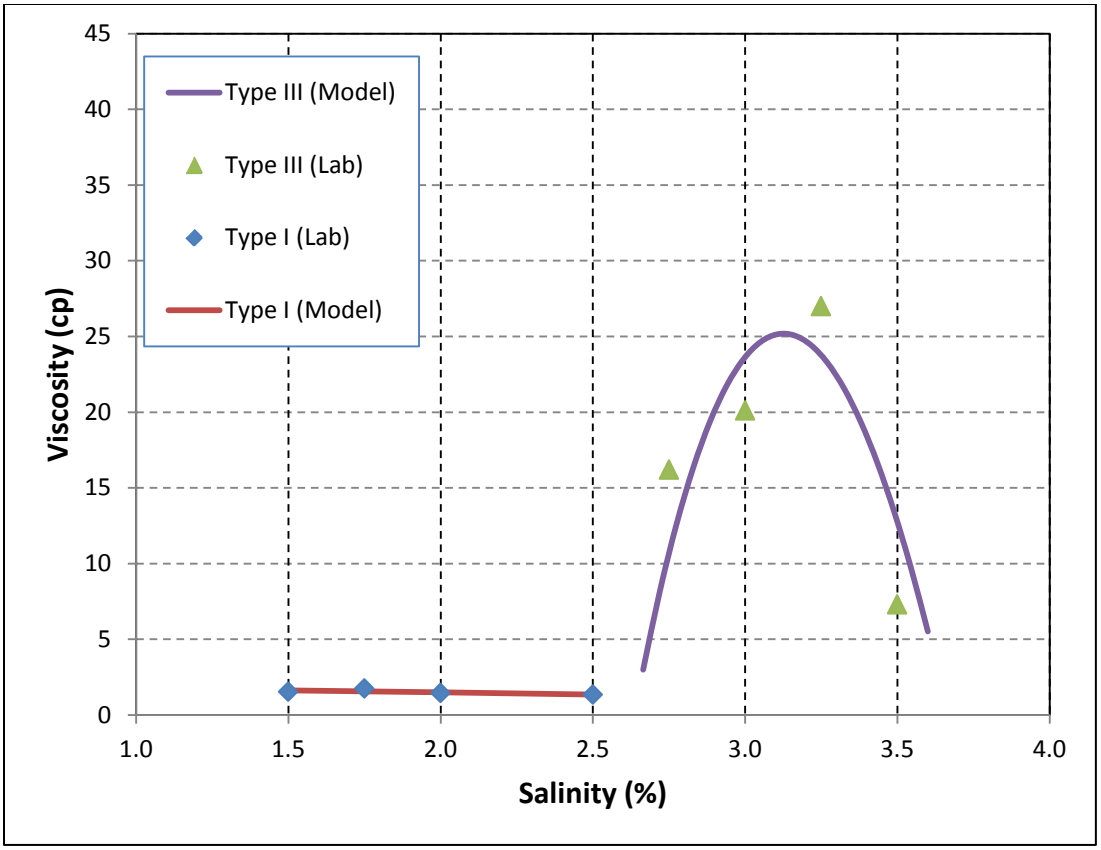

Figure 5.3: Validation of new viscosity model with experimental measurements for AO 03 data set

5.1.4 PCN 78-79

PCN 78 is made of 0.15% TDA 30, 0.15% Petrostep S2, 2.0% TEGBE and PCN 79 formula is 0.25% Enordet C0121, 0.25% Enordet J13131, 2.0% TEGBE. These samples are mixed with 30% oil. We only have the microemulsion viscosity measurements for the middle phase of samples with salinity in Type III phase behavior. Table 5.11 contains the microemulsion viscosities vs. shear rates at different salinities for PCN-78 and PCN-79.

To verify our viscosity model, we again use results at shear rates of 1 and 10 sec^{-1}. Table 5.12 and Table 5.13 show the lab measurements, coefficients, and model results for

PCN-78 and PCN-79. Figure 5.4 and Figure 5.5 show that the viscosity model matches the lab results fairly good.

Table 5.11: PCN-78 and PCN-79 microemulsion viscosity measurements

PCN-78						PCN-79					
41045	ppm TDS	46045	ppm TDS	51045	ppm TDS	41045	ppm TDS	46045	ppm TDS	51045	ppm TDS
30	% oil	30	% oil	30	% oil	30	% oil	30	% oil	30	% oil
38	oC	38	oC	38	oC	38	oC	38	oC	38	oC
Shear rate	Viscosity	Shear rate	Viscosity	Shear rate	Viscosity	Shear rate	Viscosity	Shear rate	Viscosity	Shear rate	Viscosity
s-1	cP	s-1	cP	s-1	cP	s-1	cP	s-1	cP	s-1	cP
0.10	54.46	0.10	167.00	0.10	214.50	0.10	38.85	0.10	83.50	0.10	61.33
0.18	56.84	0.18	170.80	0.18	208.30	0.18	31.30	0.18	84.98	0.18	68.60
0.32	55.75	0.32	166.39	0.32	195.90	0.32	35.98	0.32	82.99	0.32	65.34
0.56	54.85	0.56	161.25	0.56	181.20	0.56	34.23	0.56	77.86	0.56	59.29
1.00	53.22	1.00	156.26	1.00	163.06	1.00	33.70	1.00	73.88	1.00	50.95
1.78	50.85	1.78	153.90	1.78	143.45	1.78	33.27	1.78	68.76	1.78	41.06
3.16	49.53	3.16	151.87	3.16	106.26	3.16	32.89	3.16	65.99	3.16	28.43
5.62	50.14	5.62	143.45	5.62	68.89	5.62	31.78	5.62	60.65	5.62	23.53
10.00	48.21	10.00	135.20	10.00	52.88	10.00	31.39	10.00	57.91	10.00	16.32
17.78	43.85	17.78	130.38	17.78	40.12	17.78	30.98	17.78	57.10	17.78	9.87
31.62	45.00	31.62	127.01	31.62	31.62	31.62	28.96	31.62	60.69	31.62	8.41
56.23	48.46	56.23	123.96	56.23	28.66	56.23	26.09	56.23	60.43	56.23	9.18
100.00	53.60	100.00	123.60	100.00	29.20	100.00	22.47	100.00	59.01		
177.83	55.21	177.83	118.40			177.83	17.86	177.83	50.62		
316.23	45.98	316.23	103.14			316.23	13.61	316.23	42.09		
562.34	35.01	562.34	81.95			562.34	10.12	562.34	34.09		

Table 5.12: Model results vs. lab measurements for PCN-78

PCN-78						
Salinity (ppm)	Viscosity (cp)					
	Shear Rate 1 (1/sec)			Shear Rate 10 (1/sec)		
	Lab Data	Model	Relative Error (%)	Lab Data	Model	Relative Error (%)
41045	53.2	53.2	0.05	48.2	48.2	0.00
46045	156.3	156.3	0.03	135.2	135.2	0.00
51045	163.1	163.1	0.02	52.9	53.0	0.17
α5	11688.75			20539.94		
α6	-6589.08			-11058.73		
α7	-1868.67			-3613.90		

Table 5.13: Model results vs. lab measurements for PCN-79

PCN-79						
Salinity (ppm)	Viscosity (cp)					
	Shear Rate 1 (1/sec)			Shear Rate 10 (1/sec)		
	Lab Data	Model	Relative Error (%)	Lab Data	Model	Relative Error (%)
41045	33.70	33.72	0.05	31.39	31.42	0.08
46045	73.88	73.90	0.03	57.91	57.90	0.02
51045	50.95	51.00	0.09	16.32	16.32	0.01
α5	7668.48			8275.95		
α6	-4165.07			-4400.13		
α7	-1319.92			-1483.11		

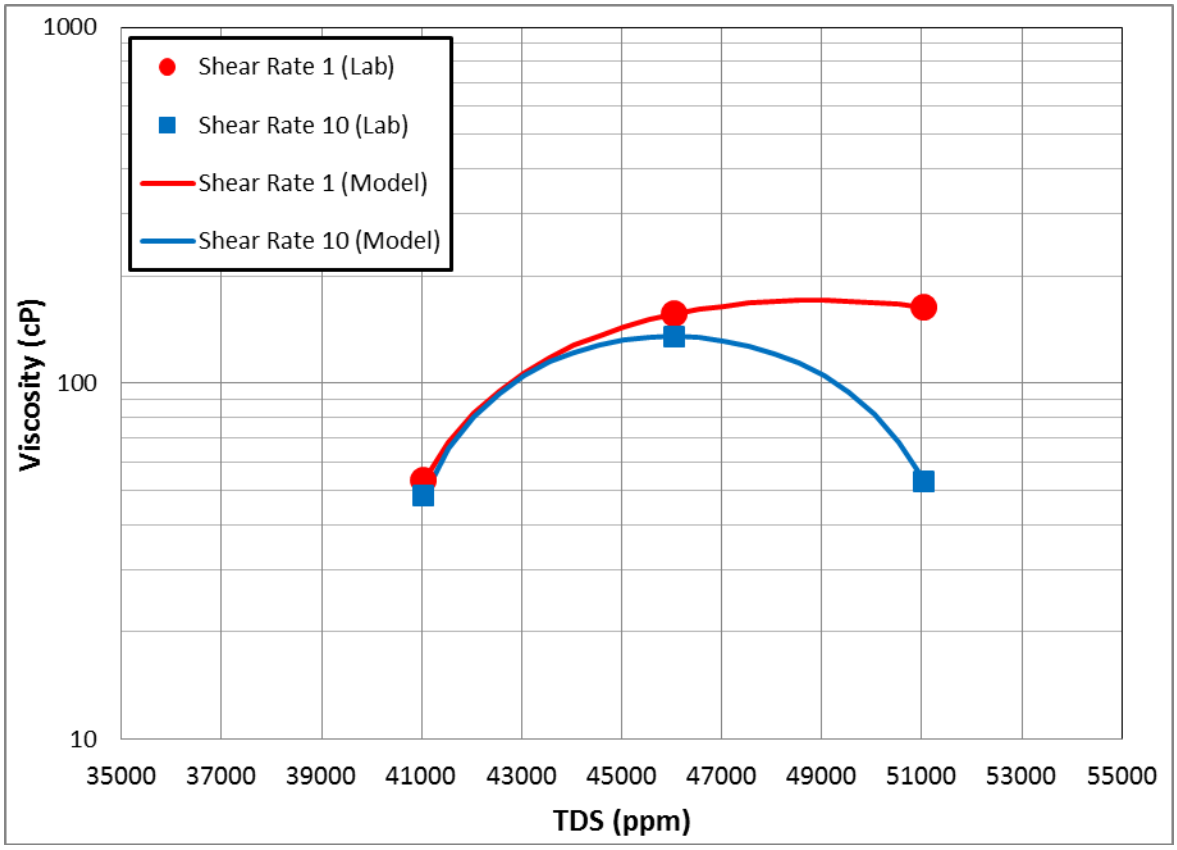

Figure 5.4: Validation of new viscosity model with experimental measurements for PCN-78

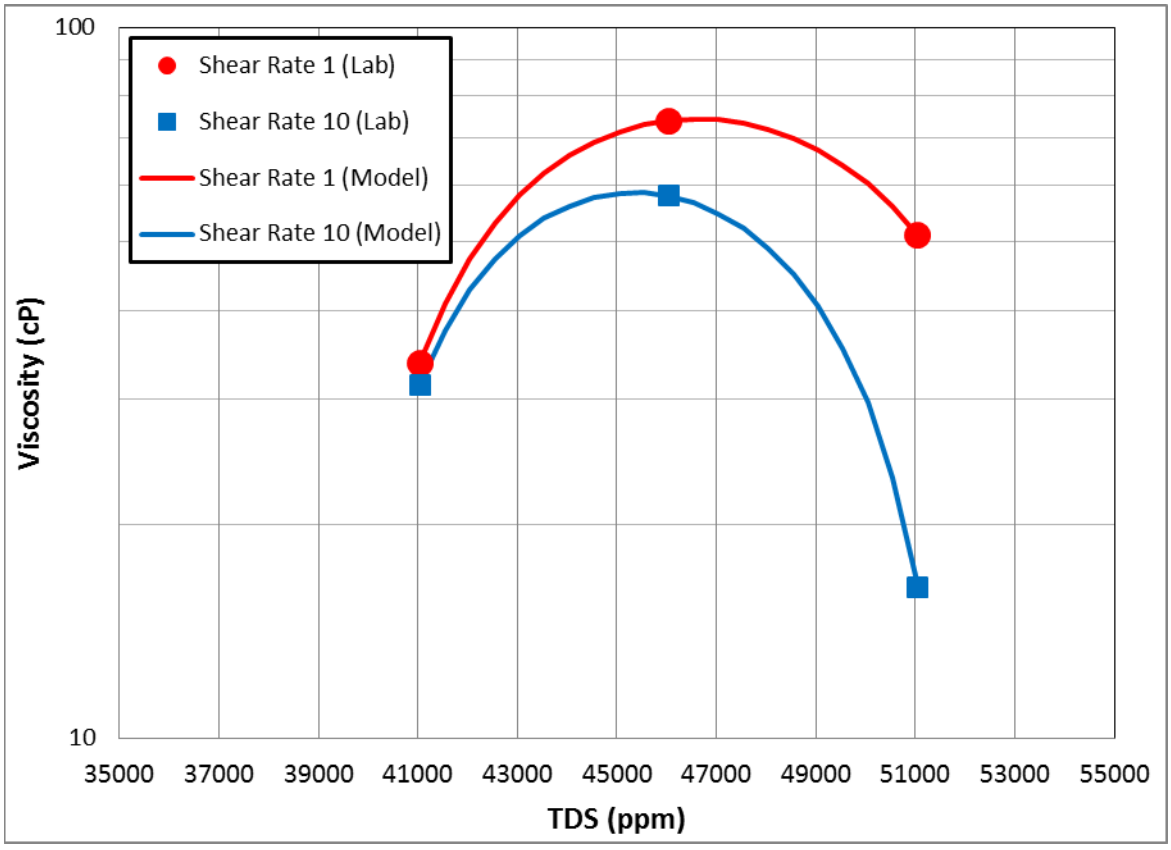

Figure 5.5: Validation of new viscosity model with experimental measurements for PCN-79

5.1.5 PCN-128 Data Set

PCN 128 is a solution of 3.0% IBA-10EO, Na_2CO_3 scan in PCNSSB with 30% oil (053-1a) at 38 °C. Two sets of lab data (with and without polymer) are available for this study. In this section we use the lab data for the set without the polymer to validate the viscosity model. The effect of polymer in microemulsion viscosity will be discussed later. We have viscosity measurements for four tubes at different salinities. Tube at 10,000 ppm Na_2CO_3 is Type I phase behavior and the rest are Type III phase behavior. Table 5.14 shows the viscosity measurements for this case.

We used the lab results at shear rate of 10 sec^{-1} for comparison with the model calculations. Table 5.15 and Figure 5.6 show good match between the lab data and the results from the model.

Table 5.14: PCN-128 microemulsion viscosity measurements

ME	No Polymer	ME	No Polymer	ME	No Polymer	ME	No Polymer
PCN-128 Re		PCN-128 Re		PCN-128 Re		PCN-128 Re	
3%	IBA-10EO	3%	IBA-10EO	3%	IBA-10EO	3%	IBA-10EO
10000	ppm Na2CO3	20000	ppm Na2CO3	30000	ppm Na2CO3	40000	ppm Na2CO3
1000	ppm Brine	1000	ppm Brine	1000	ppm Brine	1000	ppm Brine
11000	ppm TDS	21000	ppm TDS	31000	ppm TDS	41000	ppm TDS
30	% oil	30	% oil	30	% oil	30	% oil
0	ppm FP3630S	0	ppm FP3630S	0	ppm FP3630S	0	ppm FP3630S
38	oC	38	oC	38	oC	38	oC
Shear rate	Viscosity	Shear rate	Viscosity	Shear rate	Viscosity	Shear rate	Viscosity
s-1	cP	s-1	cP	s-1	cP	s-1	cP
		0.10	64.13	0.10	211.89	0.10	213.15
		0.18	58.04	0.18	210.71	0.18	210.27
		0.32	52.05	0.32	210.98	0.32	206.74
		0.56	46.46	0.56	210.10	0.56	204.62
		1.00	43.75	1.00	209.40	1.00	202.60
		1.78	41.45	1.78	210.40	1.78	202.93
3.16	1.35	3.16	39.15	3.16	209.06	3.16	201.62
5.62	1.44	5.62	37.29	5.62	209.22	5.62	201.86
10.00	1.44	10.00	35.11	10.00	208.41	10.00	199.84
17.78	1.48	17.78	34.17	17.78	205.06	17.78	196.62
31.62	1.50	31.62	26.04	31.62	195.72	31.62	189.54
56.23	1.51	56.23	23.76	56.23	175.35	56.23	178.94
100.00	1.52	100.00	27.13	100.00	134.60	100.00	156.21
177.83	1.55	177.83	32.15	177.83	94.08	177.83	119.02
316.23	1.57	316.23	27.18	316.23	66.25	316.23	84.70
		562.34	22.55	562.34	47.61	562.34	60.85

Table 5.15: Model results vs. lab measurements for PCN-128

PCN-128			
Salinity (ppm)	Viscosity (cp)		
	Shear Rate 10 (1/sec)		
	Lab Data	Model	Relative Error (%)
21000	35.1	35.1	0.06
31000	208.4	208.0	0.18
41000	199.8	202.2	1.17
α5	3118.26		
α6	-1232.82		
α7	-716.20		

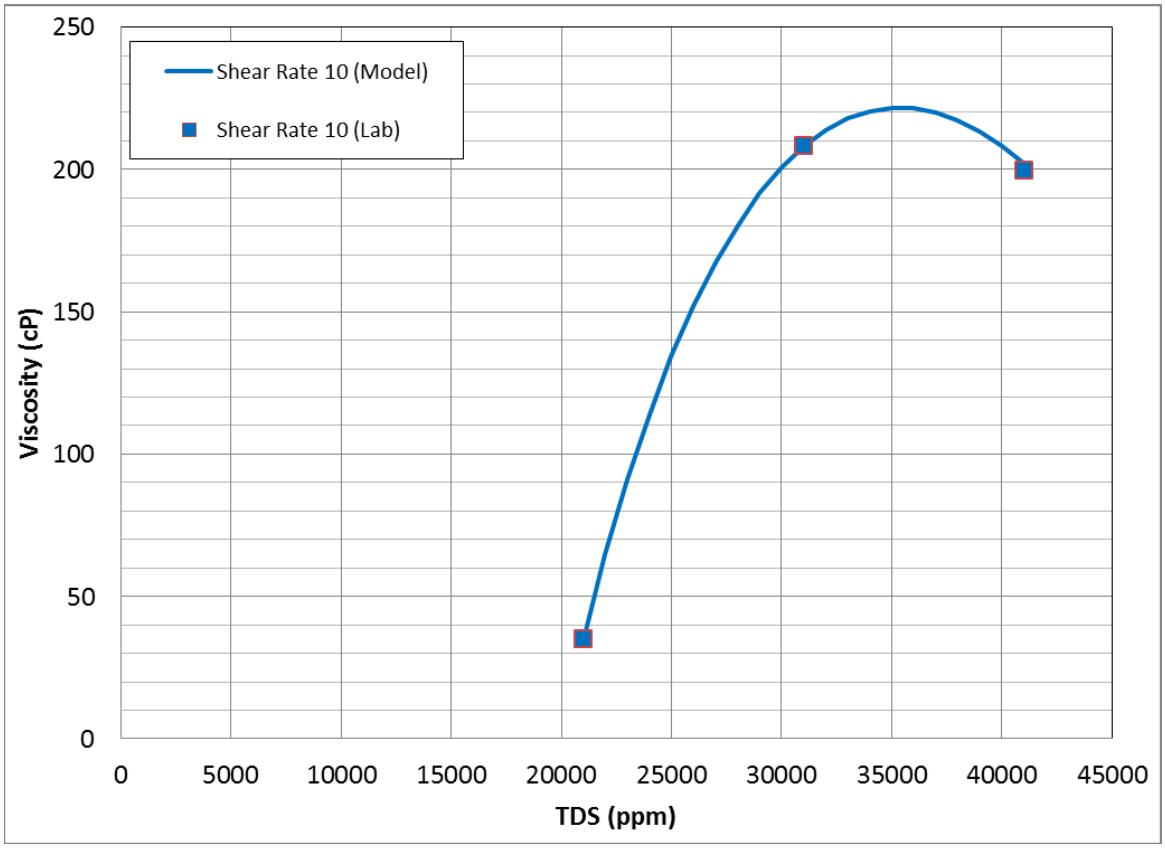

Figure 5.6: Validation of new viscosity model with experimental measurements for PCN-128

5.1.6 Field A Data Set

We have two different samples, KL-46 (1% IBA-3EO) and KL-48 (1% IBA-1EO). For sample KL-48 we have the lab results at 85 °C while for sample KL-46 we have the lab results at 65 °C and 85 °C. We do not have the exact description of the two samples but we know the oil that is used in both tests is the same and has the viscosity of 70 cP at 85 °C and 170 cP at 65 °C. Viscosities vs. shear rate were measured at different salinities for middle phase in Type III samples.

We used the lab results at shear rates of 1 sec^{-1} and 10 sec^{-1} to validate the proposed models. Table 5.16 through Table 5.18 list the lab results for the three samples

at the above mentioned shear rates. We used the above information and validated our viscosity model. The results were satisfactory and the model could match the lab results very well. Figure 5.7 shows the lab results against the model results for all samples.

Table 5.16: Viscosity measurements at shear rates of 1 and 10 sec^{-1} for KL-48ME at 85 °C

KL-48ME				
Salinity (ppm)	Salinity (meq/ml)	Viscosity (cp)		KL-24 (85 C)
		IBA-1EO(1s-1,85 C)	IBA-1EO(10s-1,85 C)	Viscosity (cp)
20000	0.3419	32.0	19.9	70
25000	0.4274	245.3	176.3	70
30000	0.5128	223.0	177.3	70
35000	0.5983	151.8	143.3	70
α5		8868.62	5856.32	
α6		-2929.54	-1983.64	
α7		-2714.32	-1733.66	

Table 5.17: Viscosity measurements at shear rates of 1 and 10 sec^{-1} for KL-46ME at 85 °C

Kali-46ME				
Salinity (ppm)	Salinity (meq/ml)	Viscosity (cp)		KL-24 (85C)
		IBA-3EO(1s-1,85 C)	IBA-3EO(10s-1,85 C)	Viscosity (cp)
35000	0.5983	2.1	1.6	70
40000	0.6838	308.8	210.1	70
45000	0.7692	246.6	160.0	70
50000	0.8547	116.4	108.9	70
α5		24029.74	14340.40	
α6		-12066.28	-7252.19	
α7		-4626.70	-2722.51	

Table 5.18: Viscosity measurements at shear rates of 1 and 10 sec^{-1} for KL-46ME at 65 °C

KL-46ME				
Salinity (ppm)	Salinity (meq/ml)	Viscosity (cp)		KL-24 (65C)
		IBA-3EO(1s-1,65 C)	IBA-3EO(10s-1,65 C)	Viscosity (cp)
45000	0.7692	261.7	125.7	170
50000	0.8547	422.3	233.9	170
55000	0.9402	420.3	353.4	170
α5		22184.60	-1304.41	
α6		-13209.37	121.11	
α7		-3179.60	598.68	

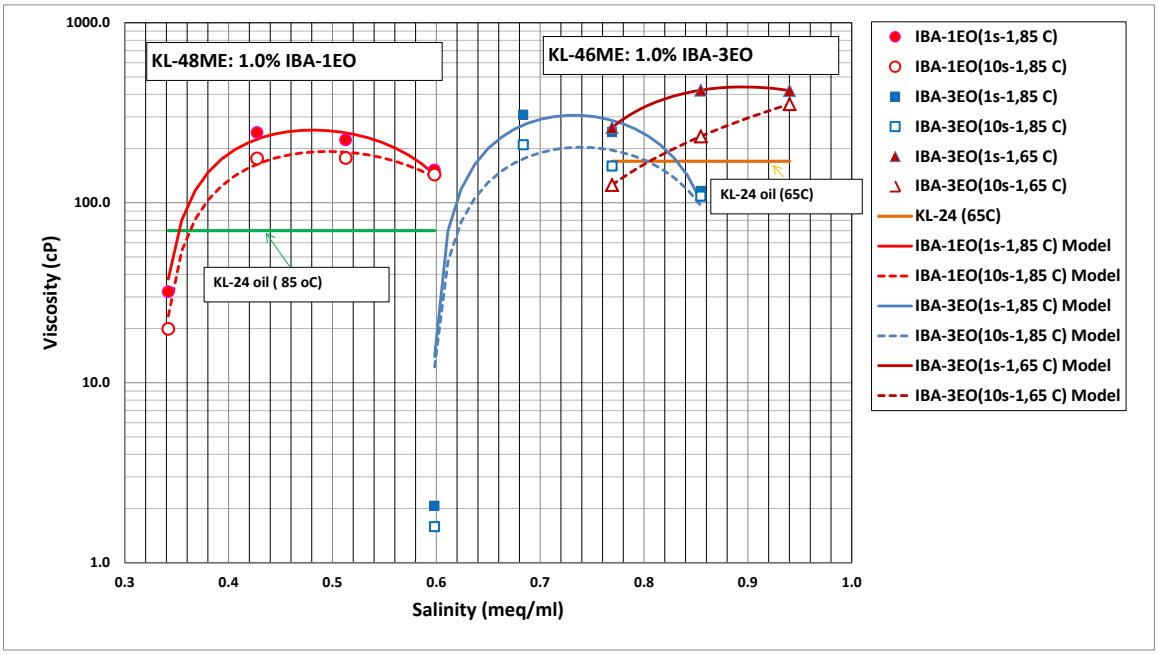

Figure 5.7: Lab measurements vs. model results for Field A data.

5.2 EFFECT OF POLYMER ON MICROEMULSION RHEOLOGY

The effectiveness of microemulsions in EOR is limited due to several factors. One of these factors is the low viscosity of majority of microemulsions. When a low viscosity fluid is used to displace a more viscose fluid, the effectiveness of displacement process

reduces due to the displacement instability known as fingering. The second important factor that limits the effectiveness of microemulsion displacement is adsorption of surfactant by formation which in turn reduces the microemulsion bank and also destabilizes the microemulsion due to loss of surfactant.

In order to improve the mobility ratio of surfactant flooding, polymer is added to the surfactant solution. The polymer microemulsion solutions are stable at high salinity and help to reduce the adsorption and retention of the surfactant in the rock formation. The complex internal microstructure of microemulsion complexes with polymer lead to a rheology behavior that is very different from conventional Newtonian and non-Newtonian fluids, especially for microemulsion phase in Type III phase behavior (bi-continuous microemulsion). In principle, adding any kind of polymeric material to a microemulsion will affect its rheological behavior; however, the kind of changes will mainly depend of polymer molecule.

In the following section, we investigate the effect of polymer on microemulsion rheology. We have experimental lab measurements for few of the data sets we discussed in Section 4.1. The experimental measurements are performed such that both data sets (with and without polymer) encompass the same range of salinity with the same salinity increment. The samples that will be used in this study and have rheology measurements for the case with and without polymer are:

- AO 352 Data Set
- AO 03 Data Set
- PCN 128 Data Set

5.2.1 Effect of Polymer on Microemulsion Phase Behavior

In microemulsion systems, several phases can coexists in equilibrium with each phase having a different microscopic and macroscopic structure. Several factors such as salinity, temperature and presence of other materials like polymer affect the phase behavior of microemulsions. Investigation of the effect of polymer on microemulsion phase behavior is outside of the scope of this study; however we would like to note couple of findings from the experimental measurements regarding the effect of polymer on microemulsion phase behavior.

The increase in salinity from low to a high values results in phase transitions from Windsor Type I to Windsor Type II going through Windsor Type III. The experimental results show that the microemulsion complexes with polymer exhibit the same phase transitions pattern that we have for the microemulsion solutions without polymer, meaning that the system goes from Windsor Type I to Windsor Type II via Windsor Type III.

Another significant finding from these measurements is the fact that the presence of polymer in a microemulsion complex changes the range of salinity that the Type III phase can form (lower and upper limits of effective salinity for Type III system have been extended). In all of our measurements, the presence of polymer widens the range of salinity that the Type III phase can exist (Table 5.19 and Table 5.20). We measured the solubilization ratios for the solutions with and without polymer in AO 352 data set which shows that the solubilization ratios are also different when polymer is added to the formulation (Figure 5.8).

Table 5.19: Phase behavior for AO 352

Salinity (wt% NaCl)	Type	
	No Polymer	With Polymer
0.00	I	I
0.25	I	I
0.50	I	I
0.75	I	III
1.00	III	III
1.25	III	III
1.50	III	III
1.75	III	III
2.00	II	III
2.25	II	II

Table 5.20: Phase behavior for AO 03 data set

Salinity (wt% NaCl)	Type	
	No Polymer	With Polymer
1.25	I	I
1.50	I	I
1.75	I	III
2.00	I	III
2.25	I	III
2.50	I	III
2.75	III	III
3.00	III	III
3.25	III	III
3.50	III	III

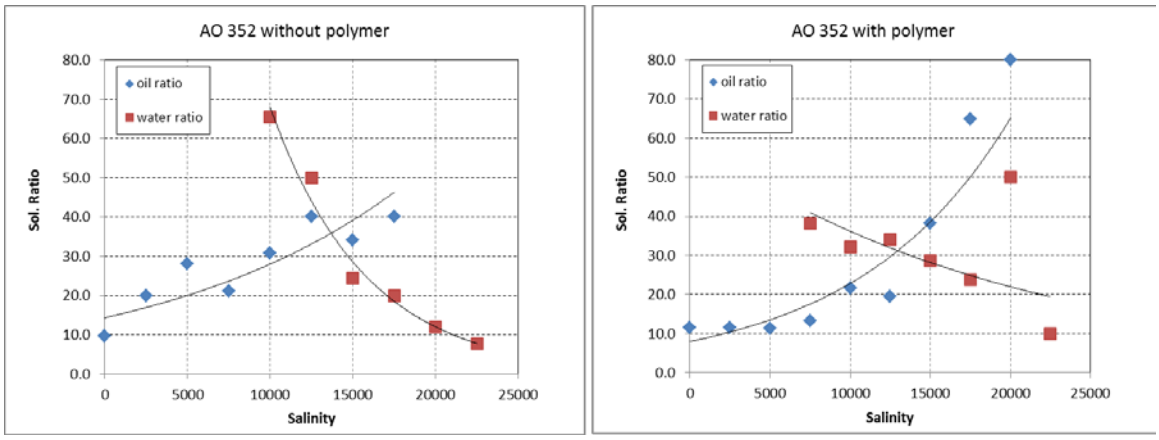

Figure 5.8: Effect of polymer on solubilization ratio (AO 352).

5.2.2 AO 352 Data Set with Polymer

2500 ppm of HPAM Floppam 3330 polymer from SNF was added to the surfactant solution used in AO 352 samples discussed in Section 4.1.2. There are 10 samples for which we have viscosity measurements for all equilibrium phases in each test tube. We carry the same study that we did for AO 352 samples without polymer and make a comparison between the results with and without the polymer.

Oil Phase Viscosity

First we plot all the oil phase viscosities in one chart (Figure 5.9 and Figure 5.10). The results show that the majority of samples follow the same trend and the top phase viscosity is almost the same as pure oil viscosity. The water and oil viscosities are 0.5 cp and 14 cp respectively. The oil phase viscosity does not change with salinity which is in consistence with the assumption that the oil phase remains intact in these two phase behaviors (Type I and Type III). The oil viscosity was also not affected by the presence of polymer which indicates that polymer concentration in oil phase is negligible. Some

samples in both Type I and Type III show slightly higher viscosity which we believe is the measurement error during the fluid extraction from the test tube.

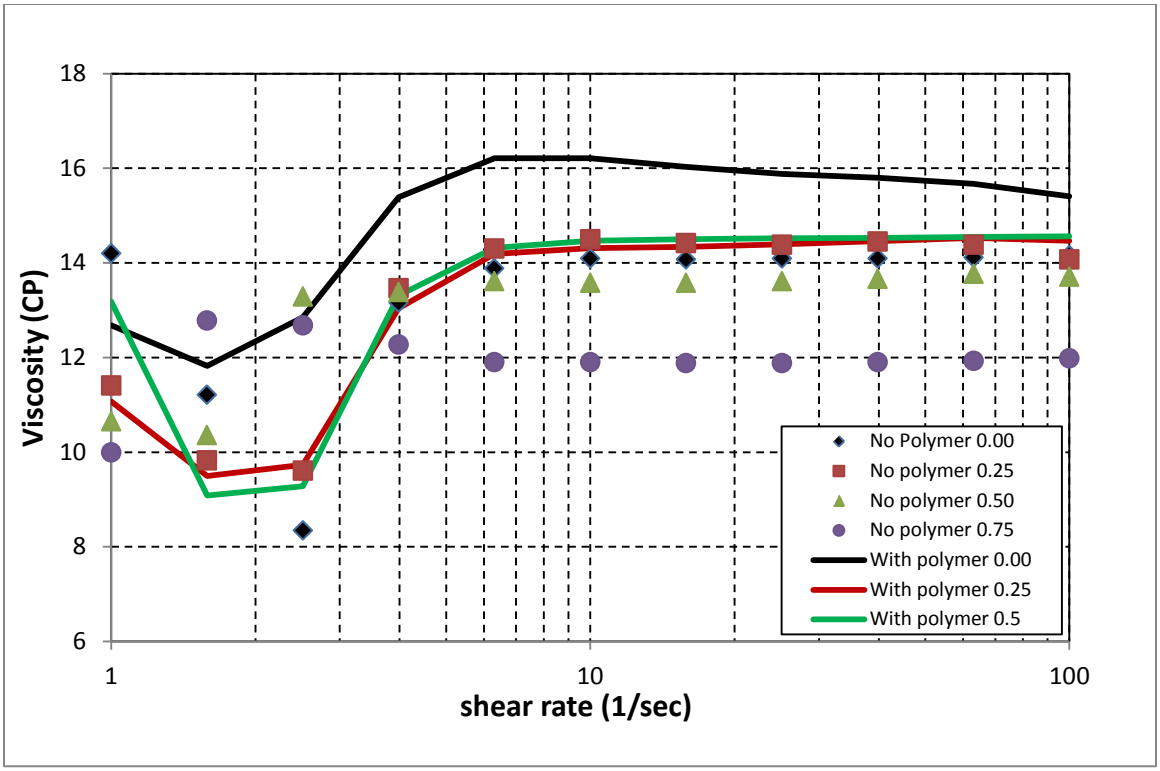

Figure 5.9: Oil phase viscosities vs. shear rates at different salinity for samples with Type I phase behavior (AO 352 samples with and without polymer).

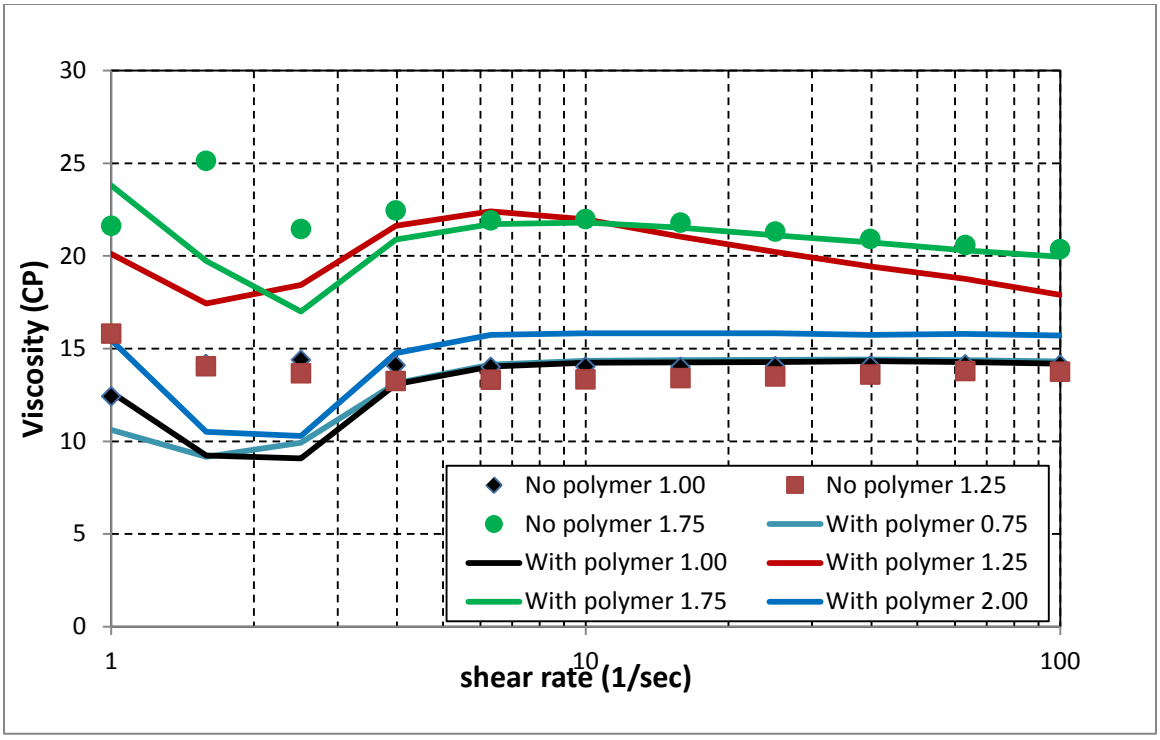

Figure 5.10: Oil phase viscosities vs. shear rates at different salinity for samples with Type III phase behavior (AO 352 samples with and without polymer).

Aqueous Phase Viscosity in Type III Systems

Figure 5.11 shows the solution viscosity for a solution with polymer and no surfactant. As it seen from the plot, the salinity does not affect polymer viscosity. The measurements at low shear rates also seem to be unreliable.

When there is no polymer in the system the water viscosity in all samples of Type III and Type II is about 0.5 cp but when the polymer is added to the solution, the bottom aqueous phase viscosity in Type III systems exhibits significantly higher viscosity compared to the water viscosity (Figure 5.12). This substantial increase in aqueous viscosity suggests that the polymer is mainly partitioned into the aqueous phase. The oleic phase viscosity remains relatively unchanged; hence the polymer partitioned

between aqueous and microemulsion phases only. We assume that the amount of surfactant in the lower aqueous phase of a Type III is negligible and the increase in the viscosity is only due to presence of polymer dissolved in the water. This conclusion is based on the observation that we have in the case without polymer where the aqueous phase viscosity was the same as water viscosity in Type III systems (Refer to Section 4.1.2 for more details).

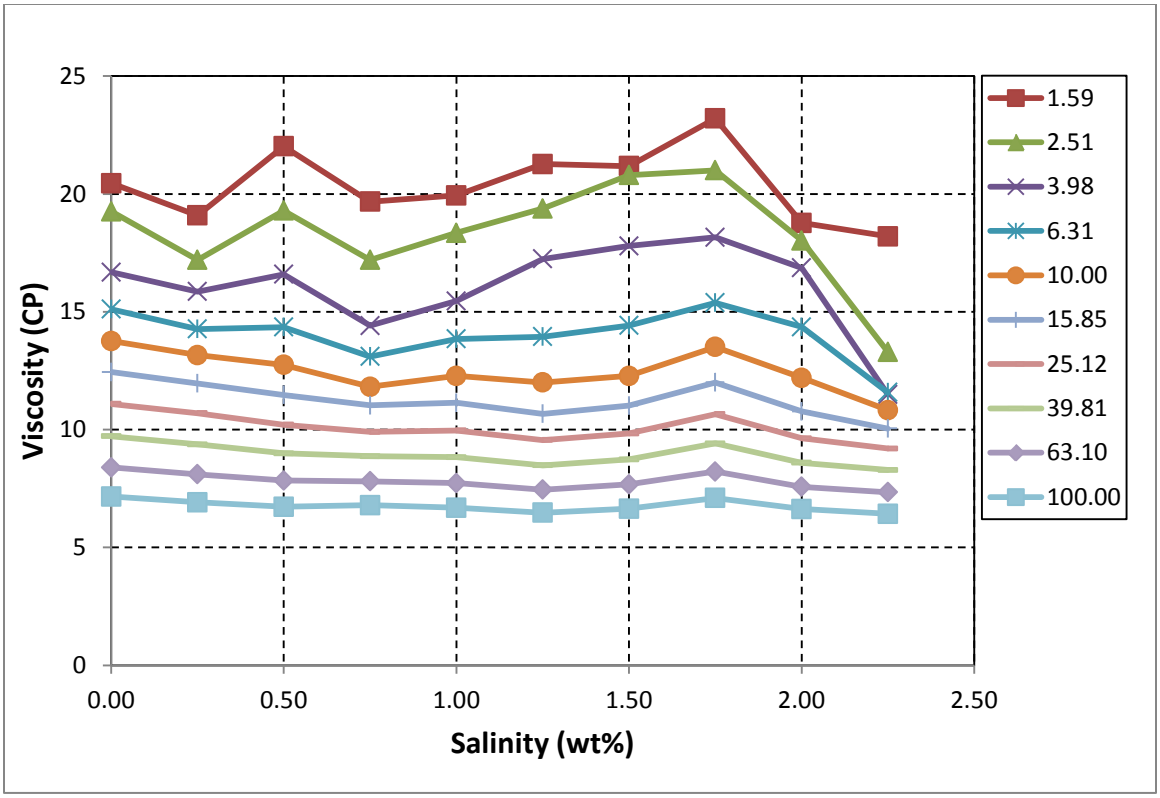

Figure 5.11: Polymer viscosity measurements vs. salinity at different shear rates in sec^{-1}.

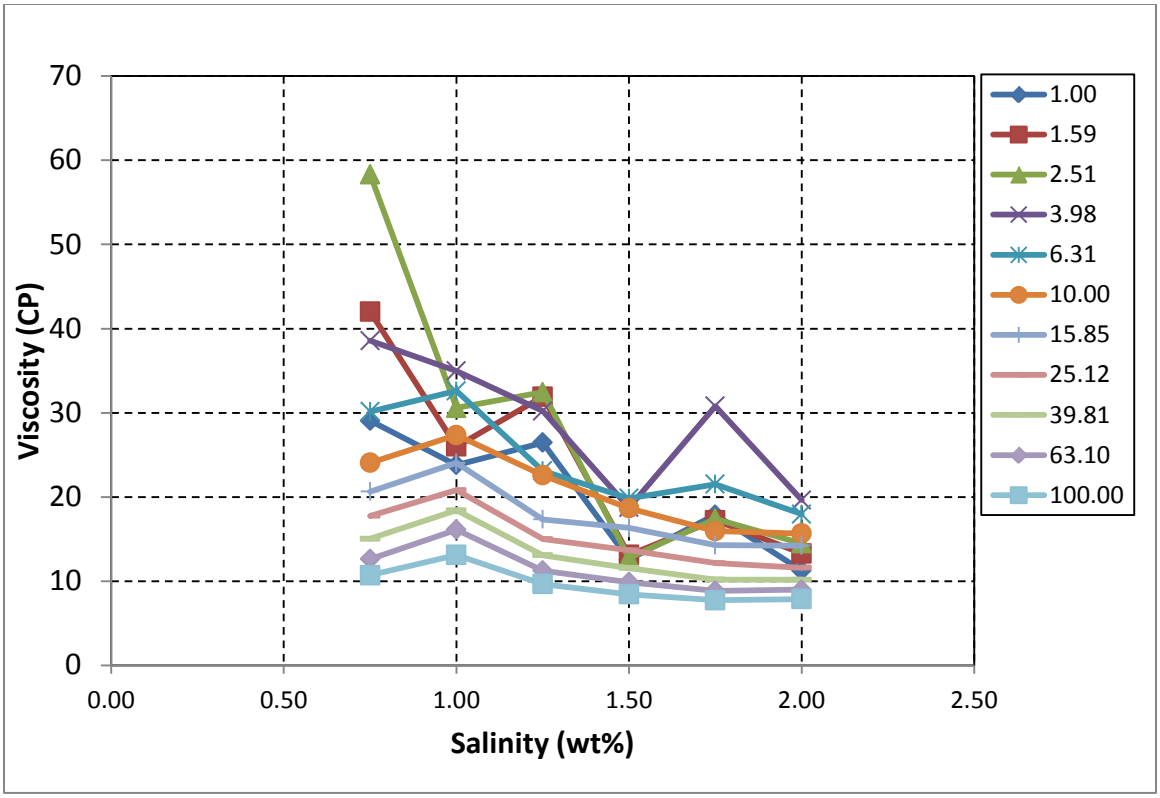

Figure 5.12: Aqueous phase viscosity for samples with Type III phase behavior at different shear rate of Sec^{-1}

Microemulsion Phase Viscosity

For solutions with Type I and Type III phase behavior, the experimental measurements with polymer show similar trend with salinity to the samples without polymer (Figure 5.13 and Figure 5.14). The microemulsion phase viscosity with Type I phase behavior has a linear correlation with salinity and with Type III phase behavior has a parabolic relation with salinity. Based on this observation, we will modify Eq. (5.2) to account for the effect of polymer on the viscosity of microemulsion phase.

We first compare the microemulsion viscosities at shear rate of 10 sec^{-1} for solutions with and without polymer. Figure 5.15 shows such a comparison for Type I phase behavior and Figure 5.16 shows the comparison for Type III phase behavior. The

results for Type I suggest that we can replace the water viscosity with polymer viscosity in the proposed viscosity model. Results for Type III show that the presence of polymer increases the microemulsion viscosity by a factor of 1 to 3 and without a correlation with polymer viscosity itself.

We only have one sample for Type II phase behavior which limits us in drawing a solid conclusion for the effect of polymer in this phase behavior.

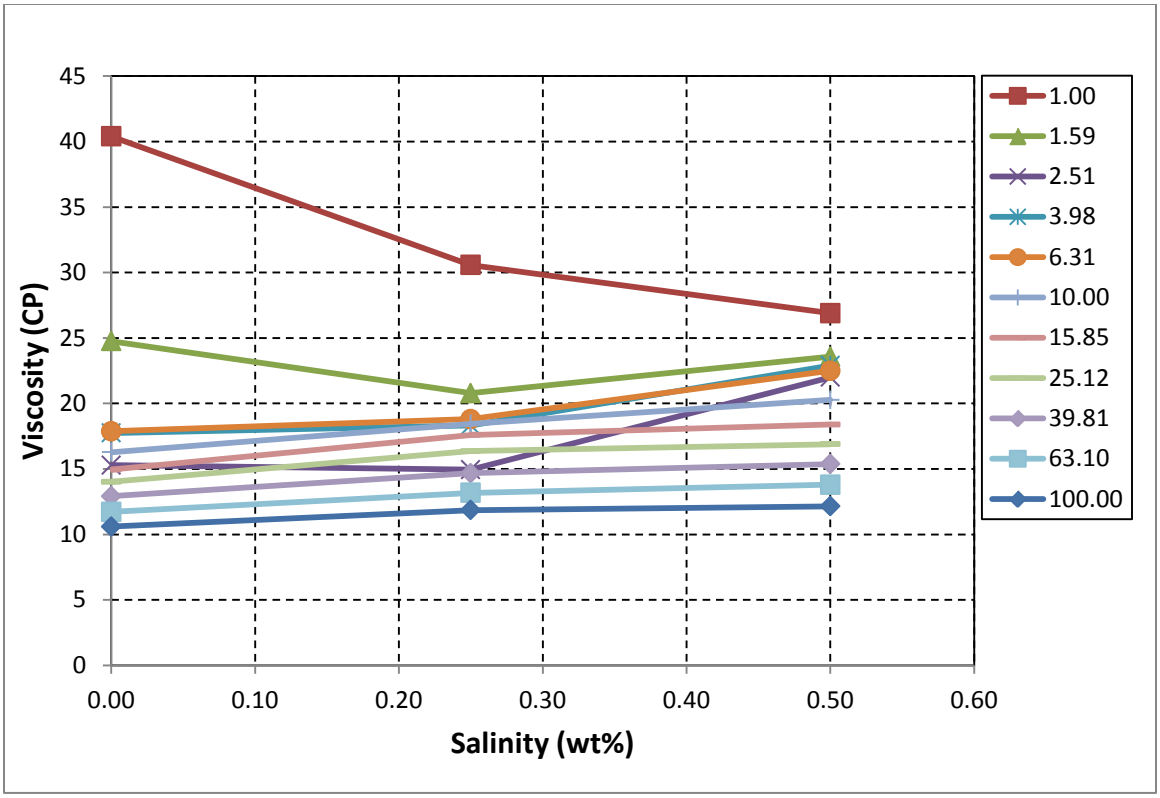

Figure 5.13: Viscosity vs. salinity for samples with Type I phase behavior (AO 352 with polymer) for different shear rates in Sec^{-1}.

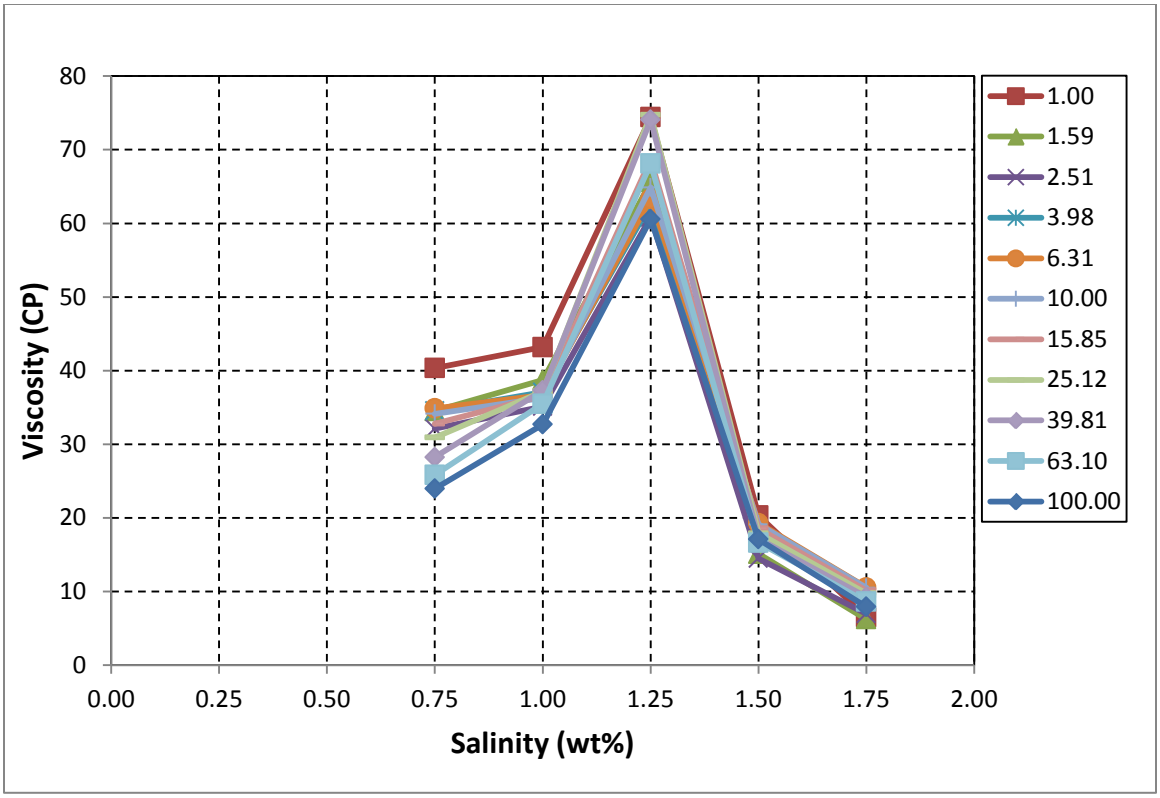

Figure 5.14: Viscosity vs. salinity for samples with Type III phase behavior (AO 352 with polymer) for different shear rates in Sec^{-1}.

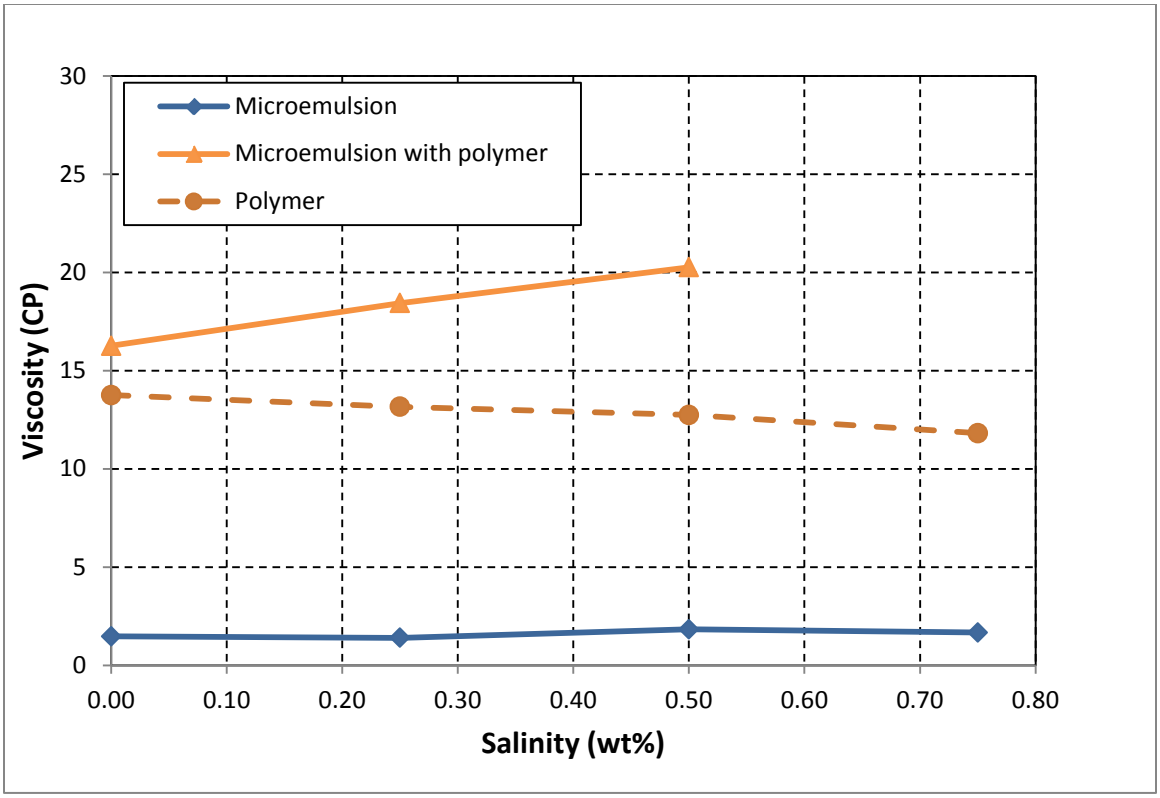

Figure 5.15: Comparison between microemulsion viscosities (with and without polymer) for system with Type I phase behavior at shear rate of 10 sec^{-1}.

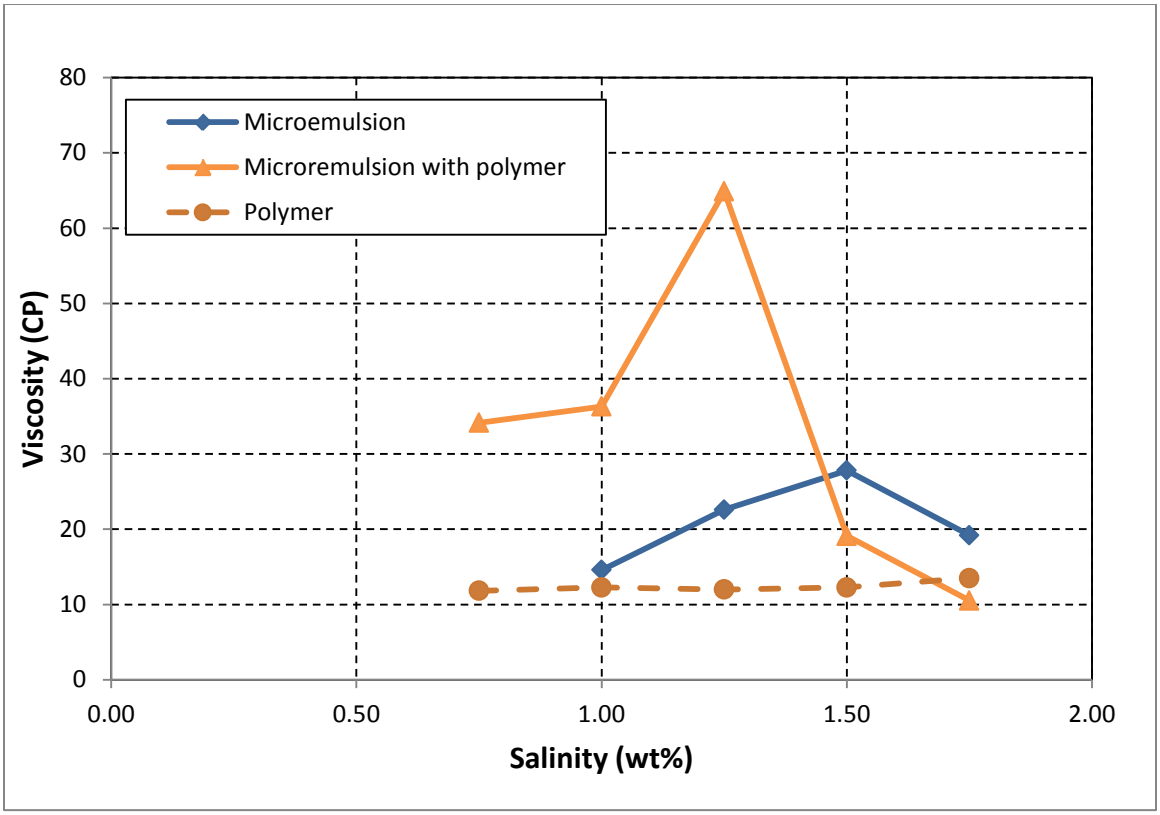

Figure 5.16: Comparison between microemulsion viscosities (with and without polymer) for system with Type III phase behavior at shear rate of 10 sec^{-1}.

5.2.3 AO 03 Data Set

2500 ppm of HPAM 3330 polymer was added to surfactant formulation used in AO 03 samples discussed in Section 4.1.3. There are 10 samples for which we have viscosity measurements for all equilibrium phases in each test tube. We make a comparison between the results with and without polymer.

Since we have viscosity measurements for microemulsion formulation with and without polymer as well as measurements for polymer viscosities at the same salinities, we investigated the polymer partitioning between different phases and its effect on

microemulsion viscosity. For more clarity, we do our analyses based on the type of phase behavior.

Type I phase behavior

A summary of viscosity measurements for samples with Type I phase behavior (formulation with and without polymer) are shown in Table 5.21. It can be concluded from the results that almost all polymer is in the bottom phase for samples with Type I phase behavior. However, when we have polymer and surfactant in a system, the overall viscosity of the bottom phase is higher than polymer viscosity. This higher viscosity could be due to some molecular interaction between polymer molecules and surfactant molecules. In almost all cases that we have, whenever polymer is present in the system, overall phase viscosities are 1.5 to 2.0 times higher than polymer viscosity.

Based on these finding, we recommend using the same correlation we offered in Eq. (5.2) to model microemulsion viscosity for Type I systems. In the absence of experimental measurements for microemulsion with polymer, we suggest the following model for the microemulsion viscosity for Type I phase behavior system.

$$\mu_1 = \beta_1 \mu_p \left(\alpha_1 + \alpha_2 C_{SE}\right) \tag{5.3}$$

In the above equation, α_1 and α_2 are matching model parameters and β_1 is a coefficient between 1.5 to 2.0 to account for the interaction effect between polymer and surfactant. μ_p is polymer viscosity.

Table 5.21: Bottom phase aqueous viscosities for samples with Type I phase behavior (AO 03 data set)

Sample #	Salinity	Bottom Phase Viscosity		Polymer Viscosity
		No Polymer	With Polymer	
1	1.25		27.41	23.85
2	1.5	1.53	38.46	25.38
3	1.75	1.74		26.05
4	2	1.45		27.51
5	2.25			27.41
6	2.5	1.34		27.62

Type II Phase Behavior

When we look at the viscosity of the bottom phase (aqueous phase) and we compare it with the polymer viscosity, we see that almost the entire polymer stays in the bottom phase and we can assume that the bottom phase viscosity is a function of polymer viscosity (Figure 5.17). The results show that when we have polymer, it increases the bottom phase viscosities to higher values by a factor of 1.5 to 2.0 times higher than polymer viscosity. Again, this could be due to molecular interaction between polymer and surfactant in the system.

Type III Phase Behavior

For the middle phase in samples with Type III phase behavior (microemulsion phase) we introduced the following equation:

$$\mu_3 = \alpha_5 + \frac{\alpha_6}{C_{SE}^{0.5}} + \alpha_7 e^{C_{SE}} \tag{5.4}$$

We used our lab results to verify the above equation for the case with and without polymer. Table 5.22 and Figure 5.18 show the model parameters and the match between lab and model results. Figure 5.18 shows an excellent match between model results and lab data for the case with and without polymer. It is interesting to note that the presence of polymer increases the microemulsion (middle phase) viscosity by a factor of 1.5 to 2.

The results show that the same equation [Eq. (5.2)] can be used to match microemulsion (middle phase) viscosity for the cases with and without polymer. However, in the absence of lab measurements for microemulsion solutions with polymer, and based on the above observations, we offer the following model for the middle phase viscosity in a Type III phase behavior system:

$$\mu_3 = \beta_2 \left(\alpha_5 + \frac{\alpha_6}{C_{SE}^{0.5}} + \alpha_7 e^{C_{SE}} \right) \tag{5.5}$$

where β_2 is a coefficient between 1.5 to 2 and α_5, α_6, and α_7 are matching parameters for the case without polymer .

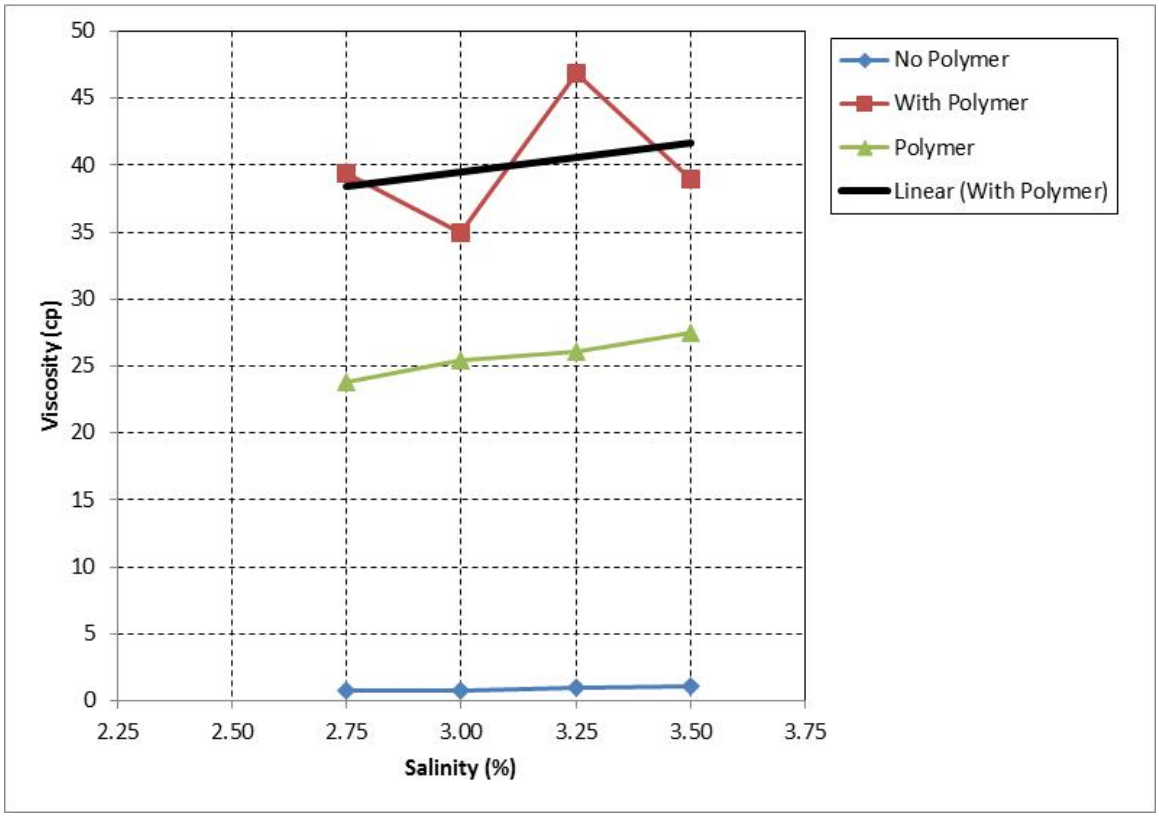

Figure 5.17: Comparison of polymer viscosity and bottom phase viscosities for samples with and without polymer in a Type III phase behavior (AO 03 data set)

Table 5.22: Microemulsion viscosities for the cases with and without polymer in Type III (AO 03 data set)

AO 03 data - Middle (microemulsion) phase viscosity		
Salinity (%)	Viscosity (cp)	
	No Polymer (10 1/s)	With Polymer (10 1/s)
2.50		33.3
2.75	16.2	44.5
3.00	20.1	37.1
3.25	27.0	40.7
3.50	7.3	27.5
α5	3476	1559
α6	-1281	-533
α7	-996	-463

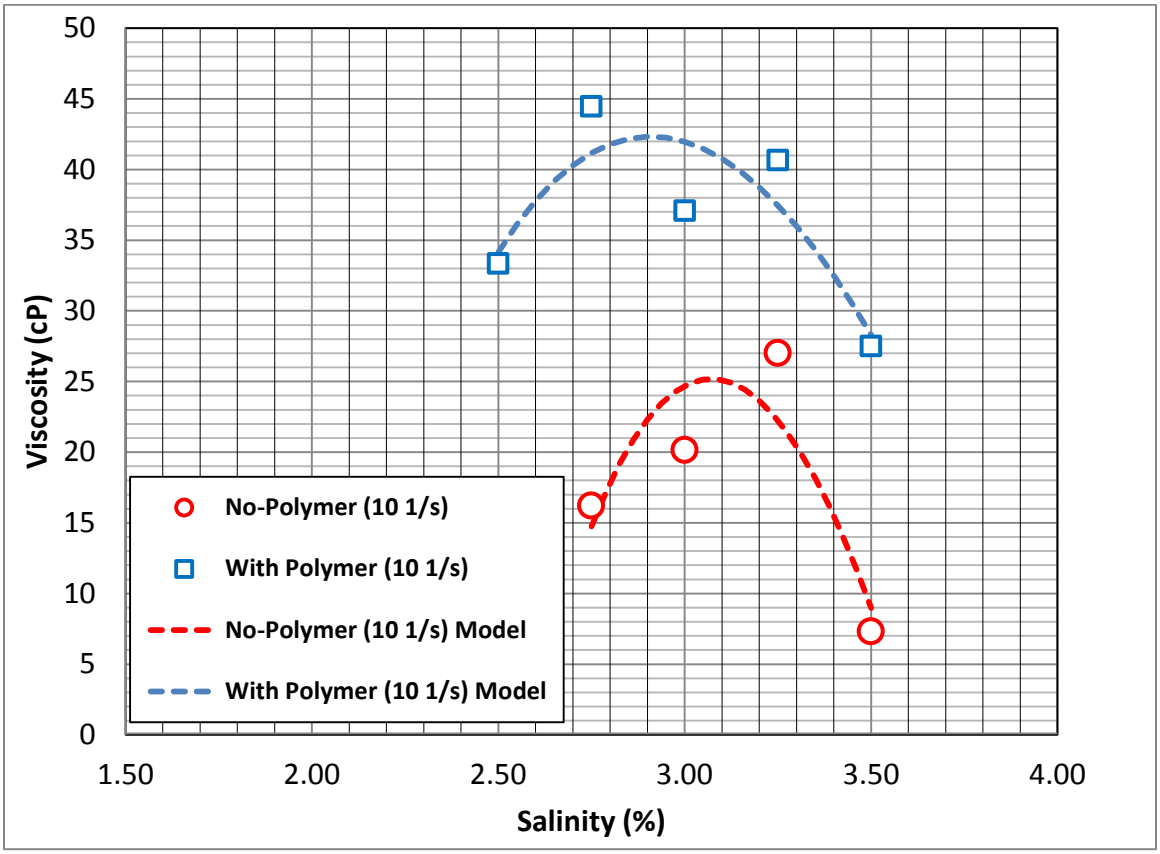

Figure 5.18: Microemulsion phase viscosity with and without polymer for a Type III phase behavior (AO 03 data set).

5.2.4 PCN 128 Data Set

PCN 128 is a solution of 3.0% IBA-10EO, Na_2CO_3 scan in PCNSSB with 30% oil (053-1a) at 38 °C. Two sets of lab data (with and without polymer) are available for this case. 4000 ppm of FP3630S polymer is used for the solution with polymer. Viscosities are measured at different salinity. Samples with polymer were prepared at higher concentration of 6000 to 8000 ppm Polymer mother solution in base brine (1000 ppm injection water), then diluted to 4000 ppm Polymer at each tubes. Na_2CO_3 are

prepared in the same way: 20% mother solution then diluted to the concentration at each tube.

Viscosity measurements are all for microemulsion phase (middle phase) in Type III. This data set is used to qualitatively investigate the effect of polymer on the microemulsion viscosity. Table 5.23 shows the experimental measurements for microemulsion viscosities with and without polymer at shear rate of 1 sec^{-1}. Figure 5.19 shows that the viscosity trend is the same for the case with and without polymer which suggests that the same equation should be applicable to both cases. Here we also see that when the polymer is added to the system, the microemulsion phase viscosity is increased by a factor of 1.5 to 2.0.

Table 5.23: Microemulsion viscosities with and without polymer at shear rate of 1 sec^{-1}

Microemulstion Viscosity at shear rate 1		
Salinity (ppm)	Viscosity (cp)	
	No Polymer (lab)	With Polymer (lab)
21000	43.8	183.5
31000	209.4	317.2
41000	202.6	290.9

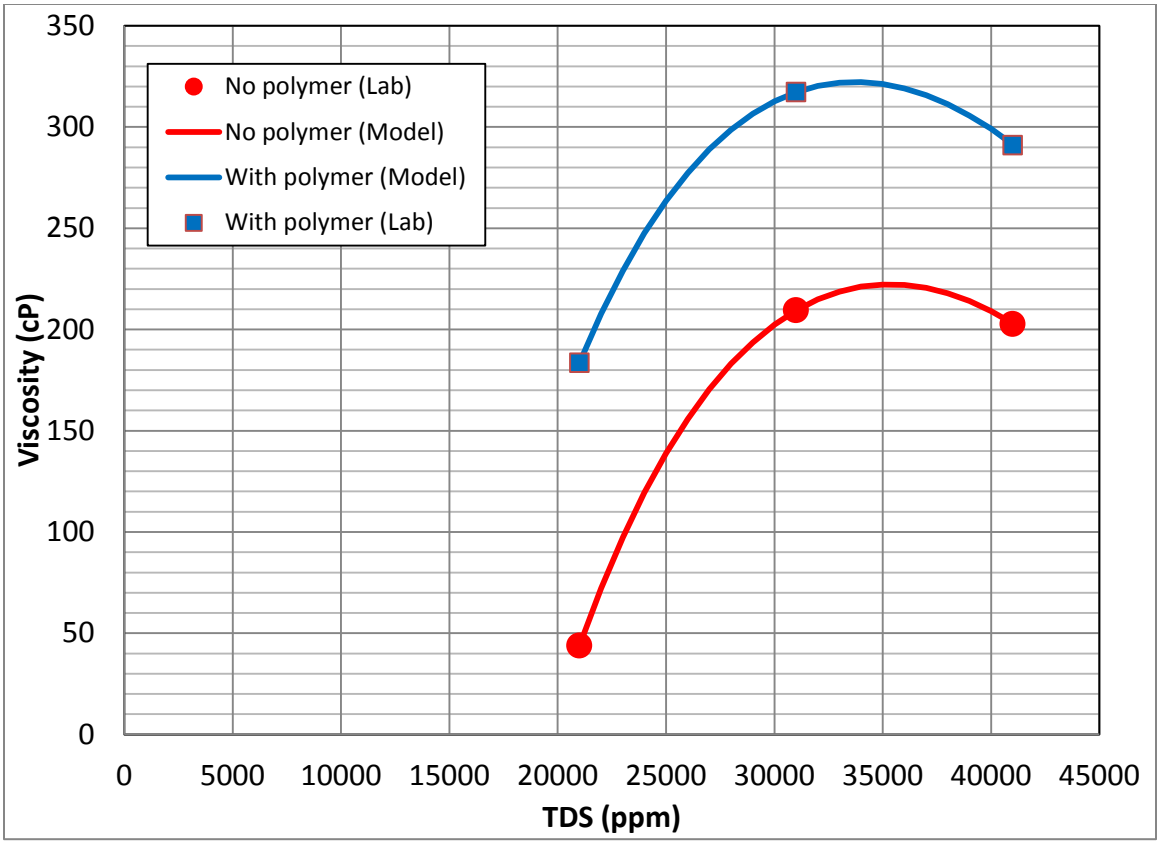

Figure 5.19: Comparison of microemulsion phase viscosity with and without polymer (PCN 128 data set).

Chapter 6: Simulation Case Study

6.1 UTCHEM SIMULATOR

UTCHEM is a three-dimensional, multiphase, multicomponent chemical flooding simulator developed at the Center for Petroleum and Geosystems Engineering at The University of Texas at Austin [(Pope, et al., 1979), (Datta-Gupta, et al., 1986), (Saad, et al., 1998), (Delshad, et al., 1996), (Delshad, et al., 2006)]. The simulator is designed to be used for complex surfactant/oil/brine phase behavior, petrophysical properties, chemical reactions, and heterogeneity in porous media. It also supports three-phase relative permeability, capillary desaturation of oil, water and microemulsion phases, shear thinning and viscoelastic polymer viscosity.

Some of the key features in UTCHEM numerical simulator include surfactant phase behavior [(Pope & Nelson, 1978); (Prouvost, et al., 1985); (Camilleri, et al., 1987)], three phase relative permeability (Delshad, et al., 1987), oil desaturation (Delshad, et al., 1986), well modeling (Saad, 1989), shear-thinning polymer viscosity (Wreath, et al., 1990), and tracer partitioning (Jin, 1995).

Advanced numerical techniques such as high-order numerical accuracy and dispersion control are implemented in UTCHEM. The solution scheme is similar to IMPES, where pressure is solved fully implicitly but concentrations are solved explicitly. UTCHEM has several applications in modeling enhanced oil recovery. Mathematical model developments are based on the following assumptions:

1. Fluids and rocks are slightly compressible.
2. Local thermodynamic equilibrium except for tracers and dissolution of organic components.
3. The solid phase is immobile.

4. Darcy's law applies.
5. Ideal mixing rule.
6. The fluid phase behavior is independent of reservoir pressure.
7. Dispersion follows a generalization of Fick's law to multiphase flow in porous media.

6.1.1 UTCHEM Viscosity Model

Liquid phase viscosities are modeled in terms of pure component viscosities and the phase concentrations of the oil, water, and surfactant ($C_{i\ell}$):

$$\mu_\ell = C_{1\ell}\,\mu_w e^{\alpha_1(C_{2\ell}+C_{3\ell})} + C_{2\ell}\,\mu_o\, e^{\alpha_2(C_{1\ell}+C_{3\ell})} + C_{3\ell}\,\alpha_3 e^{\left(\alpha_4 C_{1\ell}+\alpha_5 C_{2\ell}\right)} \qquad \textit{for } \ell = 1, 2, \textit{ or } 3 \qquad (6.1)$$

where the α parameters are determined by matching laboratory microemulsion viscosities at several compositions. In the absence of surfactant and polymer, water and oil phase viscosities reduce to pure water and oil viscosities (μ_w, μ_o). When polymer is present, μ_w is replaced by μ_p defined below.

The following exponential relationship is used to compute viscosities as a function of temperature (T).

$$\mu_\kappa = \mu_{\kappa,ref}\,\exp\left[b_\kappa\left(\frac{1}{T}-\frac{1}{T_{ref}}\right)\right] \qquad \textit{for } \kappa = \textit{ water, oil, or air} \qquad (6.2)$$

where $\mu_{\kappa,ref}$ is the viscosity at a reference temperature of T_{ref} and b_κ is an input parameter.

The viscosity of a polymer solution depends on the concentration of polymer and on salinity. The Flory-Huggins equation (Flory, 1953) was modified to account for variation in salinity as

$$\mu_p^0 = \mu_w \left(1 + \left(A_{p1} C_{4\ell} + A_{p2} C_{4\ell}^2 + A_{p3} C_{4\ell}^3\right) C_{SEP}^{S_p}\right) \qquad \textit{for } \ell = 1 \textit{ or } 3 \tag{6.3}$$

where $C_{4\ell}$ is the polymer concentration in the water or microemulsion phase, μ_w is the water viscosity, A_{P1}, A_{P2}, and A_{P3} are model parameters obtained by fitting polymer viscosity as a function of polymer concentration. The factor $C_{SEP}^{S_p}$ allows for dependence of polymer viscosity on salinity and hardness.

The reduction in polymer solution viscosity as a function of shear rate $\dot{\gamma}$ is modeled by Meter's equation (Meter & Bird, 1964):

$$\mu_p = \mu_w + \frac{\mu_p^o - \mu_w}{1 + \left(\frac{\dot{\gamma}}{\dot{\gamma}_{1/2}}\right)^{P_\alpha - 1}} \tag{6.4}$$

where $\dot{\gamma}_{1/2}$ is the shear rate at which viscosity is the average of μ_p^o and μ_w and P_α is an empirical coefficient. When the above equation is applied to flow in permeable media, μ_p is usually called apparent viscosity and the shear rate is an equivalent shear rate $\dot{\gamma}_{eq}$ The in-situ shear rate for phase ℓ is modeled by the modified Blake-Kozeny capillary bundle equation for multiphase flow [(Lin, 1981); (Sorbie, 1991)] as

$$\dot{\gamma}_{eq} = \frac{\dot{\gamma}_c |u_\ell|}{\sqrt{\bar{k} k_{r\ell} \phi S_\ell}} \tag{6.5}$$

where $\dot{\gamma}_c$ is equal to 3.97C sec^{-1} and C is the shear rate coefficient used to account for non-ideal effects such as slip at the pore walls [(Wreath, et al., 1990); (Sorbie, 1991)]. The appropriate average permeability $\bar{k}$ is given by

$$\bar{k} = \left[\frac{1}{k_x}\left(\frac{u_{x\ell}}{u_\ell}\right)^2 + \frac{1}{k_y}\left(\frac{u_{y\ell}}{u_\ell}\right)^2 + \frac{1}{k_z}\left(\frac{u_{z\ell}}{u_\ell}\right)^2\right]^{-1} \tag{6.6}$$

The main determinant of resistance to fluid flow through porous media is the fluid viscosity. Microemulsions are complex fluids which are usually produced by mixing very different components. The molecular interactions between these components can give

rise to unusual rheological properties. Modeling such complicated rheological fluids in reservoir simulators is one of the most important factors on history match processes. The effect of viscosity is more pronounced in matching pressure data. The new viscosity model developed in previous chapter was implemented in UTCHEM reservoir simulator. In this section we verify the new viscosity model by history matching two core flood experiments with special emphasis on pressure match.

We were provided with two coreflood results (PCN-01 and PCN-04), including the design and setup, core properties, and all fluid properties for modeling the corefloods. Great work was done by (Xu, 2012) on history match of the coreflood data for these two experiments. We used his results in our comparisons.

6.2 PCN-01 ACP COREFLOOD HISTORY MATCH

The performance of the ACP formulation to recover crude oil from a Bentheimer core at the reservoir temperature of 38 °C was evaluated in the laboratory. The chemical formulation was developed from phase behavior tests at 38 °C using synthetic softened brine (PCNSSB) and surrogate crude oil diluted with 7.5 wt% Decalin to achieve similar properties as the live oil. The viscosity of the diluted oil is approximately 170 cP at the reservoir temperature of 38 °C. Flopaam 3630S was used in the chemical slug to improve mobility control. From the coreflood results, the oil recovery was 69.5% of residual oil saturation after waterflood and residual oil saturation from chemical flood (S_{orc}) was 13.5%. The pressure drop at steady state looked reasonable with 5.5 psi across the whole core of 1 ft length. The result was not great, but seemed to be promising with very low usage of chemicals such as co-solvent, alkali, and polymer.

The PCN-01 core properties, the ASP slug and polymer drive designs, and brine composition are reported in Table 6.1 through Table 6.3. Microemulsion viscosity with

30% oil was measured at different shear rates at the optimum salinity of 16,000 ppm TDS and it is around 90 cp where the 7.5% Decalin-diluted oil to mimic the live oil, has a viscosity of ~ 170 cp at the reservoir temperature of 38 °C (Figure 6.1). This formulation gives a stable microemulsion viscosity at low shear rate irrespective of the salinities. The polymer slug viscosity should be around 180 cP at a shear rate of 5 sec^{-1} corresponding to insitu velocity of 1 ft/day. This value was given by the inverse total relative mobility shown in (Figure 6.2).

The coreflood was conducted by injecting 0.5 PV ACP slug at a rate of 1 ft/day chased by a polymer drive at the same rate until no more oil was produced. Figure 6.3 shows the cumulative oil recovery, oil cut, and oil saturation vs. pore volume injected.

UTCHEM simulator was used to match the coreflood results including, cumulative oil recovery, oil cut, oil saturation, and pressure drop across the core. Table 6.4 through Table 6.6 summarize input parameters used in the simulation model for this experiment. The main challenge in this history match process was to reasonably match the pressure drop across the core. With the original UTCHEM viscosity model, it was impossible to match the pressure drop (Xu, 2012). After we implemented the new viscosity model, we matched the pressure drop across the core as well as cumulative recovery and oil cut. The viscosity parameters used in the original and the new viscosity models are presented in Table 6.7.

Figure 6.4 shows the pressure drop match for the original viscosity model and the new viscosity model. The results show excellent match using the new viscosity model. Figure 6.5 and Figure 6.6 show very good match of cumulative oil recovery and oil saturation between the lab data, the original viscosity model, and the new viscosity model.

Table 6.1: PCN-01 core properties

Property	**Value**	**Unit**
Length	0.971129	ft
Diameter	0.164167	ft
Area	11.40	cm^2
Porosity	0.21	
Permeability*	2507	md
Pore Volume	0.004944	ft^3
Temperature	38	^oC
Initial Oil Saturation before ACP	0.443	
Residual Water Saturation	0.17	
Water Relative Permeability	0.07	
Oil Relative Permeability	0.95	

Table 6.2: Compositions of synthetic brine (PCNSSB) for PCN-01 coreflood.

Ion	**Concentration (ppm)**
Potassium	11.59
Sodium	300.00
Magnesium	0
Calcium	0
Chlorine	140.81
Sulfate	310.41
Bicarbonate	176.95
TDS	939.76

Table 6.3: ASP slug and polymer drive used in PCN-01 coreflood

ACP Slug	**Polymer Drive**
0.5 PV	1.4 PV
1.5% Huntsmann n-Butyl-5EO	2250 ppm Flopaam 3630S in PCNSSB (934 ppm TDS)
Frontal velocity: 1 ft/day	Frontal velocity : 1 ft/day
6,000 ppm Na_2CO_3 in PCNSSB (6,934 ppm TDS)	
2750 ppm Flopaam 3630S	
Viscosity: ~ 100 cp @ 5 s^{-1}, 38 °C	Viscosity: ~140 cp @ 5 s^{-1}, 38 °C

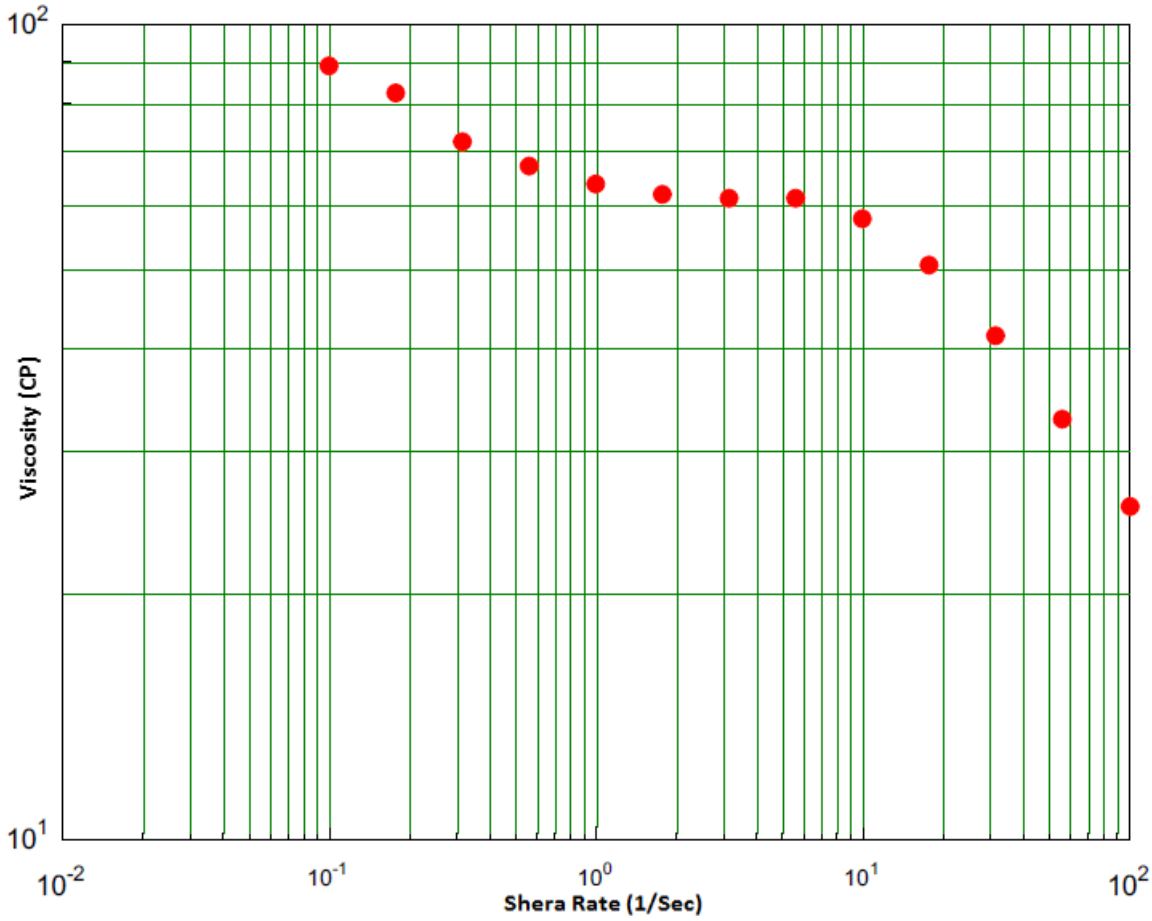

Figure 6.1: Microemulsion viscosity with 1.5% Butyl-5EO in PCNSSB at 16000 ppm TDS in 30% oil.

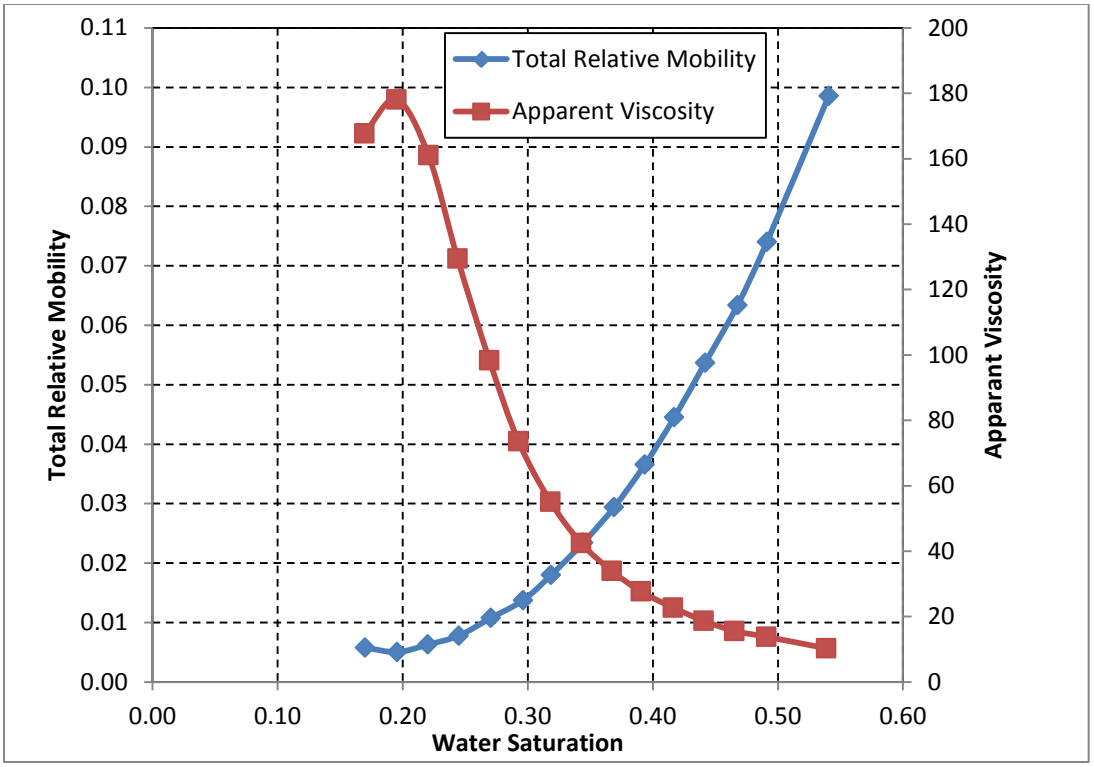

Figure 6.2: PCN-01 apparent viscosity and total relative mobility.

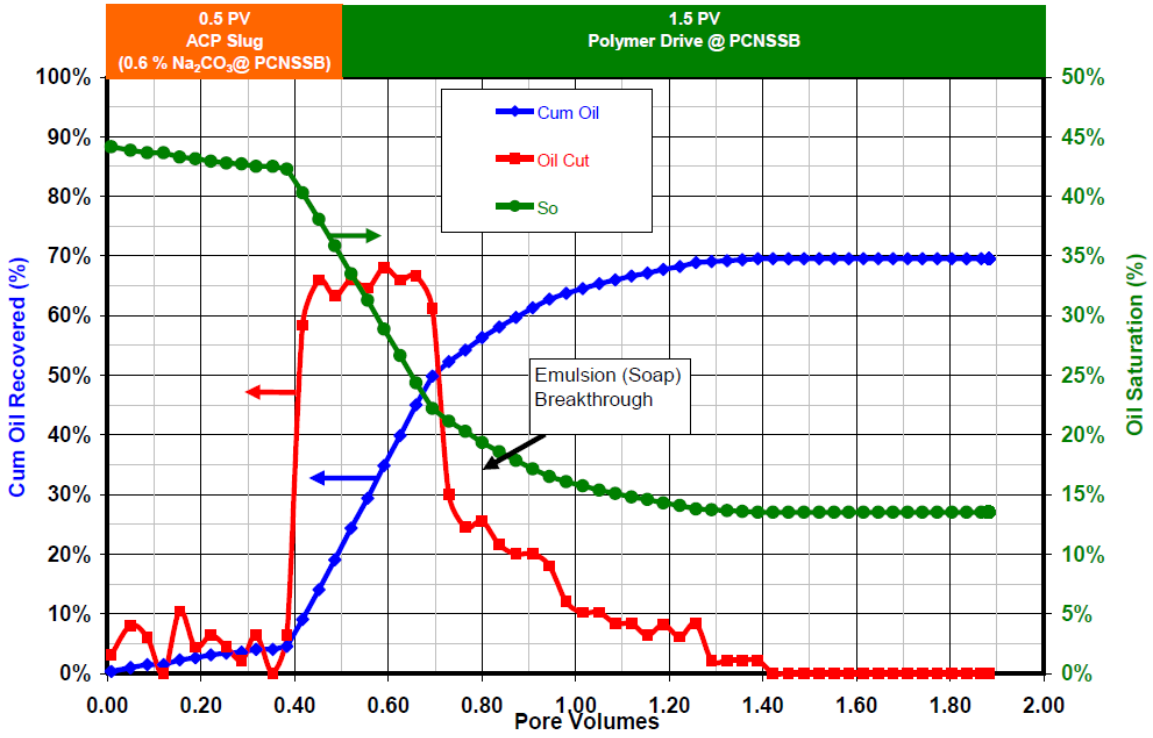

Figure 6.3: Oil recovery, oil saturation, and oil cut for PNC-01 coreflood.

Table 6.4: Co-solvent and soap phase behavior UTCHEM input parameters (Xu, 2012).

Input Parameters	**Value**
HBNC70	0.15
HBNC71	0.13
HBNC72	0.15
CSEL7, meq/mL	0.1415
CSEU7, meq/mL	0.2264
IMIX	0
CSELP, meq/mL	0.2
CSEUP, meq/mL	0.33

Table 6.5: Polymer input parameters (Xu, 2012)

Input Parameters	**Value**
AP1	50
AP2	150
AP3	1200
SSLOPE	-0.4435
GAMAC	4
GAMHF, GAMHF2	10,0
POWN	2.3
BRK	100
CRK	0

Table 6.6: Input parameters for co-solvent/microemulsion properties (Xu, 2012)

Input Parameters	**Value**
AD31	1.6
AD32	0.1
B3D	1000
AD41	0.48
AD42	0
B4D	100

Table 6.7: Viscosity parameters for the original and the new viscosity models

Input Parameters	**Original Viscosity Model**	**New Viscosity Model [Eq.** (5.2)**]**
ALPHAV1	0.1	3.15
ALPHAV2	1.7	-13
ALPHAV3	0.1	0.51
ALPHAV4	0	-1.35
ALPHAV5	0	1060
ALPHAV6	Not applicable	-100
ALPHAV7	Not applicable	-650

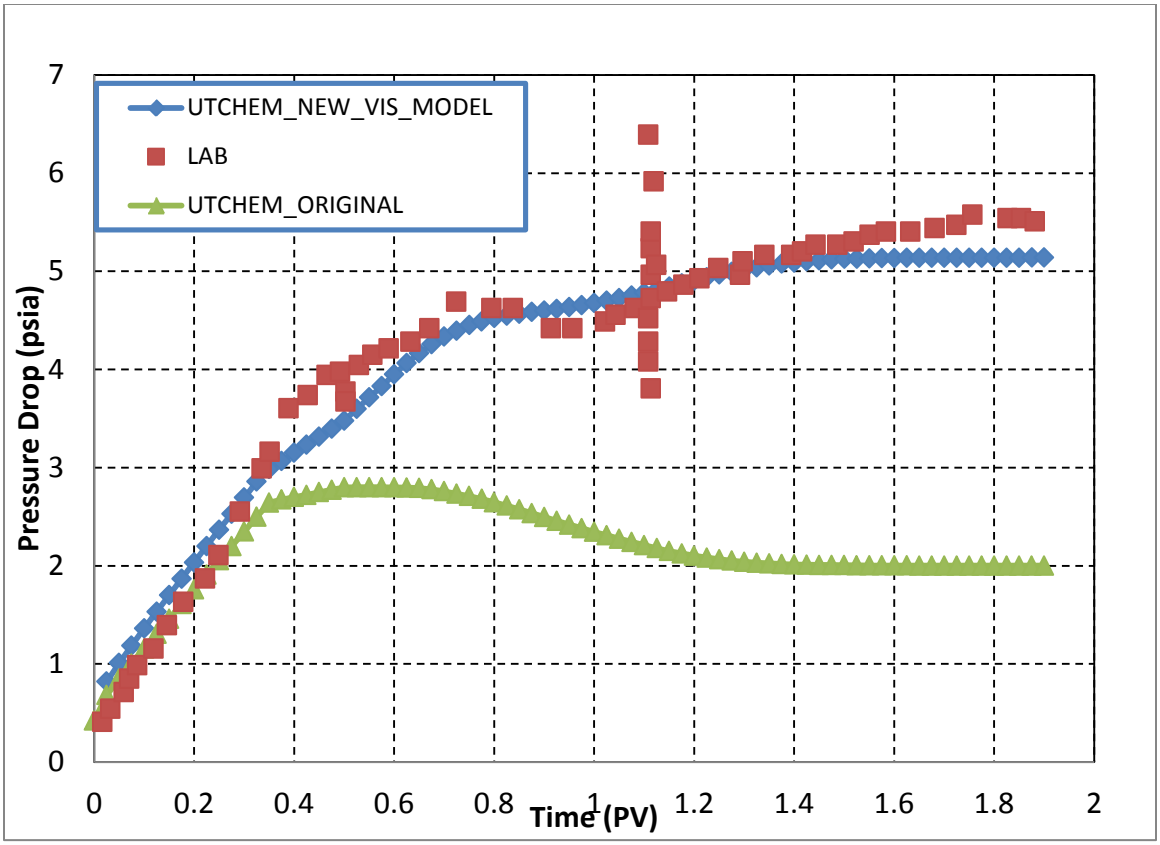

Figure 6.4: Pressure drop across entire core for PCN-01 coreflood.

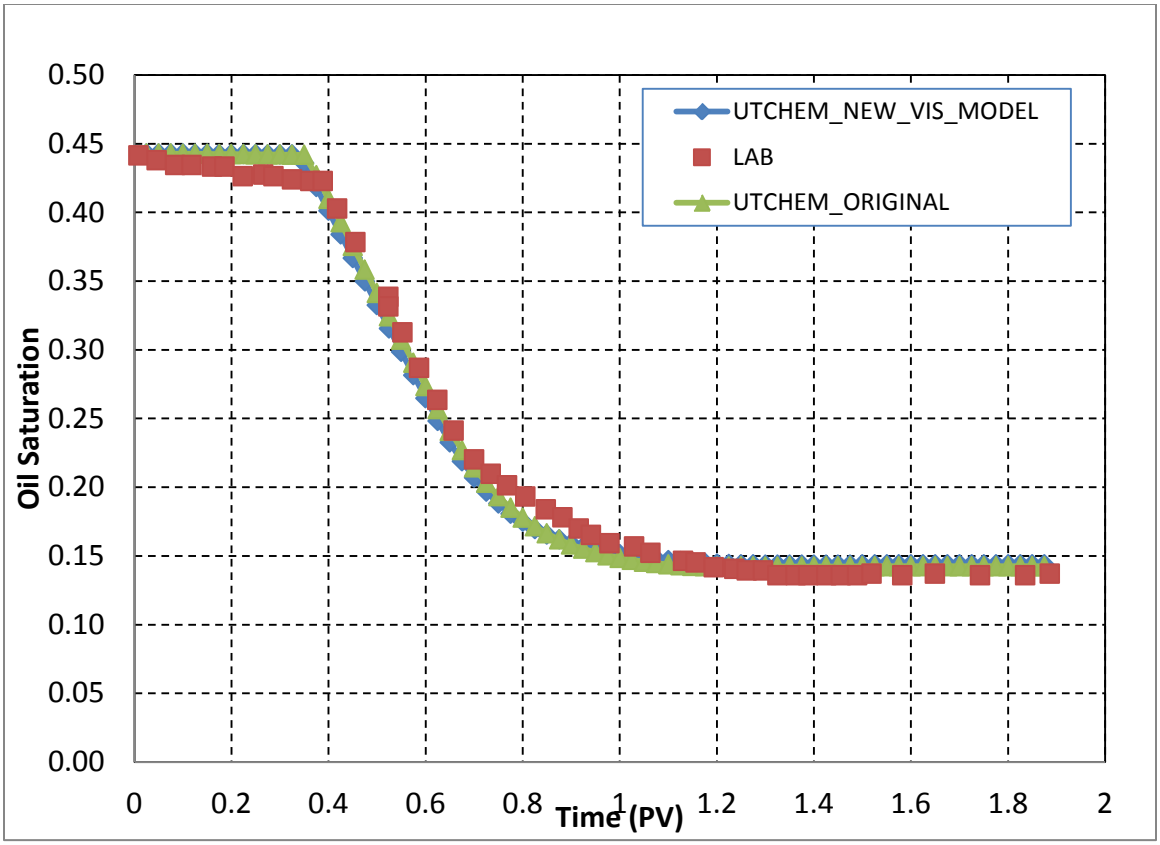

Figure 6.5: Oil saturation for PCN-01 coreflood.

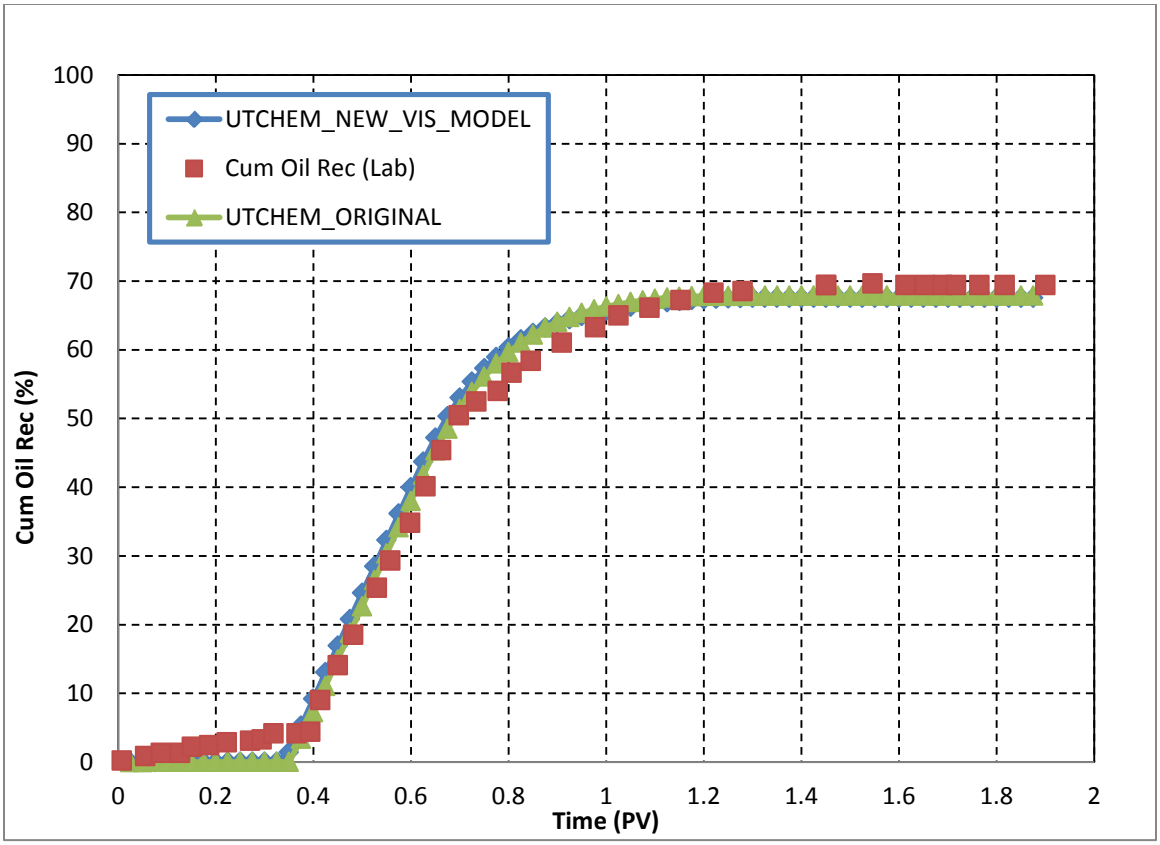

Figure 6.6: Cumulative oil recovery for PCN-01 coreflood.

6.3 PCN-04 ACP COREFLOOD HISTORY MATCH

The chemical formulation was developed using aqueous and microemulsion phase behavior tests at 38 °C using Synthetic Softened brine (PCNSSB) and surrogate crude oil diluted with 7.5 wt% Decalin. The performance of similar formulation (Iso-Butyl-10EO) was proven very well from the Bentheimer core flood. The viscosity of the oil with the dilution is approximately 170 cP at the reservoir temperature of 38 °C. The oil recovery was 98 % of residual oil saturation after water flood (36%) with an average oil cut of 60 % in the oil bank and the residual oil saturation from chemical flood (S_{orc}) was 0.8 %.

The pressure drop at steady state was measured as 12.9 psi across the whole core of 1 ft length.

Microemulsion viscosity with 30% oil was measured at different shear rates at the salinity of 31,000 ppm TDS and the viscosity was measured around 90 cp where the 7.5% Decalin-diluted oil has a viscosity of ~ 160 cp at the reservoir temperature of 38 °C. This formulation gives a stable microemulsion viscosity at low shear rate irrespective of the salinities in this measurement.

The PCN-04 core properties, the ASP slug and polymer drive designs, and brine composition used for this coreflood experiment are reported in Table 6.8 through Table 6.10.

A 0.3 PV ACP slug was injected at a rate of 1 ft/D followed by a polymer drive (~ 10,934 ppm TDS) at the same velocity until no more oil is produced. Figure 6.7 shows the cumulative oil recovery, oil cut, and oil saturation vs. pore volume injected.

UTCHEM simulator was used to match the coreflood results including, cumulative oil recovery, oil cut, oil saturation, and pressure drop across the core. Table 6.11 through Table 6.13 summarize input parameters used in the simulation model for this experiment. The viscosity parameters used in the original and the new viscosity models are presented in Table 6.14.

The main objective here is to improve the match for the pressure drop using the new proposed microemulsion viscosity model.

Figure 6.8 shows the pressure drop match for the original viscosity model [Eq. (4.1)] and the new viscosity model [Eq. (5.2)]. The results show an excellent match using the new viscosity mode. Figure 6.9 and Figure 6.10 show very good match of cumulative

oil recovery and oil saturation between lab data, the original viscosity model, and the new viscosity model.

Table 6.8: PCN-04 core properties

Property	**Value**	**Unit**
Length	0.91667	ft
Diameter	0.125	ft
Porosity	0.28	
Permeability*	1500	md
Pore Volume	0.00315	ft^3
Temperature	38	^oC
Initial Oil Saturation before ACP	0.36	
Residual Water Saturation	0.36	
Water Relative Permeability	0.03	
Oil Relative Permeability	1.0	

Table 6.9: Compositions of synthetic brine (PCNSSB) for PCN-04 coreflood.

Ion	**Concentration (ppm)**
Potassium	11.59
Sodium	300.00
Magnesium	0
Calcium	0
Chlorine	140.81
Sulfate	310.41
Bicarbonate	176.95
TDS	939.76

Table 6.10: ASP slug and polymer drive used in PCN-04 coreflood

ACP Slug	**Polymer Drive**
0.3 PV	1.6 PV
3% Huntsmann iso-Butyl-10EO	10,000 ppm Na_2CO_3 in PCNSSB (10,934 ppm TDS)
Frontal velocity: 1 ft/day	Frontal velocity : 1 ft/day
30,000 ppm Na_2CO_3 in PCNSSB (30,934 ppm TDS)	
4000 ppm Flopaam 3630S	4000 ppm Flopaam 3630S
Viscosity: ~ 125 cp @ 5 s^{-1}, 38 °C	Viscosity: ~185 cp @ 5 s^{-1}, 38 °C

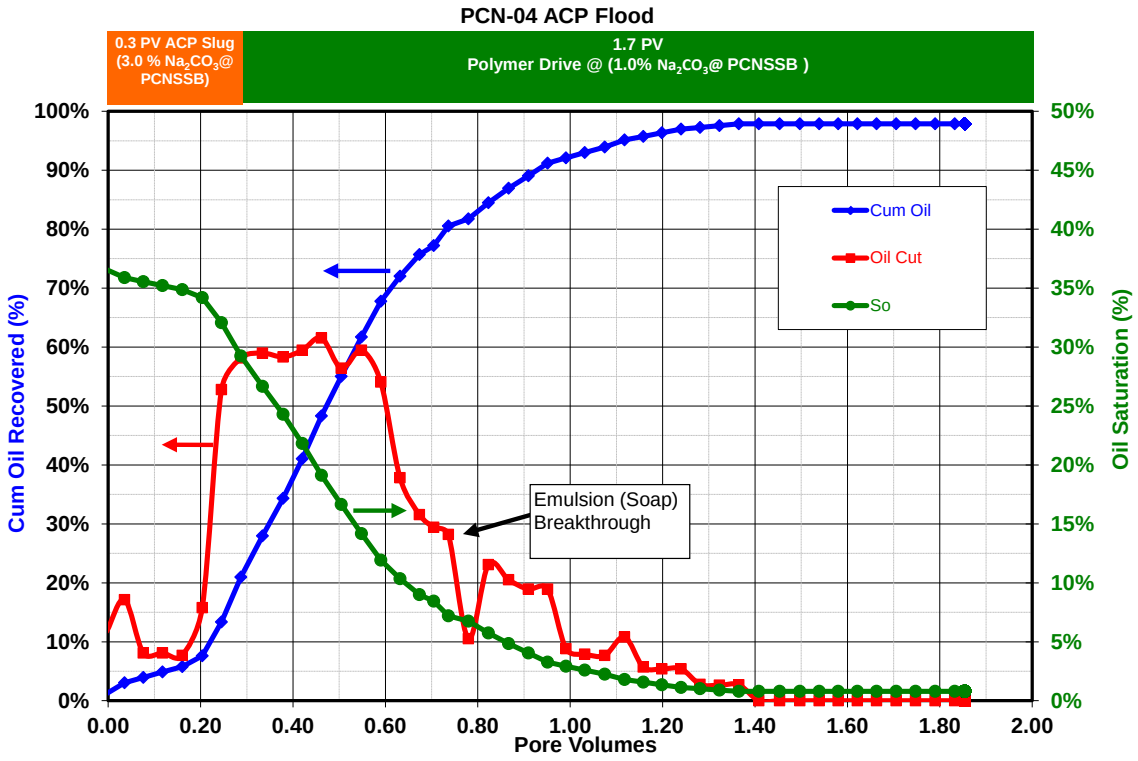

Figure 6.7: Oil recovery, oil saturation, and oil cut for PNC-04 coreflood.

Table 6.11: Co-solvent and soap phase behavior input parameters (Xu, 2012).

Input Parameters	**Value**
HBNC70	0.06
HBNC71	0.04
HBNC72	0.06
CSEL7, meq/mL	0.34
CSEU7, meq/mL	0.79
IMIX	1
HBN0	0.005
HBN1	0.0003
HBN2	0.0005
CSELP, meq/ML	0.34
CSEUP, meq/mL	0.79

Table 6.12: Polymer input parameters (Xu, 2012)

Input Parameters	Value
AP1	50
AP2	150
AP3	1200
SSLOPE	-0.389
GAMAC	4
GAMHF, GAMHF2	0.5,0
POWN	1.9
BRK	100
CRK	0

Table 6.13: Input parameters for co-solvent/microemulsion properties (Xu, 2012)

Input Parameters	Value
AD31	1.6
AD32	0.1
B3D	1000
AD41	4.5
AD42	0.5
B4D	100

Table 6.14: Viscosity parameters for the original and the new viscosity models

Input Parameters	Original Viscosity Model	New Viscosity Model
ALPHAV1	0.1	2.00
ALPHAV2	1.7	16.8
ALPHAV3	0.1	0.15
ALPHAV4	0	0.0
ALPHAV5	0	3020
ALPHAV6	Not applicable	-1155
ALPHAV7	Not applicable	-675

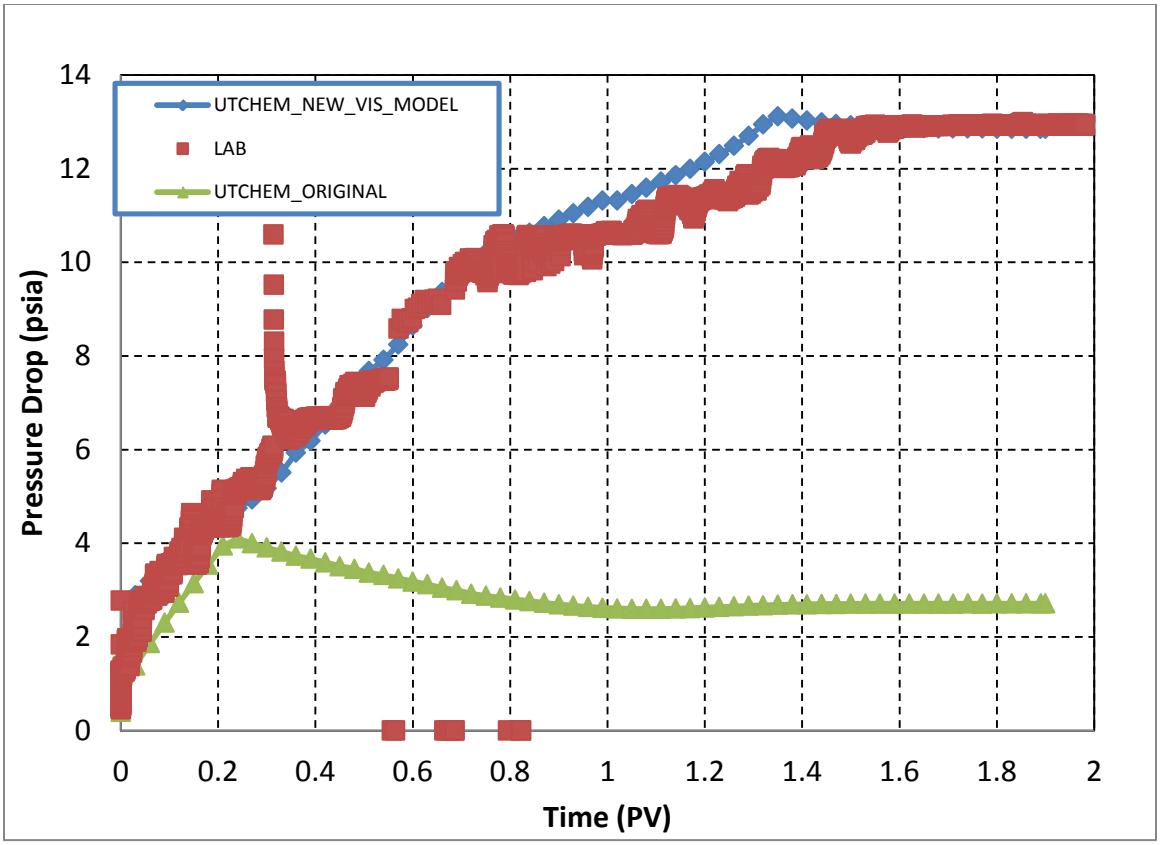

Figure 6.8: Pressure drop across entire core for PCN-04 coreflood.

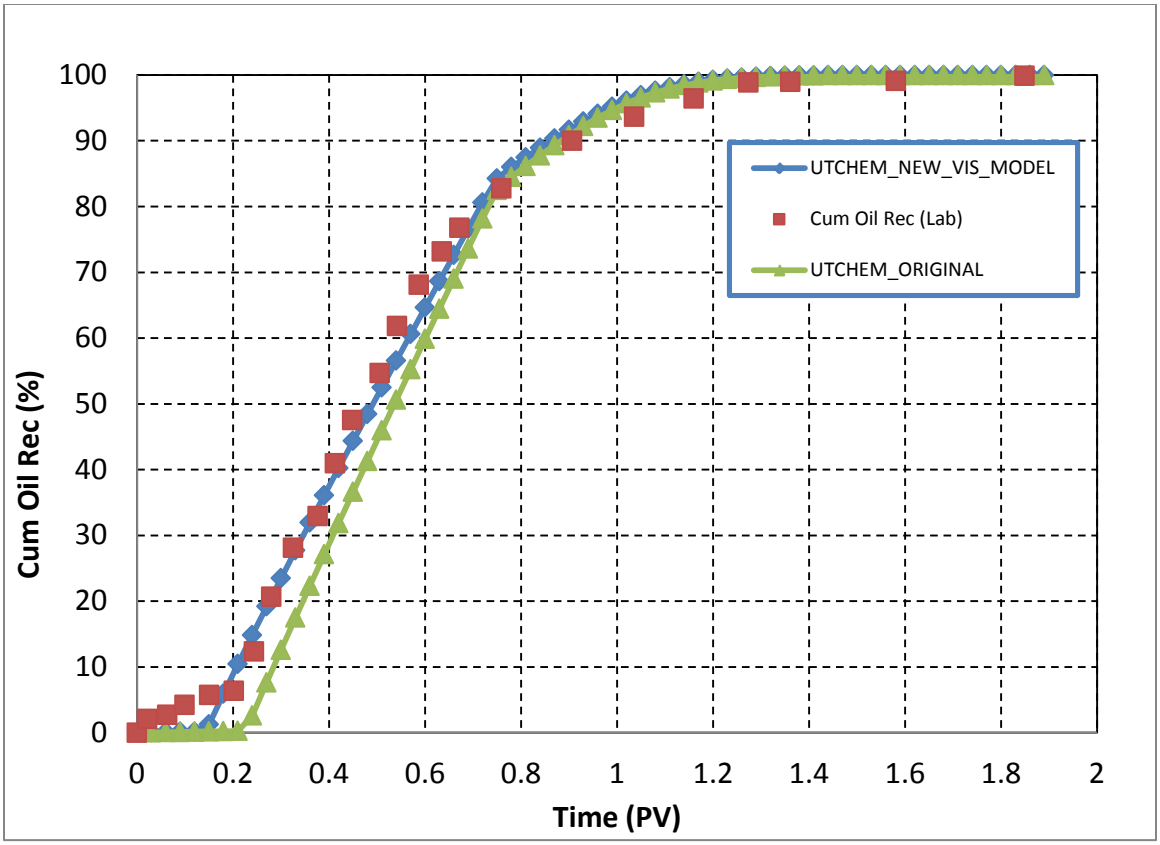

Figure 6.9: Cumulative oil recovery for PCN-04 coreflood.

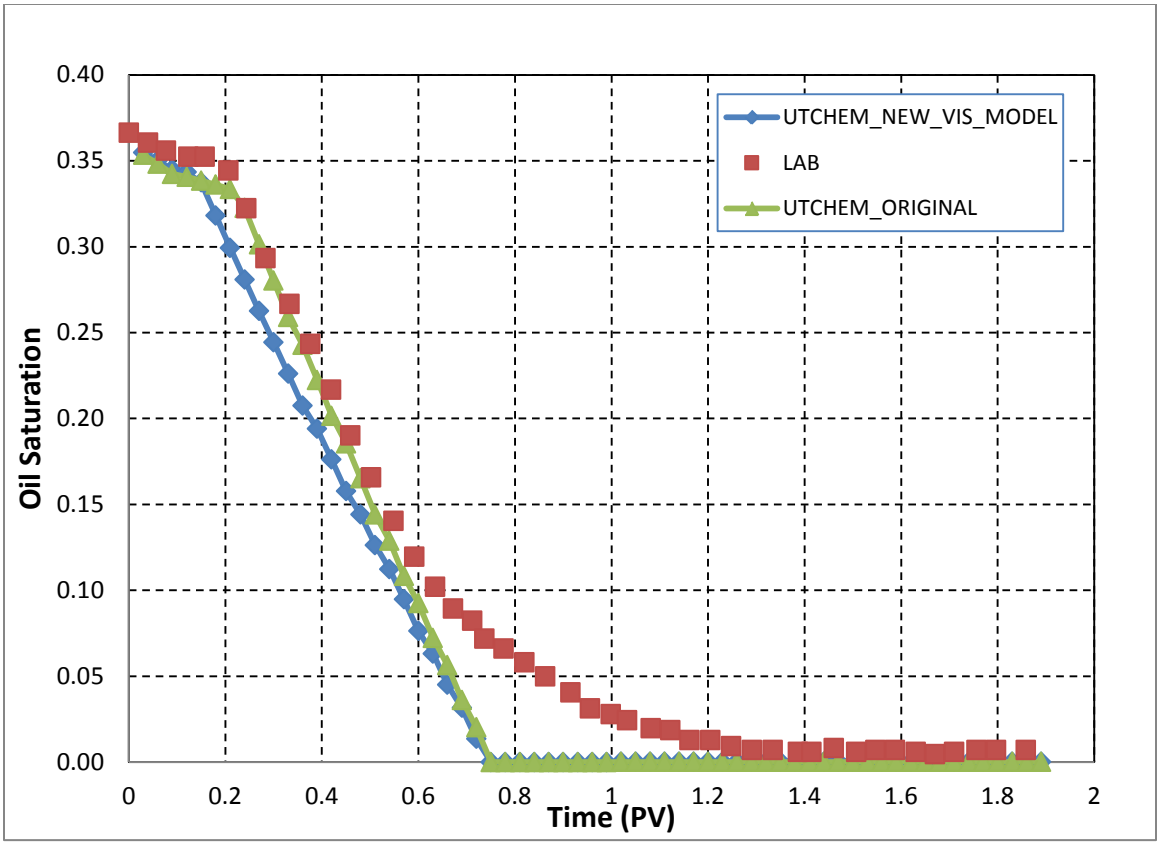

Figure 6.10: Oil saturation for PCN-04 coreflood.

Chapter 7: Effect of Co-Solvent on Microemulsion Viscosity

The high viscosity of microemulsion system would prohibit the application of surfactant flooding in EOR processes. During the surfactant screening process at laboratory, we must verify that the microemulsion formulation has low viscosity without gels or macroemulsions. Adding a co-solvent to the surfactant solution reduces the viscosity and has a positive impact on microemulsion phase behavior with more rapid equilibration. Co-solvents are chemical agents that are used to improve the performance of surfactant/polymer flooding. Co-solvent molecules line up between the surfactant hydrocarbon groups at the oil-water interface which results in lowering the viscosity of the microemulsion phase. Co-solvents also minimize the occurrence of liquid crystals and gels (Bourrel & Schechter, 1988). They also reduce the equilibration time and improve the stability of the microemulsion solutions [(Sanz & Pope, 1995), (Flaaten, et al., 2009), (Levitt, et al., 2006)]. Some study also show that the co-surfactants can be used to modify the optimum salinity and the surfactant formulation [(Lelanne-Casso, et al., 1983), (Bourrel & Schechter, 1988)].

Taghavifar et al. (2013) devleoped a theoretical framework to explain the micoremulsion rheological behavior when co-solvent and branched surfactants are added to the system. They also used the same approach to qualitatively describe the effect of temperature on the rheology of microemulsion. They used their framework to describe the experimental measurements obtained by Walker (2011). However, all the samples analyzed are of Windsor Type III in equilibruim with excess oil and brine. They concluded that the addition of co-solvent reduces the bending modulus of the interface which increases the fluidity and also breaks the long-range interactions through electorstatic charge or composition heterogeneity. These two phenomena make the

inteface more fluid or ideal and express Newtonian-like rheological behavior. The effect of temperature was related to the disruption of the natural hydrogen bonding network of water which makes the interface more flexible. Based on their study, the reduction of the bending modulus and increase of the saddle-splay modulus break the long-rang interactions and improve the microemulsion rehology. Co-solvent modifies both moduli and become the most effective method in breaking the long-range interaction while the increase in temperature or adding branched surfactant only modifies one of the moduli.

In this section we study the effect of co-solvent on microemulsion viscosity. In general the addition of co-solvent to surfactant formulation improves the aqueous stability (i.e. clear aqueous solutions), helps in faster equilibration time in presence of oil, reduces the microemulsion viscosity. On the other hand, co-solvents can increase or decrease the optimum salinity compared to the formulation without co-solvent and will reduce the solubilization ratio (i.e. increase interfacial tension). The reduction factor in microemulsion viscosity depends on many factors including type of co-solvent, salinity, and the co-solvent concentration. We have few lab tests that to some extent show the effect of co-solvent on microemulsion viscosity but almost none of the tests provide adequate and sufficient information to draw any conclusion and develop a model to account for the effect of co-solvent on microemulsion viscosity.

We first present a review of the available test data and then propose a preliminary model to account for the effect of co-solvent on microemulsion viscosity.

7.1 DATA SET 1

This data set includes few samples of microemulsion with different surfactant concentration, co-solvent concentration, and total dissolve solids (TDS). In each set, a given concentration of surfactant was mixed with different concentrations of co-solvent.

The co-solvent used in these experiments is Iso Butyl Alcohol (IBA). We have plotted the solubilization ratios of water and oil vs. the salinity to determine the lower, upper, and optimum salinities for each set. The middle phase microemulsion viscosities are measured for the test tube at the optimum salinity. Figure 7.1 shows the measured microemulsion viscosity as a function of shear rate for different surfactant and co-solvent concentrations at optimum salinity. Table 7.1 gives the summary of lab data. The viscosities in Table 7.1 are at shear rate of 1 sec^{-1}.

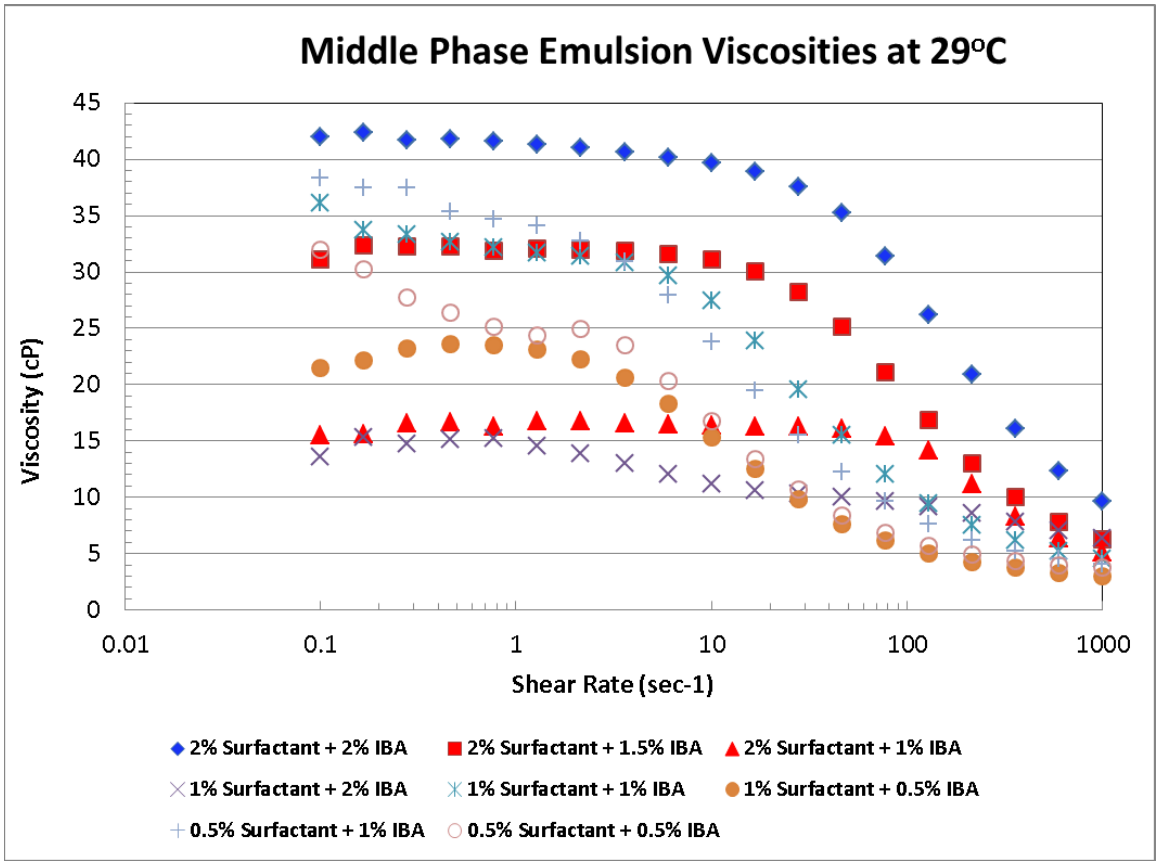

Figure 7.1: Middle phase viscosities vs. shear rates at different surfactant and co-solvent concentrations.

Table 7.1: Microemulsion viscosity at different surfactant and co-solvent concentrations

Set Number	Surfactant (wt%)	IBA (wt%)	C_{SEL}	C_{SEU}	Opt Salinity	Opt Sol Ratio	Viscosity (cP)
							1 sec^{-1}
1	2.00	2.0	3.0	3.4	3.4	13.0	41.3
2	2.00	1.5	3.2	3.6	3.4	20.0	32.1
3	2.00	1.0	3.6	3.8	3.6	25.0	16.7
4	1.00	2.0	2.8	3.0	3.0	12.0	14.6
5	1.00	1.0	2.8	3.1	3.1	36.0	31.7
6	1.00	0.5	3.2	3.4	3.3	36.0	23.1
7	0.50	2.0	2.2	2.6	2.6	12.0	
8	0.50	1.0	2.2	2.6	2.6	30.0	34.1
9	0.50	0.5	2.4	2.7	2.7	3.8	24.4
10	0.15	2.0	1.4	1.8			
11	0.15	1.0	No middle phase	No middle phase			
12	0.15	0.5	No middle phase	No middle phase			

The samples can be divided into three sub-sets based on the surfactant concentration. Since the viscosities were measured only at optimum salinity for the middle phase, not all samples in Table 7.1 have values for viscosities.

Co-solvents are generally used to improve microemulsion stability and lower the microemulsion viscosities. The data in Table 7.1 shows that the optimum solubilization ratio decreases with the increase in co-solvent concentration which indicates that the co-solvent reduces the solubility of the surfactant and increases the interfacial tension. However, the benefits of reducing the viscosity and coalescence time (i.e. faster equilibration) overcome the lower solubilization ratios with superior performance in oil recovery coreflood experiments (Dwarakanath, et al., 2008). Also, the microemulsion viscosity increases with the increase in co-solvent concentration which also reduces the surfactant formulation performance. We expect that the co-solvent is used to improve the aqueous stability and microemulsion stability for in this case.

Another observation is that the co-solvent changes the lower and upper limits of the salinity which indicates the co-solvent changes the phase behavior of the microemulsion formulation. The optimum salinity seems to be relatively insensitive to the co-solvent concentration for this data set.

Plotting the microemulsion viscosity vs. co-solvent concentration shows a linear trend (Figure 7.2). We ignored one of the points in 1 wt% surfactant data set because of the measurement error. Since all of these viscosity measurements are done at almost the same salinity these effect are merely due to co-solvent concentration. The results also show that the slope of the lines is almost the same (i.e. parallel lines). We use the above observation and trend of the data to develop a model to account for the effect of co-solvent on microemulsion viscosity at different salinities. Since co-solvent changes the

phase behavior and the lower and upper limits of salinity and also changes the viscosity, we need to modify the viscosity model to reflect these two effects. The above observations help to offer a modification to the existing UTCHEM viscosity model.

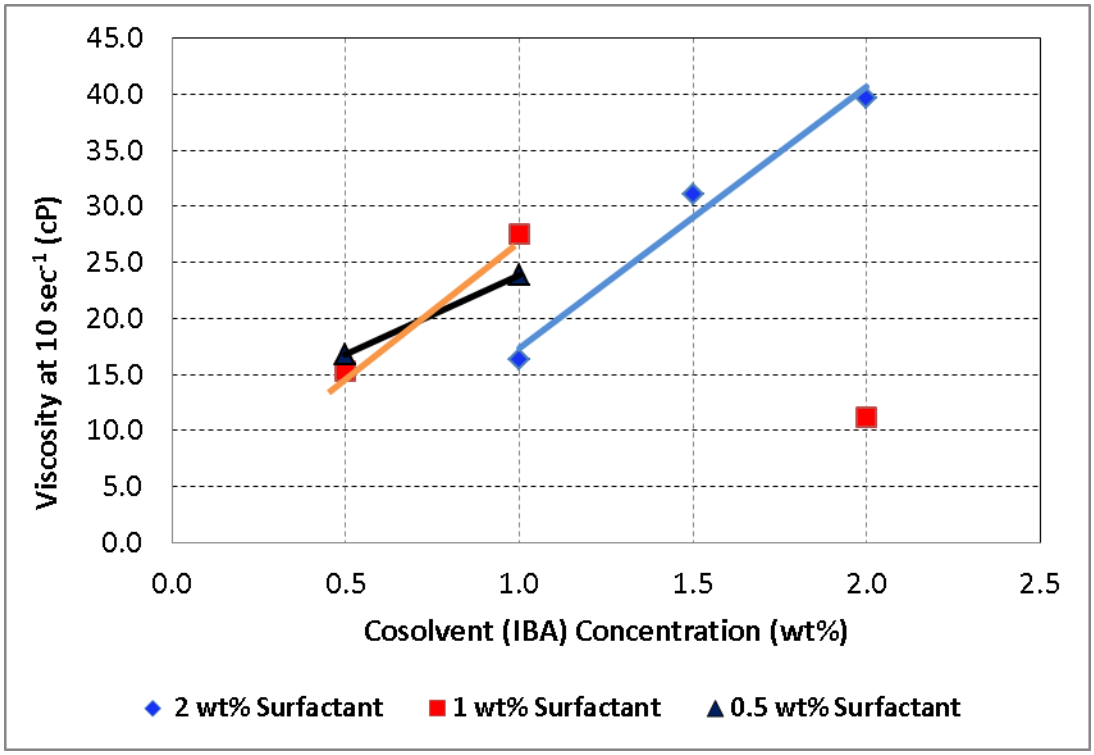

Figure 7.2: Microemulsion viscosity vs. co-solvent concentration at constant surfactant concentration and a given salinity

7.2 VISCOSITY MODEL TO INCORPORATE CO-SOLVENT EFFECTS

Salter 1977 conducted series of interesting experiments and shed light on to some effects of co-solvents on microemulsion properties. The main focus of his study devoted to the effect of co-solvent on optimal salinity and optimal interfacial tension but he also plotted the effect of co-solvent on microemulsion viscosity. The main points of his study related to viscosity behaviors are:

1. When excess oil and water exist their viscosities are independent of salinity.
2. The viscosity of microemulsion phase is initially less than the viscosity of oil phase (when no excess-brine exists - Type I phase behavior) and increases with the increase in salinity. The viscosity increases to a maximum and then decreases with the increase in salinity.
3. The maximum microemulsion viscosity decreases with the increase in amount of alcohol added.

In one of his experimental data sets, Salter investigated the effect of nine different 'small molecule' alcohols using salt optimization process. For each alcohol, he used four different alcohol-to-surfactant ratios over the 0 to 3.6 wt% NaCl. Phase behavior, interfacial tension, and phase viscosity data were measured and reported for all of the samples. He observed that the range of salinities for which phase transition happened were depended on the type and amount of the alcohol. His results showed that in all three groups of alcohols (water soluble, intermediate solubility, and oil soluble), the upper limits of salinity increased with the increase in alcohol concentration.

We have digitized and plotted his results in Figure 7.3 through Figure 7.6. These results are only for one set that the optimal salinity does not change with the changes in amount of co-solvent. According to (Salter, 1977) , the acronyms such as AA TAA (12.5) describes the mixture components, where the first part (AA) designates the surfactant, the second part (TAA) designates the alcohol, and the number in parenthesis (12.5) designates the wright percent of the combined mixture which is alcohol.

To identify different phase behavior, we draw two lines for C_{SEL} and C_{SEU}. In Figure 7.3 and Figure 7.4 we can fairly assume that we only have Type I and Type II phase behavior.

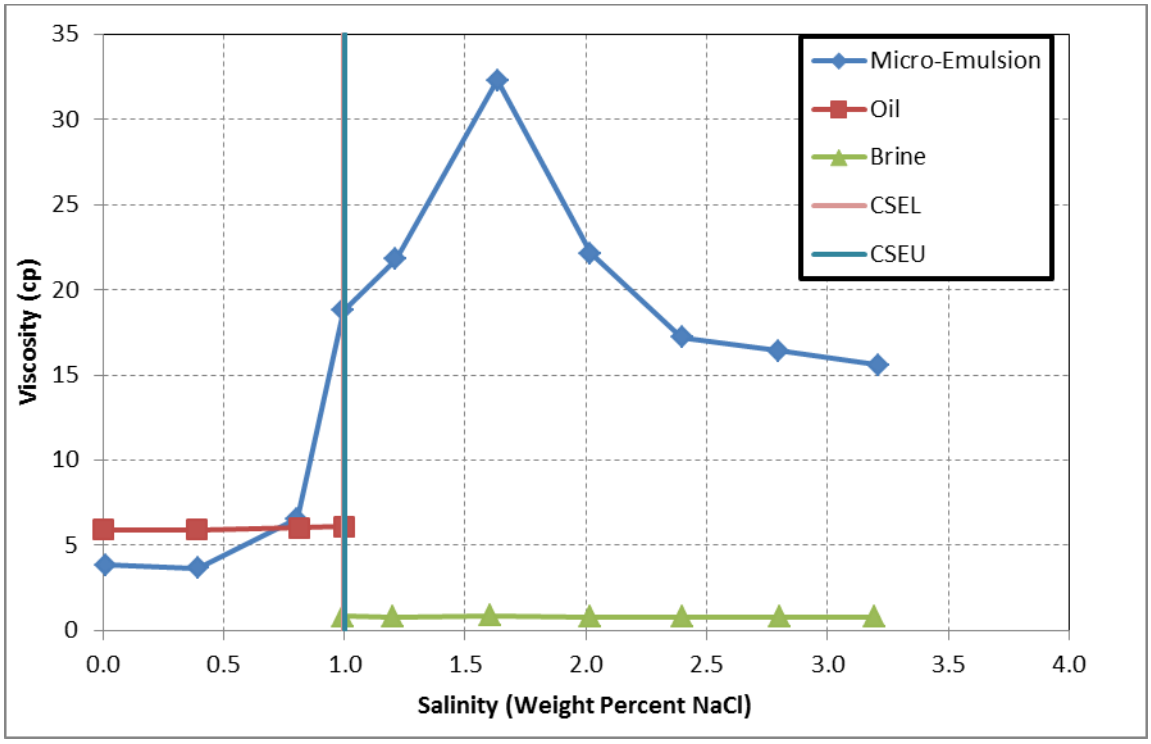

Figure 7.3: Microemulsion viscosity vs. salinity for Surfactant AA TAA (12.5). CSEL and CSEU nearly coincide (Salter, 1977)

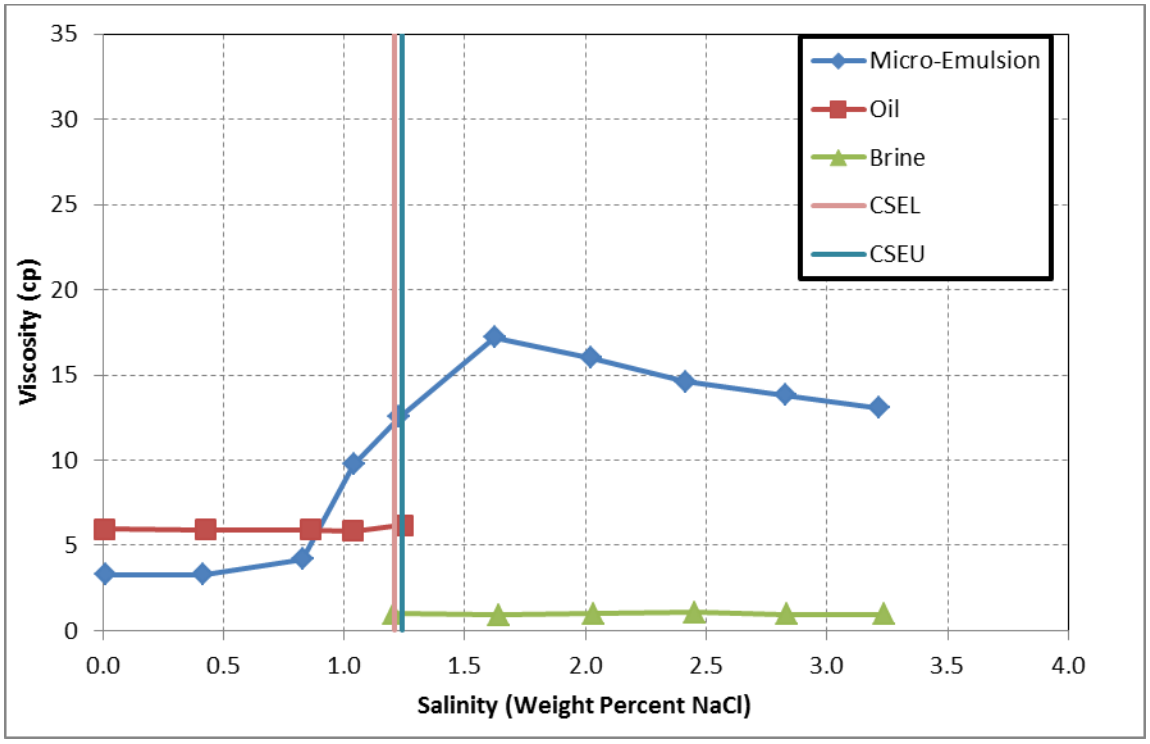

Figure 7.4: Microemulsion viscosity vs. salinity for Surfactant AA TAA (25) (Salter, 1977)

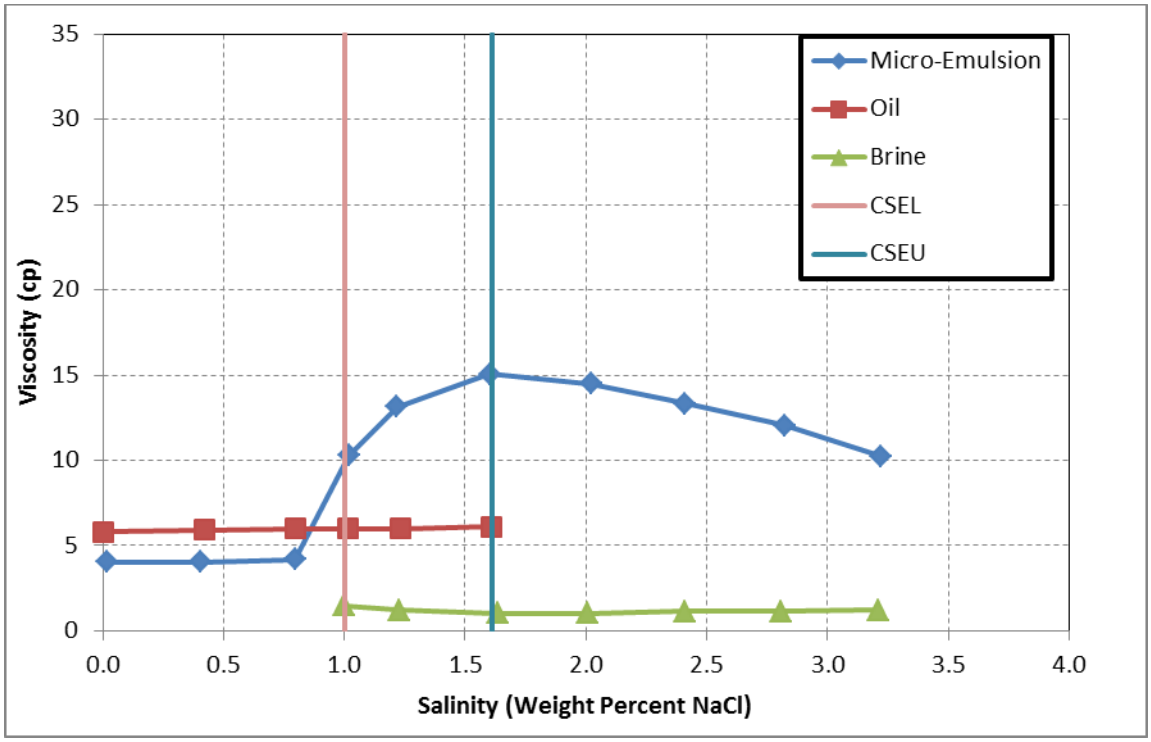

Figure 7.5: Microemulsion viscosity vs. salinity for Surfactant AA TAA (37.5) (Salter, 1977)

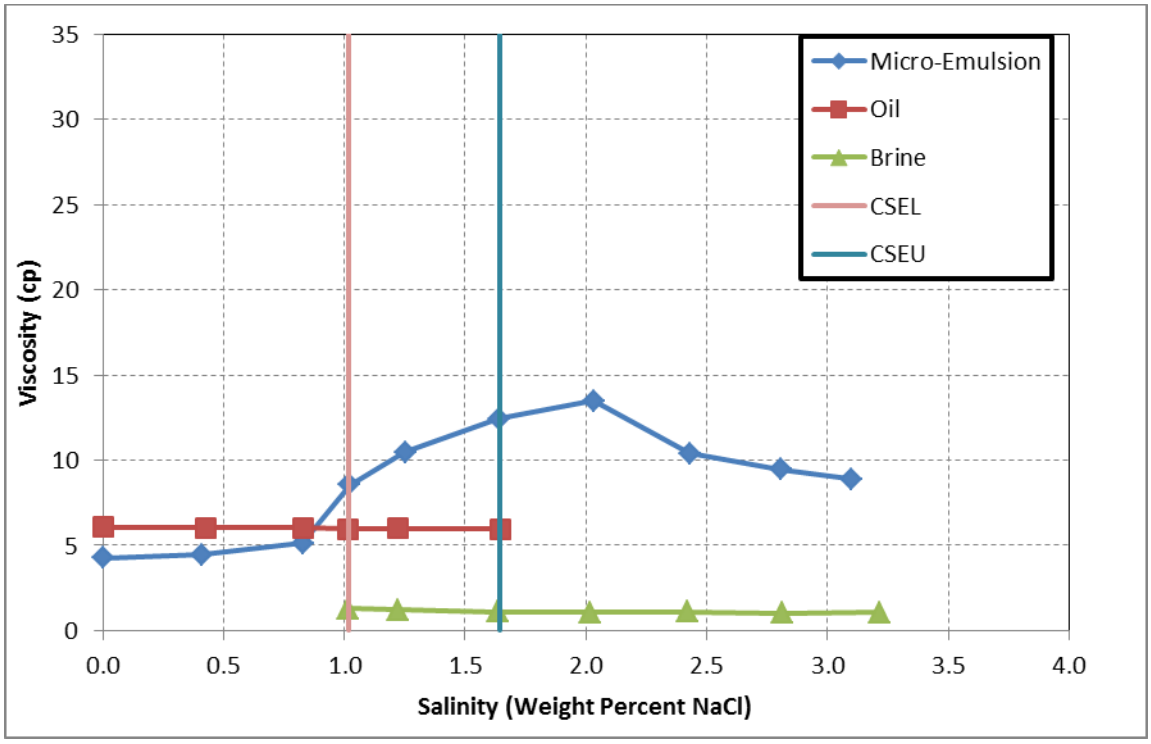

Figure 7.6: Microemulsion viscosity vs. salinity for Surfactant AA TAA (50) (Salter, 1977)

In order to analyze the data we divide the lab data into three sections based on three phase behavior types. In each type, we introduce a normalize salinity such that we have the same reference for all the data. The mathematical definition of the normalized salinity is different for each type of phase behavior and will be described in sections below.

7.2.1 Type I Phase Behavior

Since the lower limit salinity (C_{SEL}) changes with the concentration of co-solvent, we use C_{SEL} to normalize the salinity for each data set. We introduce the normalized effective salinity (C_{SE}^{1}) for systems with Type I phase behavior as follow:

$$C_{SE}^{1} = \frac{C_{SE}}{C_{SEL}} \tag{7.1}$$

Using the above definition, the normalized effective salinity for system with Type I phase behavior is between 0 and 1. Figure 7.7 shows the viscosity of Type I phase behavior at each concentration of co-solvent vs. normalized effective salinity. From the results it can be concluded that the amount of co-solvent does not affect the viscosity of tubes with Type I phase behavior. The results also show a linear trend between viscosity and normalized effective salinity.

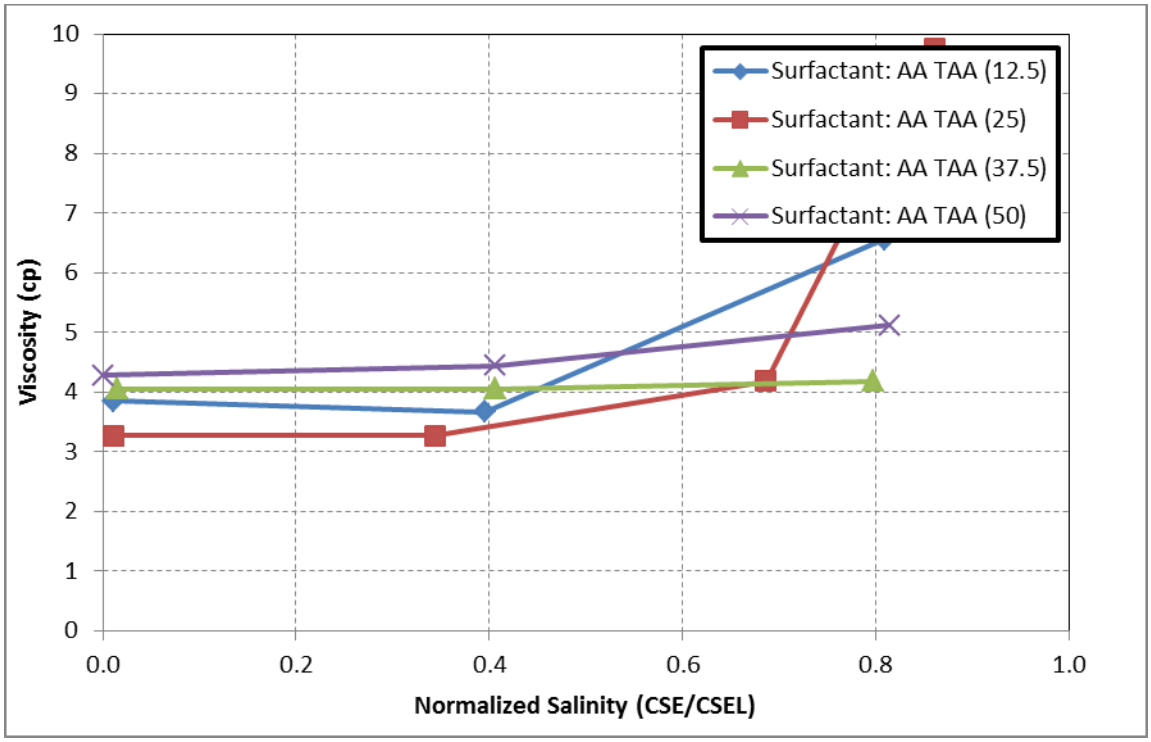

Figure 7.7: Viscosity vs. normalized salinity for Type I samples with different co-solvent concentrations (indicated in the parenthesis) of Salter (Salter, 1977) .

The above observations suggest that the co-solvent does not change the viscosity of microemulsion phase in Type I system and if we modify the viscosity model by replacing C_{SE} with C_{SE}^{1} as:

$$\mu_m = \mu_w\left(\beta_1 + \beta_2 C_{SE}^{1}\right) \qquad for\, C_{SE} < C_{SEL} \tag{7.2}$$

In the above equation μ_m is the microemulsion viscosity, μ_w is the water viscosity, C_{SE}^{1} is the normalized effective salinity (Eq. 7.1), and β_1 and β_2 are the constant coefficients obtained by matching the measured viscosities.

7.2.2 Type III Phase Behavior

We introduce the normalized effective salinity for samples with Type III phase behavior as follows:

$$C_{SE}^{3} = \frac{C_{SE} - C_{SEL}}{C_{SEU} - C_{SEL}} \tag{7.3}$$

Using the above definition, the normalized effective salinity for system with Type III phase behavior is between 0 and 1. Using the effective salinity into new viscosity model incorporates the effect of co-solvent concentration on lower and upper limits salinities.

Figure 7.8 shows the viscosity of Type III phase behavior for each concentration of co-solvent vs. normalized salinity [Eq. (7.3)]. The results show that the co-solvent reduces the viscosity and the coefficient is constant for all salinities (the two lines are parallel). Now we need to introduce another coefficient that takes into account the effect of co-solvent concentration on microemulsion viscosity. We need additional experimental data to formulate how this model coefficient changes with co-solvent concentration but what we can conclude from the results in Figure 7.8 is that the reduction or increase is constant for all salinities. We introduce this coefficient as a change in the microemulsion viscosity per one unit of co-solvent concentration as follow:

$$RF = \frac{\mu_{m,2} \diagup \mu_{m,1}}{C_{7,2} - C_{7,1}} \tag{7.4}$$

In the above equation RF is the reduction factor, $\mu_{m,1}$ is the microemulsion viscosity at co-solvent concentration $C_{7,1}$, and $\mu_{m,2}$ is the microemulsion viscosity at co-solvent concentration $C_{7,2}$. RF has unit of $1/C_{\cos olvent}$ where the co-solvent concentration unit is volume fraction. In order for RF to be positive, $C_{7,2}$ must be greater than $C_{7,1}$. For example, for the results shown in Figure 7.8 at salinity of 0.4, the microemulsion viscosity is 13.13 and 10.3 for the co-solvent concentration of 37.5 and 50 respectively. Hence the reduction factor is about 0.063 for this data set for all salinities.

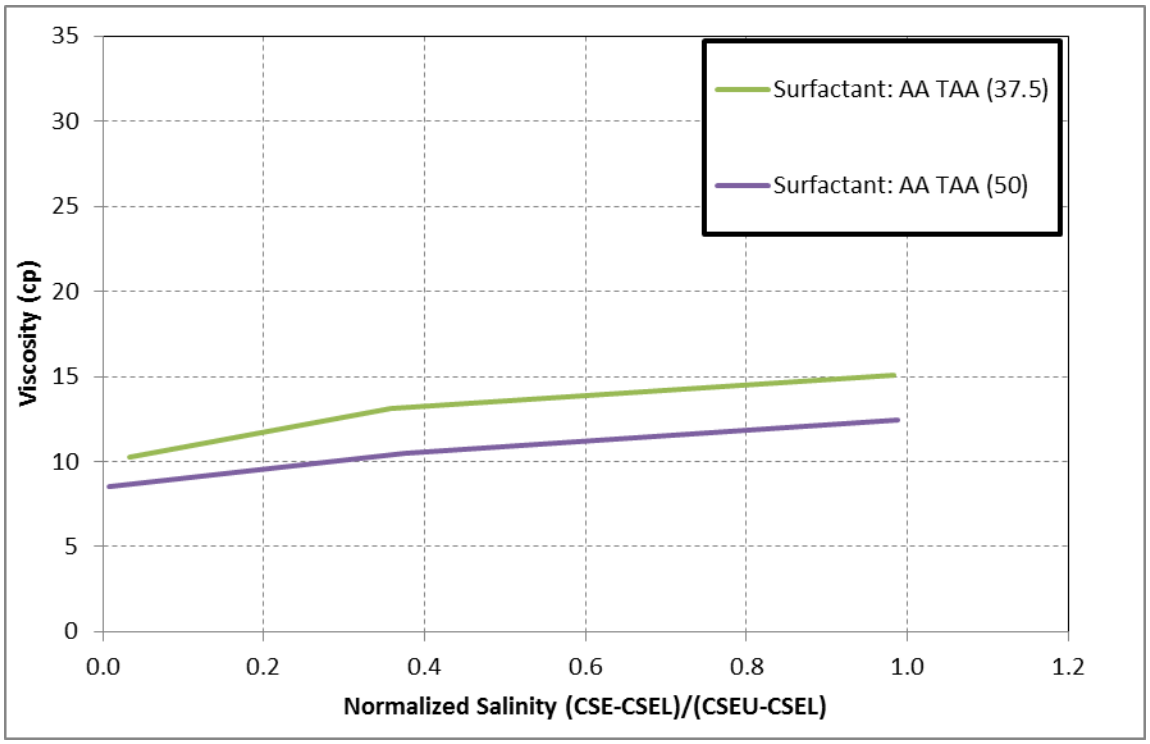

Figure 7.8: Viscosity vs. normalized salinity for Type III samples at different concentrations of co-solvent vs normalized salinity using data of Salter (Salter, 1977).

Using the normalized effective salinity and the reduction factor, we modify our viscosity model for Type III phase behavior as follow:

$$\mu_m = RF \times C_7 \times \left(\beta_5 + \frac{\beta_6}{\sqrt{C_{SE}^3}} + \beta_7 e^{C_{SE}^3} \right) \qquad for\, C_{SEL} \le C_{SE} \le C_{SEU} \tag{7.5}$$

In the above equation C_7 is the co-solvent concentration at which the microemulsion viscosity is calculated and β parameters are matching constants. Since RF is a function of co-solvent concentration, $C_{co-solvent}$ must have a value within the range of the two concentrations used in calculating RF [Eq. (7.4)].

7.2.3 Type II Phase Behavior

The normalized form that we use for samples with Type II phase behavior using the upper Type III effective salinity (C_{SEU}) is as follows:

$$C_{SE}^{2} = \frac{C_{SE}}{C_{SEU}} \tag{7.6}$$

Using the above definition, the normalized effective salinity for Type II phase behavior starts at a value of 1. Figure 7.9 shows the viscosity of Type II phase behavior at each co-solvent concentration vs. the normalized salinity [Eq. (7.6)]. If we ignore the data for Surfactant AA TAA (12.5) then there is a constant reduction factor for co-solvent concentrations at all salinities. In general the reduction factor depends on co-solvent concentration. However, it seems that the reduction factors are almost identical for all co-solvent concentrations for this data set (Table 7.2).

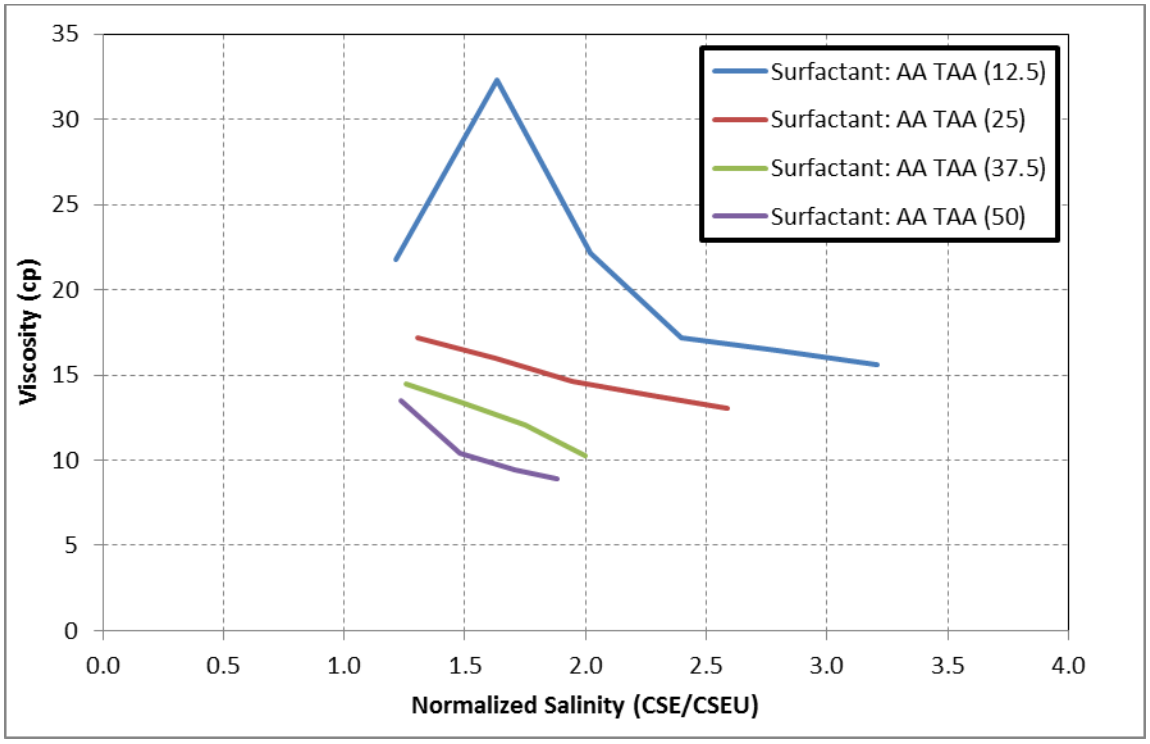

Figure 7.9: Microemulsion viscosity vs. normalized salinity for Type II samples at different concentrations of co-solvent vs normalized salinity using Salter's data (Salter, 1977).

Again, we use the normalized effective salinity to account for the effect of co-solvent on the upper limit of effective salinity and we use the reduction factor to incorporate the effect of co-solvent concentration on the microemulsion viscosity. We have to note that the reduction factors for samples with Type II and Type III phase behavior are different but they may be very close as in this case.

From Figure 7.9 at normalized effective salinity of 1.6, the microemulsion viscosities are 15.99, 12.65, and 9.78 cp for co-solvent concentrations of 25%, 37.5%, and 50% respectively. The reduction factors (RF) are 0.063 and 0.062 for the co-solvent concentrations between 25 – 37.5% and 37.5 – 50% respectively. These results show that

we can use a constant reduction factor for both Type II and Type III for all co-solvent concentrations and salinities for this data set (Table 7.2).

Table 7.2: RF at different co-solvent concentrations

Alcohol Concentration	Type II		Type III	
	Viscosity (cp)	RF	Viscosity (cp)	RF
25	15.99			
37.5	12.65	0.0633	13.13	
50	9.78	0.0618	10.30	0.0628

Based on the above conclusions, we modify microemulsion viscosity model for Type II phase behavior as follows:

$$\mu_m = RF \times C_7 \times \mu_o \left(\beta_3 + \beta_4 C_{SE}^2\right) \qquad for\, C_{SE} > C_{SEU} \tag{7.7}$$

Therefore, the proposed microemulsion viscosity model is:

$$\mu_m = \begin{cases} \mu_w \left(\beta_1 + \beta_2 C_{SE}^1\right) & C_{SE} < C_{SEL} \quad , C_{SE}^1 = \dfrac{C_{SE}}{C_{SEL}} \\ RF \times C_7 \times \mu_o \left(\beta_3 + \beta_4 C_{SE}^2\right) & C_{SE} > C_{SEU} \quad , C_{SE}^2 = \dfrac{C_{SE}}{C_{SEU}} \\ RF \times C_7 \times \left(\beta_5 + \dfrac{\beta_6}{\sqrt{C_{SE}^3}} + \beta_7 e^{C_{SE}^3}\right) & C_{SEL} \le C_{SE} \le C_{SEU} \quad , C_{SE}^3 = \dfrac{C_{SE} - C_{SEL}}{C_{SEU} - C_{SEL}} \end{cases} \tag{7.8}$$

7.2.4 Model Verification

To verify our model, we used the data sets from Salter for microemulsion viscosities at 37.5 and 50 wt% alcohol concentrations. We calculated β parameters at 37.5 wt% of alcohol and used Eq. (7.8) to calculate the viscosities at 50 wt% alcohol. The water and oil viscosities used in these calculations are 1 cp and 6 cp respectively.

Table 7.3 gives the microemulsion viscosities for the microemulsion with 37.5 wt% alcohol and Table 7.4 contains the model parameters for this data set. The RF calculated is 0.063. Table 7.5 contains the calculated values for microemulsion viscosities at 50 wt% alcohol concentration and Figure 7.10 shows the model validation. The results show excellent match between calculated and experimental measurements.

Table 7.3: Microemulsion viscosities for sample with 37.5 wt% alcohol concentration

Salinity (wt% NaCl)	Viscosity (cp)
0.02	4.05
0.41	4.05
0.80	4.18
1.02	10.29
1.22	13.13
1.60	15.06
2.02	14.48
2.41	13.32
2.82	12.03
3.22	10.23

Table 7.4: Model parameters at 37.5 wt% alcohol concentration

Model Parameters	Value
β1	4.10
b2	0.16
β3	3.61
b4	-0.94
β5	12.42
b6	-0.62
β7	1.22

Table 7.5: Microemulsion viscosities for sample with 50 wt% alcohol concentration

Salinity (wt% NaCl)	Viscosity (cp)	Model Viscosity (cp)
0.00	4.28	4.10
0.41	4.44	4.17
0.83	5.12	4.23
1.02	8.56	5.15
1.25	10.46	10.54
1.64	12.41	12.06
2.03	13.47	11.77
2.43	10.38	10.68
2.81	9.46	9.64
3.10	8.87	8.85

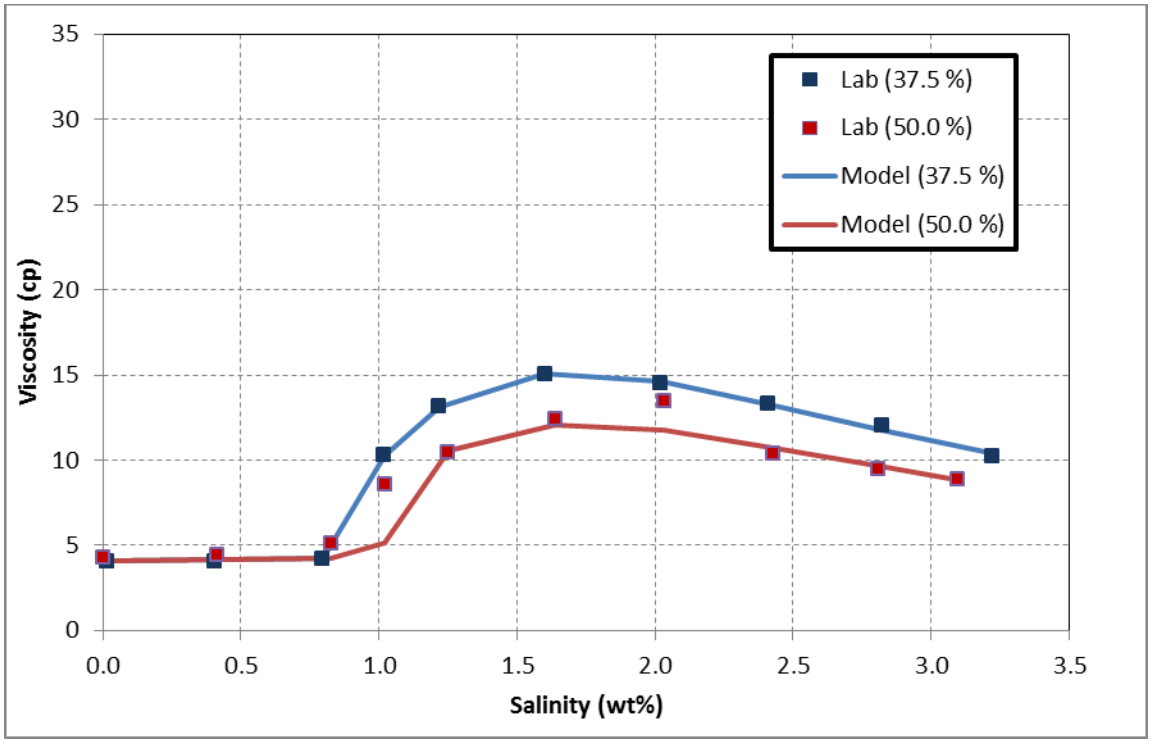

Figure 7.10: Model validation for microemulsion viscosities at 37.5 and 50 wt% alcohol concentrations (Date from Salter (Salter, 1977).

7.3 SUMMARY

We addressed the effect of co-solvent on microemulsion rheology by modifying the microemulsion viscosity model [Eq. (7.8)] to account for the effect of co-solvent on microemulsion viscosity. The effect of co-solvent on the microemulsion viscosity was incorporated by introducing a reduction factor (RF) and normalized effective salinities. We have verified the model using experimental data from (Salter, 1977).

The proposed microemulsion viscosity model [Eq. (7.8)] was developed and validated based on limited experimental data. We offer the following recommendation for future validation and enhancement of the viscosity model:

- Further validation of the proposed equations over a wider range of alcohol types, concentrations and surfactant formulations.
- Future testing of the proposed viscosity model [Eq. (7.8)] for consistency and physical microemulsion viscosity before implementation into UTCHEM is recommended.
- Need to validate the model to account for microemulsion viscosity in the presence of both polymer and co-solvent.
- Need to develop the shear thinning rheology model for microemulsion phase. The following model which is implemented in UTCHEM can be used as a preliminary model:

$$\mu_{me} = \mu_{me}^{\infty} + \left(\mu_{me}^{0} - \mu_{me}^{\infty}\right)\left[1 + \left(\lambda_{me}\gamma_{eq}\right)^2\right]^{\left(\frac{m-1}{2}\right)} \tag{7.9}$$

where μ_{me} is the microemulsion viscosity, μ_{me}^{0} and μ_{me}^{∞} are limiting Newtonian viscosities at the low and high shear limits, respectively; γ_{eq} is the effective shear rate [Eq. (7.10)]; λ_{me} and m are microemulsion-specific empirical constants.

$$\gamma_{eq} = \left(\frac{3m+1}{4m}\right)^{\frac{m}{m-1}} \frac{4\left|\vec{u}_{me}\right|}{\sqrt{8\bar{k}k_{r,me}\phi S_{me}}} \tag{7.10}$$

In the above equation, $\vec{u}_{me}$ is the Darcy velocity of microemulsion phase; $\bar{k}$ is the permeability; $k_{r,me}$ is the microemulsion relative permeability; ϕ is porosity; and S_{me} is microemulsion viscosity.

- Need to include the effect of temperature on both polymer viscosity and microemulsion viscosity. Currently, only water and oil viscosities are calculated as a function of temperature in the microemulsion viscosity model.

Chapter 8: Summary, Conclusions, and Recommendations

8.1 SUMMARY AND CONCLUSIONS

In this chapter, we summarize the key findings of the research performed herein on the rheology of the microemulsion and the effect of co-solvent and polymer on the microemulsion phase viscosity.

The rheological behavior of microemulsion systems is largely dependent on the phase behaviors, i.e., oil-in-water or water-in-oil emulsions. Different phase behavior can have significantly different rheological properties for the microemulsion. The microemulsion viscosity of test tubes with Windsor Type I and Type II shows a linear trend with salinity while test tubes with Windsor Type III phase behavior show a parabolic correlation with salinity. There are abrupt changes in the microemulsion viscosity at the phase transitions. For Windsor Type I and Type II phase behavior, the microemulsion phase viscosity is similar to the viscosity of the continuous phase (i.e. oil and aqueous phases), while for test tubes with Windsor Type III phase behavior, much larger viscosity values are observed.

The viscosity of a microemulsion phase is highly affected by oil composition, the chemical formulation, and composition of the microemulsion phase. A system that is oil continuous can change into a bicontinuous system and finally to a water continuous system. These phases (oil continuous phase, bicontinuous phase, or water continuous phase) have very different structure organizations and result in distinct changes in viscosity. We have observed the same behavior in microemulsion viscosity from our lab measurements. We propose a new empirical viscosity model for the viscosity of microemulsion phase as a function of salinity. The proposed model is not continuous across the phase behavior boundaries; rather, we introduce empirical correlations for the

microemulsion phase for each type of phase behavior consistent with phase composition calculation using Hand's rule.

The proposed viscosity model was verified against several experimental data sets using different surfactant formulations, crude oil, and temperatures. The results showed an excellent match between experimental lab measurements and the viscosity calculated from the model. The proposed viscosity model was also implemented in UTCHEM reservoir simulator and history matching two core flood experiments with special emphasis on pressure drop match. Excellent agreement of pressure drop between the model and measurements was obtained.

In microemulsion systems, several phases can coexist in equilibrium with each phase having a different microscopic and macroscopic structure. Several factors such as salinity, temperature and presence of other materials like polymer and co-solvent affect the phase behavior and rheological properties of microemulsions.

The experimental results show that the microemulsion complexes with polymer exhibit the same phase transitions pattern that we have for the microemulsion solutions without polymer, meaning that there is a transition from Windsor Type I to Windsor Type II via Windsor Type III. Also, the presence of polymer in a microemulsion complex impacts the optimum salinity and the range of salinity that the Type III phase can form (lower and upper limits of effective salinity for Type III system have been extended). In all of our measurements, the presence of polymer widens the range of salinity that the Type III phase can exist.

When polymer is added to chemical formulation, the aqueous phase viscosity for systems of Windsor Type III and Type II exhibits significantly higher viscosity compared to the water viscosity. This substantial increase in aqueous viscosity suggests that the

polymer is mainly partitioned into the aqueous phase. The oleic phase viscosity remains relatively unchanged; hence the polymer partitioned between aqueous and microemulsion phases only. When we have polymer and surfactant, the microemulsion phase viscosity is higher than polymer viscosity. This higher viscosity could be due to some molecular interaction between polymer molecules and surfactant molecules. In almost all cases that we have, whenever polymer is present, microemulsion phase viscosities are 1.5 to 2.0 times higher than polymer solution viscosity.

To account for effect of polymer on the microemulsion viscosity, we modified the proposed viscosity model by replacing water viscosity with polymer viscosity in the correlations and by introducing a new factor to account for the interaction effect between polymer and surfactant.

Adding a co-solvent to the surfactant solution reduces the viscosity and has a positive impact on microemulsion phase behavior with more rapid equilibration. Co-solvent also changes the lower and upper limits of salinity where Windsor Type III forms. The effect of co-solvent on the microemulsion viscosity was incorporated into the proposed viscosity model by introducing a reduction factor (RF) and normalized effective salinities. The normalized effective salinities account for effect of co-solvent on lower and upper limits of salinity for Windsor Type III system. However, additional data are needed to more accurately model the impact of co-solvent on microemulsion viscosity.

8.2 RECOMMENDATIONS

The proposed microemulsion viscosity model and the modifications were developed and validated based on limited experimental data. We offer the following recommendation for future validation and enhancement of the viscosity model:

- Validate the model to account for microemulsion viscosity in the presence of both polymer and co-solvent.
- Further test the shear thinning rheology model for microemulsion phase in the presence of polymer.
- Include the effect of temperature on both polymer viscosity and microemulsion viscosity. Currently, only water and oil viscosities are changed as a function of temperature in the microemulsion viscosity model.
- Further validation of the proposed models over a wider range of alcohol types, concentrations, and surfactant formulations.

BIBLIOGRAPHY

Ajith, S., Jhon, A. C. & Rakshit, A. K., 1994. Physiochemical Studies of Microemulsions. *Pure Appl. Chem.,* pp. 509-514.

Anklam, M., Prudhomme, R. & Warr, G., 1995. Shear Thinning in Ternary Bicontinuous and Water-in-Oil Microemulsions. *AIChE,* pp. 677-682.

Baker, R. C., Florence , A., Ottewill, R. & Tadors, T., 1984. Investigations into the Formation and Characterization of Microemulsions. II. Light Scattering Conductivity and Viscosity Studies of Microemulsions. *J. Colloid and Interface Science,* Volume 100, pp. 332-349.

Beckstrom, R. S. & Van Tuyl, F. M., 1927. The Effect of Flooding Oil Sands with Alkaline Solutions. *American Association of Petroleum Geologists,* pp. 223-235.

Bidyut, P. K. & Satya, M. P., 2000. The Viscosity Behaviours of Microemulsions: An Overview. *PINSA,* pp. 499-519.

Bourrel, M. & Schechter, R. S., 1988. *Microemulsions and Related Systems.* New York, NY: Marcel Dekker.

Camilleri, D. et al., 1987. Comparison of an Improved Compositional Micellar/Polymer Simulator With Laboratory Corefloods. *SPE Journal,* 2(4), pp. 441-451.

Chen, C. & Warr, G., 1992. Rheology of Ternary Microemulsions. *J. Phys. Chem,* pp. 9492-9497.

Chiang, Y. M. & Shah., O. D., 1980. *The Effect of Alcohol on Surfactant Mass Transfer Across the Oil/Brine Interface and Related Phenomena.* SPE Oilfield and Geothermal Chemistry Symposium, 28-30 May 1980, Stanford, California, SPE.

Costello, B., 2005. *The AR-G2 Magnetic Bearing Rheometer,* Fleming Way, Crawley, West Sussex RH10 9NB: TA Instruments Ltd.

Datta-Gupta, A., Pope, G. A., Sepehrnoori, K. & Thrasher, R., 1986. A Symmetric, Positive Definite Formulation of a Three-Dimensional Micellar/Polymer Simulator. *SPE Reservoir Engineering,* 1(6), pp. 622-632.

Delshad, M. et al., 1986. Effect of Capillary Number on the Residual Saturation of a Three-Phase Micellar Solution. *SPE Conference Paper.*

Delshad, M., Delshad, M., Pope, G. & Lake, L., 1987. Two- and Three-Phase Relative Permeabilities of Micellar Fluids. *SPE Journal,* 2(3), pp. 327-337.

Delshad, M. et al., 2006. *Modeling Wettability Alteration in Naturally Fractured Reservoirs.* Tulsa, SPE Symposium on Inproved Oil Recovery.

Delshad, M., Pope, G. A. & Sepehrnoori, K., 1996. A Compositional Simulator for Modeling Surfactant Enhanced Aquifer Remediation, 1. Formulation.. *Journal of Contaminant Hydrology*, 23(4), pp. 303-327.

Dwarakanath, V. et al., 2008. Using Co-solvents to Provide Gradients and Improve Oil Recovery During Chemical Flooding in a Light Oil Reservoir. *SPE-113965-MS.*

Eicke, H. F., Kubik, R., Hasse, R. & Zschokkel, I., 1984. Surfactant in Solutions. *K. L. Mittal and B. Lindman, eds,* Volume 3, p. 1533.

Flaaten, A. K., Nguyen, Q. P., Pope, G. A. & zhang, J., 2009. A Syatematic Laboratory Approach to Low-Cost, High-Performance Chemical Flooding. *SPE Reservoir Evaluation and Engineering*, pp. 713-723.

Flory, P., 1953. *Principles of Polymer Chemistry.* Ithaca, New York: Cornell University Press.

Garcia-Rio, L. et al., 1994. Effects of Additives on the Internal Dynamics and Properties of Water/AOT/IsoOctane Microemulsions. *Langmuir,* Volume 10, pp. 1676-1683.

Gogarty, W. B. & Tosch, W. C., 1968. Miscible-Type Waterflooding: Oil Recovery with Micellar Solutions. *Journal of Petroleum Technology,* Volume 20, pp. 1407-1414.

Healy, R. N. & Reed, R. L., 1974. Physiochemical Aspects of Microemulsion Flooding. *SPEJ,* Volume 14, pp. 491-501.

Healy, R. N. & Reed, R. L., 1976. Multiphase Microemulsion Systems. *SPE J,* Volume 16, pp. 147-160.

Hsieh, W. C. & Shah, D. O., 1977 Copyright 1976. *The Effect of Chain Length of Oil and Alcohol As Well as Surfactant to Alcohol Ratio on the Solubilization, Phase Behavior and Interfacial Tension of Oil/Brine/Surfactant/Alcohol Systems.* s.l., s.n.

Jin, M., 1995. *A Study of Nonaqueous Phase Liquid Charactrization and Surfactant Remediation,* Austin, Texas: University of Texas at Austin.

Jones, S. C. & Dreher, K. D., 1976. Cosurfactants in Micellar Systems Used for Tertiary Oil Recovery. *SPE Journal,* Volume 16, pp. 161-167.

Lake, L., 1989. *Enhanced Oil Recovery.* Upper Saddle River, NJ: Prentice-Hall.

Lelanne-Casso, C. et al., 1983. Binary Surfactant Mixtures for Minimizing AlcoholCo-solvent Requirements. *SPE 12035.*

Levitt, D. B. et al., 2006. Identification and Evaluation of High-Performance EOR Surfactants. *SPE 100089.*

Lin, E., 1981. *A Study of Micellar/Polymer Flooding Using a Compositional Simulator,* Austin, Texas: University of Texas at Austin.

Meter, D. & Bird, R., 1964. Tube Flow of Non-Newtonian Polymer Solutions, Parts I and II Laminar. *AIChE J.,* pp. 878-881, 1143-1150.

Pope, G. A., Wang, B. & Kerming, T., 1979. A Sensitivity Study of Micellar/Polymer Flooding. *SPE Journal,* p. 357.

Pope, G. & Nelson, R., 1978. A Chemical Flooding Compositional Simulator. *SPEJ,* Volume 18, pp. 339-354.

Prouvost, L., Pope, G. A. & Rouse, B., 1985. Microemulsion Phase Behavior: A Thermodynamic Modeling of the Phase Partitioning of Amphiphilic Species. *SPE Journal,* Volume 25, pp. 693-703.

Saad, N., 1989. *Field Scale Studies With a 3-D Chemical Flooding Simulator,* Austin, Texas: University of Texas at Austin.

Saad, N., Pope, G. A. & Sepehrnoori, K., 1998. Simulation of Big Muddy Surfactant Pilot. *SPE Reservoir Engineering,* pp. 24-34.

Sahni, V. et al., April 2010. The Role of Co-Solvent and Co-Surfactants in Making Chemical Floods Robust. *SPE 130007.*

Salter, S. J., 1977. The Influence of Type and Amount of Alcohol on Surfactant-Oil-Brine Phase Behavior and Properties. *SPE 6843.*

Sanz, C. A. & Pope, G. A., 1995. Alcohol-Free Chemical Flooding: From Surfactant Screening to Coreflood Design. *SPE 28956, SPE Symposiom on Oilfield Chemistry.*

Snaz, C. & Pope, G. A., 1995. Alcohol-Free Chemical Flooding: From Surfactant Screening to Coreflood Design. *SPE 28956.*

Sorbie, K. S., 1991. *Polymer-Improved Oil Recovery.* London: Blackie.

Taghavifar, M., Sepehrnoori, K. & Pope, G., 2013. *On the Rheology of Microemulsions – Part I: Mechanisms of Alteration,* Ausitn, Texas: Department of Petroleum and Geosystems Engineering, the University of Texas at Austin.

Tosch, W., Jones, S. & A.W., A., 1969. Distribution equilibria in a micellar solution system. *Journal of Colloid and Interface Science,* 31(3), p. 297–306.

Trushenski, S. P., Dauben, D. L. & Parrish, D. R., 1974. Micellar Flooding - Fluid Propagation, Interaction, and Mobility. *SPEJ,* Volume 14, p. 633.

Vand, V., 1948. Viscosity of solutions and suspensions. I Theory. *J. Phys. Colloid Chem.*, pp. 277-299.

Walker, D., 2011. *Experimental Investigation of the Effect of Increasing the Temperature on ASP Flooding,* Austin, Texas: University of Texas at Austin.

Winsor, P., 1954. *Solvent Properties of Amphiphilic Compounds.* London: s.n.

Wreath, D., Pope, G. & Sepehrnoori, K., 1990. Dependence of Polymer Apparent Viscosity on the Permeable Media and Flow Conditions. *In Situ,* pp. 263-284.

Xu, H., 2012. *Potential for Non-thermal Cost-effective Chemical Augmented Waterflood for Producing Viscous Oils,* Austin: University of Texas at Austin.